Effects of $f(R)$ Gravity on the Gravitational Bound States of Ultra-cold Neutrons: A Laboratory Scale Detection Technique for Dark Energy?

By
Michael Jonathan Brown (BSc)

Thesis submitted by Michael Jonathan Brown (BSc) in partial fulfillment of the requirements for the Degree of Bachelor of Science with Honours in School of Engineering and Physical Sciences at James Cook University.

School of Engineering and Physical Sciences,
James Cook University.

11 July 2012

Declaration

I declare that this thesis is my own work and has not been submitted in any form for another degree or diploma at any university or other institute of tertiary education. Information derived from the published and unpublished work of others has been acknowledged in the text and a list of references is given.

Michael Jonathan Brown (BSc)
11 July 2012

Statement of Access to Thesis

I, the undersigned, the author of this thesis, understand the James Cook University will make it available for use within the University Library and, by microfilm or other photographic means, allow access to users in other approved libraries. All users consulting this thesis will have to sign the following statement:

"In consulting this thesis I agree not to copy or closely paraphrase it in whole or in part without the written consent of the author; and to make proper written acknowledgement for any assistance which I have obtained from it."

Beyond this, I do not wish to place any restriction on access to this thesis.

....

Acknowledgements

I would like to thank my supervisor Prof. Ian Whittingham for his endless patience, encouragement, support and also for introducing me to the field of $f(R)$ gravity. I would also like to thank:

Bronson Philippa, the numerical guru, for helpful advice.

David Breitkreutz *et al.* for making their incredibly useful LyX template freely available (https://github.com/davidjb/JCU-Thesis-LyX-Layout), and the many LyX developers for making academic typesetting so much easier.

All my friends and family. Jake and Elwood, for always making me laugh.

Last but not least, my wife Amy, for her love, patience, and encouragement. She also gave generously of her time to proofread this thesis.

Abstract

$f(R)$ theories are the simplest generalisations of General Relativity, Einstein's theory of gravity. $f(R)$ theories, and modified gravity theories more broadly, have been invoked to explain the accelerated expansion of the universe. A number of "viable" models have been proposed which satisfy cosmological tests and get around present day laboratory and solar system constraints by invoking the chameleon mechanism. It is important to determine whether such alternative models can be distinguished by precision experiments at the laboratory scale. This thesis focuses on recently proposed $f(R)$ models in the context of the upcoming neutron quantum bouncer experiment GRANIT [1], which has the potential to directly observe violations of Einstein gravity. This experiment works by precisely measuring the energy levels of ultra-cold neutrons trapped in the Earth's gravitational field above a mirror. Neutrons in these states have energies of the order of 10^{-12} eV (peV) and wavefunctions with spatial extents of ~ 10 μm. The size of the neutron wavefunctions gives gravitational spectroscopy sensitivity to any change of the Newtonian potential above the mirror surface on a scale of tens of microns. These experiments have a unique opportunity to study gravity and quantum mechanics in an unprecedented regime. GRANIT claims an energy sensitivity of 0.01 peV with an improvement of one or two orders of magnitude expected over the next several years. The theoretical limit to the sensitivity is 10^{-7} peV. Previous work by Brax and Pignol [2] has shown that scalar-tensor theories, which are closely related to $f(R)$ theories, can give rise to detectable shifts in the energy levels from their Newtonian values.

Here the energy levels shifts are examined for three viable $f(R)$ models: the exponential gravity model of Linder [3], the model of Hu and Sawicki [4] and the "new" exponential gravity model of Xu and Chen [5]. It is found that exponential gravity predicts energy level shifts of the order $\exp\left(-10^{19}\right) m_N c^2$, where m_N is the neutron mass. This is unobservable in any experiment lasting less than the age of the universe. The Hu-Sawicki model predicts much larger shifts which depend on the model parameters n and c_2, where $n, c_2 > 0$. It is found that the shifts are below the theoretical sensitivity limit for $n \geq \frac{1}{2}$, with shifts at $n = \frac{1}{2}$ of the order of 10^{-19} peV. It is unlikely, though not yet ruled out, that $n \ll 1$ models could be observed at neutron bouncer experiments operating under extreme conditions. The computation of the shifts for $n \ll 1$ models is hampered by convergence issues. This may be immaterial, however, because Hu-Sawicki models with $n < 2$ are not compatible with cosmological inflation in the early universe. The Xu-Chen model is shown to be indistinguishable from an $n > 2$ Hu-Sawicki model at laboratory scales, hence it is unobservable at a neutron bouncer experiment.

The reason for the difference between these results with those of Brax and Pignol is shown to be due to the special form of the scalar potential and matter coupling, which are free in scalar-tensor theory and can be chosen to give a large effect, but are constrained in $f(R)$ gravity. Because of these special features the neutron bouncer experiment can distinguish between $f(R)$ and non-$f(R)$ modified gravity, but not between the $f(R)$ models examined in this thesis.

Contents

List of Tables

List of Figures

Chapter 1

Introduction

1.1 Challenges of cosmology

Scientific cosmology is in trouble. The 2011 Nobel Prize for physics was awarded to Perlmutter, Schmidt and Riess for the surprising discovery that the expansion of the universe is accelerating rather than slowing down [10]. The current standard model of cosmology, the concordance or ΛCDM[1] model, successfully accounts for the observed acceleration of the universe. However, to achieve this ΛCDM requires a composition of the universe that Sean Carroll[2] describes as preposterous [11]. This chapter explains what would lead a cosmologist to describe such an empirically successful model this way. Several of the challenges facing modern cosmology are briefly reviewed as motivation for the topic of this thesis: $f(R)$ gravity.

The composition of the universe according to ΛCDM is shown in Figure 1.1.1. Roughly 73% of the energy density of the universe is in the form of dark energy: a very uniform energy density of unknown origin that does not dilute with the cosmic expansion [7]. The simplest model of dark energy is Einstein's cosmological constant Λ. Λ is the coefficient of a term that appears in the field equation of General Relativity (GR), equation (2.1.23). It enters the theory as a tunable parameter and, despite the empirical success of ΛCDM, there is no theoretical reason whatsoever to expect Λ to take the value it does [12, 13].

Roughly 23% of the energy density of the universe is cold dark matter of unknown composition. The leading hypothesis is that it consists of massive particles which do not interact with electromagnetism or the strong nuclear force. These weakly interacting massive particles (WIMPs) form the bulk of the matter density of the universe. Ordinary (baryonic) matter makes up the remaining four percent of the energy density, apart from a minuscule fraction (5 parts in 10^5) of radiation [7].

This incredible picture is the result of a theory founded on two assumptions [6]:

1. General relativity is the correct theory of gravity at cosmological scales.
2. We do not occupy a special position in the universe. The universe is homogeneous on large scales.

These assumptions together with the observation that the universe is isotropic to one part in 10^5 determine the Friedmann equation for the evolution of the universe [6, 14, 15] (in units where

[1] ΛCDM stands for cosmological constant Λ and Cold Dark Matter.
[2] The California Institute of Technology

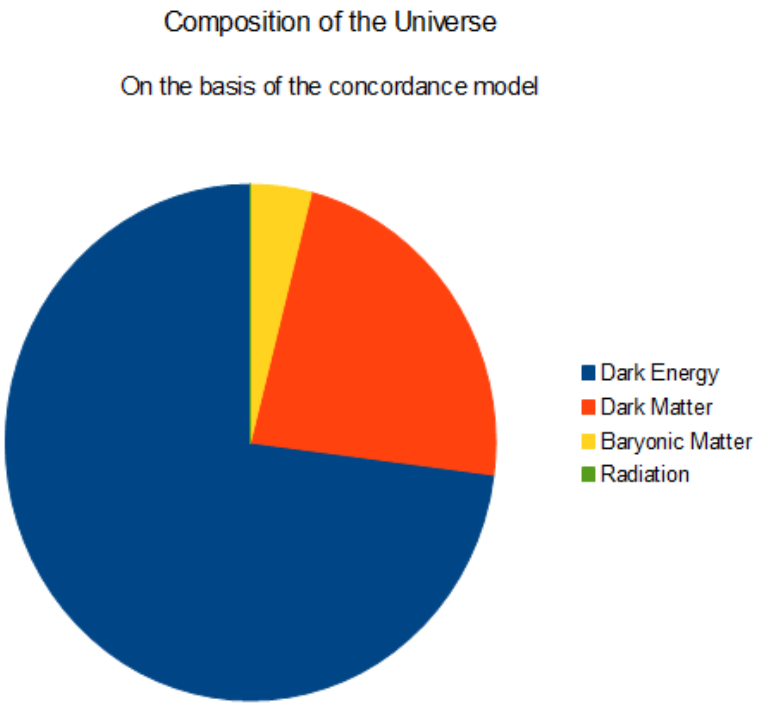

Figure 1.1.1: Composition of the universe on the basis of the concordance model, ΛCDM [6]. The radiation component is a thin (single pixel on the screen version) wedge at twelve o'clock.

$c = 1$):

$$\left(\frac{\dot{a}}{a}\right)^2 = \frac{8\pi G}{3}\rho - \frac{k}{a^2} + \frac{\Lambda}{3} \tag{1.1.1}$$

and the law of conservation of energy

$$\dot{\rho} = -3\frac{\dot{a}}{a}\left(\rho + p\right). \tag{1.1.2}$$

In these equations a is the cosmic scale factor, which measures the size of the universe (more accurately, the average separation of galaxies which are not bound together gravitationally). a is conventionally normalised so that at the present day $a\,(t = 0) \equiv a_0 = 1$. The combination $\dot{a}/a$ is often denoted H, the Hubble parameter. The observed value of the Hubble parameter in the recent universe is [8] $H_0 = 70.4 \pm 2.5$ km/s/Mpc where 1 Mpc = 1 megaparsec $\approx 3\times10^{22}$ m. In units where $\hbar = c = 1$, H can be written as an energy and the present day value is $H_0 = 1.50 \times 10^{-42}$ GeV. Frequently the Hubble parameter is written as $H_0 = h \times 100$ km/s/Mpc for convenience. The remaining quantities in equations (1.1.1) and (1.1.2) are: Newton's gravitational constant G, the energy density ρ, and the pressure p. k is the spatial curvature which determines the spatial geometry of the universe according to:

$$k = \begin{cases} +1 & \text{spherical} \\ 0 & \text{flat} \\ -1 & \text{hyperbolic} \end{cases}$$

All of the evidence is consistent with a flat universe, $k = 0$, and the cosmological parameters are often fit to data assuming $k = 0$. The error bars generally widen slightly if this assumption

is relaxed. Λ is the cosmological constant, but any form of energy density associated with a negative pressure (i.e. tension) $p = -\rho$ does not dilute with the cosmic expansion (1.1.2) and is indistinguishable from Λ (1.1.1). Thus the cosmological constant can be viewed as an effective dark energy density $\rho_\Lambda \equiv \Lambda/8\pi G$.

Every component of the universe for which $p > -\rho$ dilutes with the cosmic expansion. Eventually Λ dominates on the right hand side of (1.1.1). The expanding solution in this regime is

$$a = a_0 \mathrm{e}^{\sqrt{\frac{\Lambda}{3}}t},$$

which is an accelerating expansion of the kind seen by Perlmutter, Schmidt and Riess. The model universe where this exponential expansion is exact is called de Sitter space. In order for late time acceleration to be "natural" a cosmological model is required to have an attractive de Sitter point.

The Friedmann equation and density parameters are commonly recast in terms of dimensionless variables. The natural scale for cosmological densities is the critical density defined by

$$\rho_{\mathrm{crit}} \equiv \frac{3H_0^2}{8\pi G}. \tag{1.1.3}$$

This is the density which gives a flat universe when $\Lambda = 0$. The dimensionless density parameters are

$$\begin{aligned} \Omega_m = \frac{\rho_m}{\rho_{\mathrm{crit}}},\ \Omega_{DM} = \frac{\rho_{DM}}{\rho_{\mathrm{crit}}}, \\ \Omega_r = \frac{\rho_r}{\rho_{\mathrm{crit}}},\ \Omega_\Lambda = \frac{\Lambda}{3H_0^2}, \\ \Omega_k = -\frac{k}{a_0^2 H_0^2}, \end{aligned}$$

where ρ_m, ρ_{DM}, ρ_r are the baryonic matter, dark matter and radiation densities respectively. $\Omega_M = \Omega_m + \Omega_{DM}$ is the total matter density parameter. In terms of these variables the Friedmann equation is

$$\Omega_M + \Omega_r + \Omega_\Lambda + \Omega_k = 1.$$

The fit of these parameters to observation can be seen in Figure 1.1.2. The best fit values for the cosmological parameters vary somewhat depending on what data sets are used, but all fall within compatible ranges [8]:

$$\begin{aligned} \Omega_m &= 0.0458 \pm 0.0016 \\ \Omega_{DM} &= 0.229 \pm 0.015 \\ \Omega_\Lambda &= 0.725 \pm 0.016. \end{aligned}$$

The data are consistent with a flat universe with a big bang at $t = -13.77 \pm 0.13$ Gyr [8].

Frequently a barotropic equation of state is assumed for the cosmological components:

$$p = w\rho,$$

where the equation of state parameter w is[3]

$$w = \begin{cases} 0 & \text{nonrelativistic matter} \\ \frac{1}{3} & \text{radiation} \\ -1 & \text{cosmological constant} \end{cases}$$

Using the equation of continuity (1.1.2) each component evolves as $\rho = \rho_0 a^{-3(1+w)}$. If dark energy is the result of some dynamical mechanism rather than a cosmological constant it is possible for w to vary with time as the universe expands. Any such variation constitutes a prediction of the dark energy theory which can, in principle, be tested against observational data. The current constraint on variation of w for dark energy is shown in Figure 1.1.3.

It can be seen that ΛCDM fits the data well. Despite this it is worth entertaining doubt about the model for several reasons:

1. It seems mysterious that 95% of the energy density of the universe cannot be observed directly. The current state of dark matter direct detection is confused: the DAMA [16] and CoGeNT [17] collaborations report statistically significant detections but are contradicted by null results from CDMS-II [18] and XENON100 [19]. To date there have been no convincing reports of observations of physics responsible for dark energy apart from the standard cosmological data.

2. It is known that GR is not the ultimate theory of gravity (if there even is such a thing). Although GR is founded on deep principles and is very successful empirically [20], it is not unique as a classical theory of gravity. Further, GR is not compatible with quantum mechanics. As a quantum field theory GR is nonrenormalizable, meaning that it has an infinite number of free parameters and can no longer be predictive. The standard effective field theory picture views GR as a zeroth order theory subject to quantum corrections which are suppressed by powers of the Planck scale $E/M_{\rm pl}$, where $M_{\rm pl} \equiv (8\pi G)^{-1/2} \approx 10^{18}$ GeV is the scale at which gravity becomes strong and quantum gravity must be taken into account [21]. If this were the case then quantum modifications to general relativity would be suppressed by $H_0/M_{\rm pl} \sim 10^{-60}$ at the Hubble scale. However, this expectation is violated in concrete models such as brane-world scenarios where the 4-dimensional universe is embedded in a higher dimensional bulk spacetime. Such theories involve large distance corrections to GR and explain cosmic acceleration by an effective weakening of gravity at the Hubble scale [22].

3. ΛCDM suffers three classic problems involving flatness, horizons and monopoles [6]:

   (a) The flatness problem is that if Ω_k is small at the present day it must have been much smaller in the early universe. This requires that the universe be fine tuned for flatness. Indeed, imagine a time reversed cosmological scenario where the universe is collapsing[4]. Due to the attractive nature of gravity it is far more likely for the matter in the universe to clump into a large number of black holes than it is for it to spread out in an extremely smooth distribution. This shows that the universe began in a special, rather than generic, state.

   (b) The horizon problem is that there is not enough time in the early stage of ΛCDM expansion for regions on opposite sides of the observable universe to come into thermal equilibrium with each other. This contradicts the observed isotropy of the universe.

[3] Recall that units are used where $c = 1$. Restoring c: $w = p/\rho c^2 \ll 1$ for non-relativistic matter.
[4] General relativity is time reversal invariant.

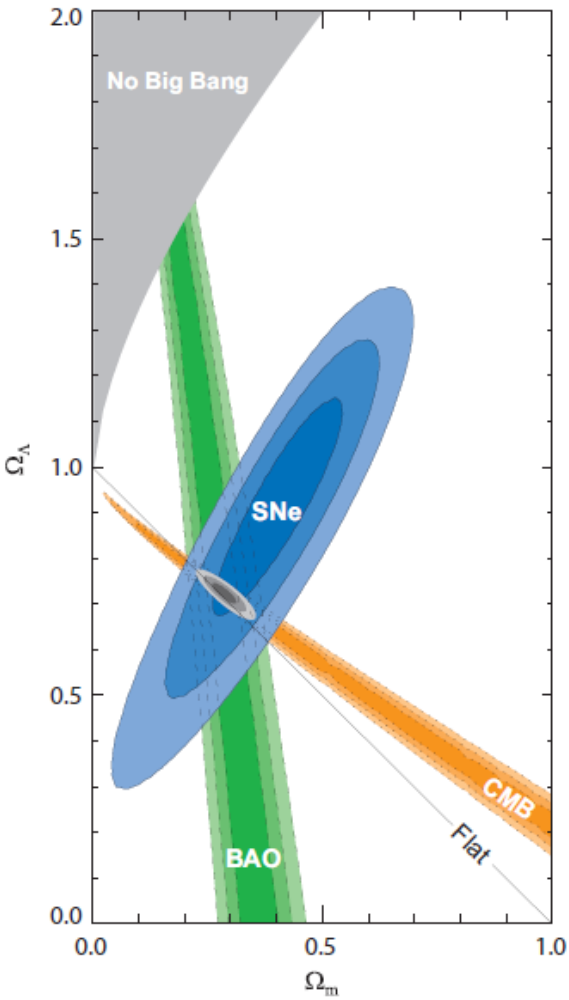

Figure 1.1.2: Fit of ΛCDM to supernova (SNe), cosmic microwave background (CMB) and baryon acoustic oscillation (BAO) data showing concordance for a flat universe with $\Omega_M \sim 0.25$ and $\Omega_\Lambda \sim 0.75$. Contours are 1, 2 and 3σ confidence intervals. Reproduction of Figure 21.1 of [7].

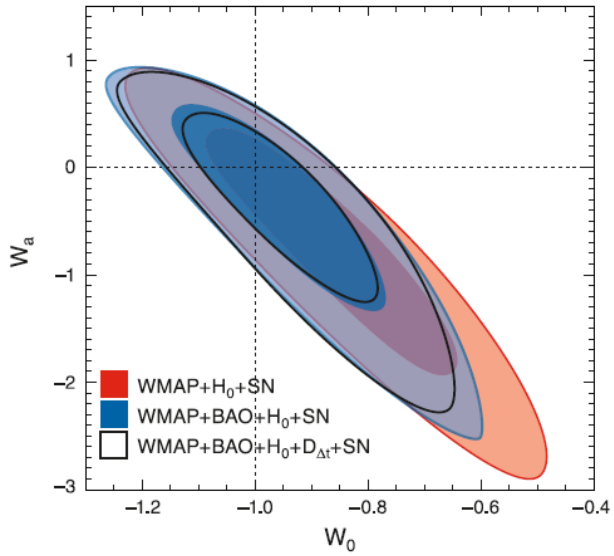

Figure 1.1.3: Constraints on a model with linear variation of w for the dark energy component according to $w = w_0 + w_a\,(1-a)$. The intersection of the dashed lines denotes the ΛCDM model ($w_0 = -1,\ w_a = 0$). The contours are 68% and 95% confidence intervals. Reproduction of Figure 13 of [8].

(c) The monopole problem is that grand unified theories (GUTs) of particle physics predict the existence of magnetic monopoles with a number density that can be computed for a given expansion history. The predicted value is in gross violation of the observational bounds on monopoles.

These problems are alleviated by postulating a period of exponential inflation in the early universe dominated by a slowly rolling scalar field [6, 23]. The potential for such a field mimics a cosmological constant. Inflationary theory correctly predicted the nearly scale invariant spectrum of density fluctuations in the early universe, but current observations remain limited in their ability to constrain inflation models. Despite the apparent success of inflation it faces a number of difficulties of its own and it is worth entertaining alternatives such as cyclic universe models [24].

4. The cosmological constant problem is that the observed value of Λ can not be computed from any known fundamental theory [12, 13]. In fact the scale of dark energy $\rho_\Lambda \approx \left(2.4 \times 10^{-3}\ \text{eV}\right)^4$ is very small compared to typical scales of particle physics such as the electro-weak symmetry breaking scale $M_{\text{ew}} \sim 10^{12}$ eV. This renders the cosmological constant extremely sensitive to corrections (both classical and quantum) from particle physics. Obtaining a small value of the cosmological constant without resorting to a delicate fine tuning is a major challenge of theoretical physics today.

These concerns present challenges to theoretical cosmologists and are goalposts against which progress in the field is measured.

Finally, it is important to note that the third and fourth of these problems are "naturalness" problems in that they require delicately chosen initial conditions to reproduce the universe we observe. Since a theory of initial conditions for the universe is lacking this is not a desirable state of affairs, but calling these "problems" is a matter of theoretical prejudice. As far as the experimental situation is concerned, it could be that nature is genuinely fine tuned and concerns about naturalness are misguided. These issues are beyond the scope of this thesis.

1.2 Attempts to address the challenges

A number of theoretical concerns regarding ΛCDM were brought up in the previous section. Attempts to address them have been many and varied. Recent reviews addressing the question of dark energy alone are of the order of one hundred pages [25, 26]. No attempt is made to thoroughly review the current state of dark energy theory here, but two important hypotheses to the nature of dark energy are relevant to this thesis: quintessence and modified gravity. This thesis focuses on a particular class of modified gravity models called $f(R)$ which relax the assumption that GR is the correct theory of gravity. It is the chameleon mechanism [27–30], discovered in the context of quintessence, that allows the construction of viable $f(R)$ models which evade stringent solar system and laboratory constraints on modified gravity [3–5, 31–33].

Quintessence models are inspired by the theory of inflation. The exponential expansion provided by inflation in the early universe is repeated at late times at a much lower energy scale to explain the exponential expansion of the universe at the present day. Quintessence models introduce a scalar field ϕ which has a potential energy density $V(\phi)$. The scalar field is minimally coupled to gravity as described by GR (meaning simply that a lump of excited scalar field will fall in the

same time as a feather, or a bowling ball), and does not couple to matter at all except through gravity. The evolution of the scalar field is governed by

$$\ddot{\phi} + 3H\dot{\phi} + \frac{\mathrm{d}V}{\mathrm{d}\phi} = 0,$$

and the equation of state is

$$w = \frac{p}{\rho} = \frac{\frac{1}{2}\dot{\phi}^2 - V(\phi)}{\frac{1}{2}\dot{\phi}^2 + V(\phi)}.$$

If the scalar field is "slowly rolling," i.e. $\dot{\phi}^2 \ll V(\phi)$, then $w \approx -1$ and the scalar potential mimics a vacuum energy density $\rho_\Lambda = V(\phi)$. Since the mass of a scalar field is given by [34]

$$\frac{\mathrm{d}V}{\mathrm{d}\phi} = m_\phi^2 \phi + \mathcal{O}\left(\phi^2\right),$$

then, for the scalar to be slowly rolling over the lifetime of the universe, it is necessary that

$$H^2\phi \sim m_\phi^2 \phi.$$

This implies a very small mass $m_\phi \sim H \sim 10^{-33}$ eV for the scalar field.

Quintessence suffers from two fine tuning problems in addition to the usual one (the smallness of ρ_Λ). It is important to note that these fine tuning problems are "naturalness" problems but they do not affect the mathematical consistency of the theory. First, scalars tend to be heavy unless a symmetry protects their mass from enormous quantum corrections. Second, it is unnatural for a scalar field to not interact with matter at all. Indeed, since the interaction potential energy of two bodies with couplings g_1 and g_2 to the scalar field is [34]

$$U(r) = -\frac{g_1 g_2}{4\pi r}\mathrm{e}^{-m_\phi r},$$

the scalar field will generate long range forces which would have been detected by now unless a) the couplings are unnaturally small or b) the interaction is screened in dense environments like the solar system where the most stringent constraints on new forces obtain.

There are three known screening mechanisms. The Symmetron mechanism causes the couplings $g_{1,2}$ to vanish in dense environments [35]. The Vainshtein screening mechanism makes the effective mass of the scalar environment dependent through derivative self interactions. This is realised in so called Galilean models [36]. Finally, and most importantly for this thesis, the chameleon mechanism causes the scalar mass to become environment dependent through an environmental dependence of the effective scalar potential $V(\phi)$ [29]. The chameleon mechanism is the only type of screening available to $f(R)$ theories. Further, the environmental dependence of the scalar potential depends on a particular type of interaction (universal, conformal) with all types of matter. This special interaction must be put into quintessence models by hand (this is how it was first discovered [28]), but it comes out of $f(R)$ automatically. This makes $f(R)$ an attractive candidate for studying the phenomenology of modified gravity theories.

The phenomenology of the original chameleon theory (and several slight variations of it) is rich and well developed [2, 28, 37–64], but the results from this literature do not directly apply to $f(R)$ gravity for several reasons. First, the scalar-matter interactions of the original chameleon theory are characterised by a dimensionless coupling constant β which is a free parameter. In $f(R)$ gravity $\beta = 1/\sqrt{6}$ is fixed. Second, the form of the scalar potential used in the original chameleon theory is not the same as that coming from $f(R)$. Finally, the original chameleon theory is formulated

in the Einstein frame whereas $f(R)$ theory is formulated in the Jordan frame. These terms are explained in the next chapter.

1.3 Scope of the present work

This thesis focuses on the energy spectrum of ultra-cold neutrons bound in the gravitational field of the Earth. The neutrons are kept from sinking through the floor of the experiment by a specially designed mirror and from flying out the top by the gravitational potential of the Earth. Since the system is bound the quantum states form a discrete spectrum. The problem with the classical gravitational potential $V = mgz$ is textbook [65] and can be solved exactly (the wavefunctions are Airy functions). Due to the weakness of gravity the lowest lying quantum states have remarkable properties [1, 66]: the typical extent of the wavefunction is of the order of tens of microns and the energies are of the order of 10^{-12} eV. Remarkably, the GRANIT project, at Institut Laue–Langevin (ILL) in Grenoble, has demonstrated the existence of these states and upgrades currently under way will allow the direct measurement of the energy splittings between the first few states by resonance spectroscopy [1, 66, 67] within the next several years! A diagram of the GRANIT spectrometer is shown in Figure 1.3.1 and the arrangement of the experiment is shown in Figure 1.3.2.

The macroscopic size of the neutron wavefunctions gives gravitational spectroscopy sensitivity to any change of the Newtonian potential above the mirror surface over a scale of tens of microns. These experiments have a unique opportunity to study gravity and quantum mechanics in an unprecedented regime. Previous work on the original chameleon theory [2] has shown that GRANIT has the potential to discover chameleons. This thesis investigates whether recently proposed viable $f(R)$ models predict modifications of the gravitational potential that could be discovered by GRANIT or a similar experiment involving gravitational bound states of ultra-cold neutrons.

This thesis is organised into four chapters and three appendices. Chapter 2 develops the formalism required to compute the predictions of $f(R)$ gravity for a neutron bouncer experiment. Included in Chapter 2 is a brief review of GR, enough to set the scene and establish notations. This introductory material is standard. A fairly standard review of $f(R)$ gravity is given including the equivalence to scalar-tensor theory, the chameleon mechanism and the so called "viable" $f(R)$ models. The calculation of the scalar potential $V(\phi)$ for these models is, to my knowledge, novel work. A calculation of the scalar field profile above a mirror, performed approximately in [2] for the original chameleon theory, is extended to the case of $f(R)$ gravity. Then the equation of motion of a neutron bouncing above a mirror is derived. Two calculations which would naturally be placed there are tedious and unenlightening, so are deferred to the Appendices A and B. They are included because they concern a topic, the Dirac equation in curved spacetime, not well known outside a specialist community. It is reassuring to see that the full relativistic theory reduces to an acceptable non-relativistic limit even in the case of $f(R)$ gravity. Chapter 3 is devoted to solving the system of equations developed in Chapter 2. It is shown that a quick estimate is sufficient to show that the energy level shifts predicted by most viable models are undetectable at GRANIT, even with significant improvements of the sensitivity. The energy level shifts are computed in first order perturbation theory for an "optimistic" model and shown to be twelve orders of magnitude smaller than the theoretical limit of the experimental sensitivity. Chapter 4 discusses the significance of these results and the potential for future work. Finally, Appendix C is a Mathematica script to compute the scalar potential $V(\phi)$ for one of the viable $f(R)$ models.

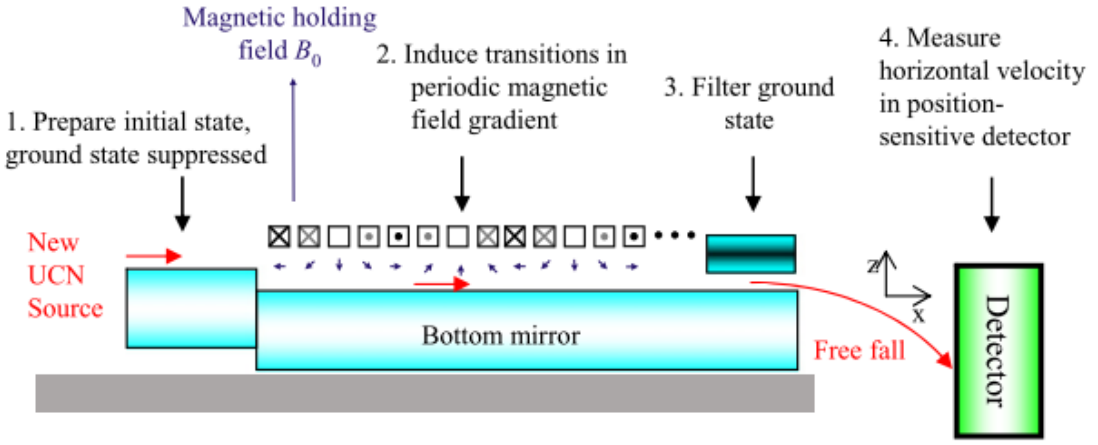

Figure 1.3.1: Schematic of GRANIT in flow through spectroscopy mode. Neutrons coming in from the left are prepared in the third gravitational quantum state by a drop off a small ledge. Following this an oscillating magnetic field induces transitions to the ground state if the frequency is on resonance for the $3 \rightarrow 1$ transition. A neutron absorbing filter then selects only those neutrons in the ground state. The frequency of the oscillating magnetic field depends on the horizontal velocity of the neutron, so only neutrons with a particular velocity are on resonance hence driven to the ground state. This velocity is measured by measuring the free fall drop of the neutrons at the end of the experiment. The velocity determines the frequency, hence the energy splitting $\Delta E_{3\rightarrow 1}$. Reproduction of Figure 11 of [1].

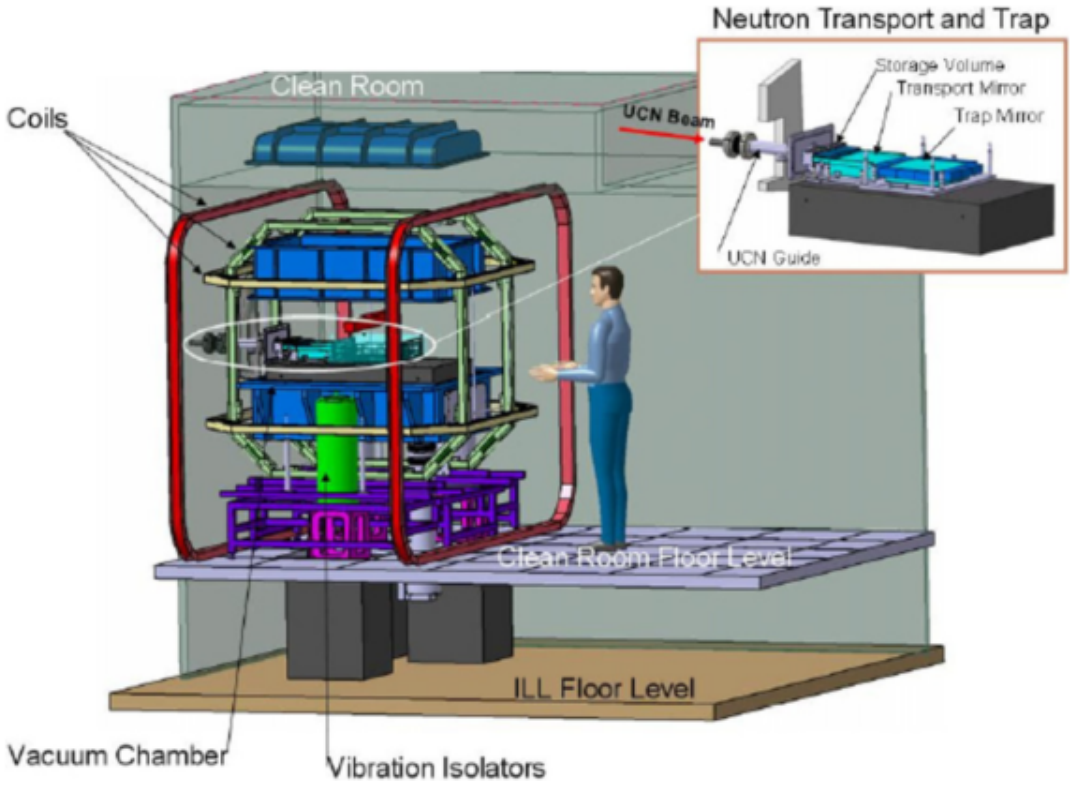

Figure 1.3.2: Schematic of GRANIT in neutron trapping mode showing the clean room arrangement, vibration isolators, vacuum chamber and Helmholtz coils for cancelling stray magnetic fields. Inset is a close up of the neutron beam-line and mirror assembly. Reproduction of Figure 5 of [1].

Chapter 2

Formulation of the problem

This chapter develops the analytical formulation of the neutron quantum bouncer experiment in the context of $f(R)$ gravity. It is necessary to state the basic principles of $f(R)$ theory and derive the equations governing the experiment. It is convenient to transform the $f(R)$ equations in the "Jordan frame" to an equivalent scalar-tensor theory in the "Einstein frame" (the meaning of these terms will become clear). This reduces the system to a non-linear Poisson type equation for the scalar field and a Schrödinger equation for the neutron. Then the geometry of the real quantum bouncer experiment GRANIT is idealised to a one dimensional model. This greatly simplifies the problem, while retaining all of the conceptual features of the full problem. In this form the problem is amenable to numerical computation.

2.1 Introduction to $f(R)$ Gravity

2.1.1 Geometric Framework of Spacetime

$f(R)$ gravity is a geometrical theory of spacetime which shares a common formulation with General Relativity. This section introduces the relevant concepts from GR and establishes the notation used here. No effort is made to comprehensively review GR as that would require at least 1200 pages [14], only a few of which are needed here. Everything in this section is standard material and can be found, up to notational differences, in any relativity text[1].

Key to GR, and the vast majority of modified gravity theories following it, is the notion of *spacetime*: the three dimensions of space and the single dimension of time unified into a single mathematical structure (a *manifold*). Points, or *events*, in spacetime can be labelled by arbitrary coordinate functions, which are denoted $\{x^\mu\}$, $\mu = 0, 1, 2, 3$. Tensors are objects that have a well defined geometrical meaning independent of any particular coordinate choice. They are classified according to rank, and the set of all tensors of a given rank form a linear vector space: the sum of two tensors of compatible rank is again a tensor, and a scalar multiple of a tensor is a tensor.

A coordinate system $\{x^\mu\}$ defines a set of basis vectors labelled $\left\{\partial_\mu \equiv \frac{\partial}{\partial x^\mu}\right\}$. Heuristically one can think of ∂_μ pointing in the direction of increasing x^μ. An arbitrary vector can be expanded in this basis $V = V^\mu \partial_\mu$ (repeated indices are summed over all possible values unless noted otherwise) and frequently the vector is identified with its components V^μ. Dual vectors, or one-forms, are tensors defined with a lower index: W_μ. These are dual to vectors in the sense that each one-form defines a linear scalar valued function on vectors: $W : V \mapsto W_\mu V^\mu$. A tensor with p upper indices and q lower indices is said to be a rank (p, q) tensor.

[1] A helpful list of relativity texts is found at the beginning of [15].

The basic geometrical quantity is the *metric tensor* which describes the length of curves in spacetime. The length of an infinitesimal displacement $\mathrm{d}x^\mu$ is determined by the metric $g_{\mu\nu}$:

$$\mathrm{d}s^2 = g_{\mu\nu}\mathrm{d}x^\mu \mathrm{d}x^\nu. \tag{2.1.1}$$

In the special case of flat spacetime, which corresponds to special relativity, coordinates can be found such that $g_{\mu\nu} = \eta_{\mu\nu} \equiv \mathrm{diag}\,(-1,1,1,1)$ and $\mathrm{d}s^2 = -\mathrm{d}t^2 + \mathrm{d}x^2 + \mathrm{d}y^2 + \mathrm{d}z^2$. In a curved spacetime it is not possible to find coordinates such that $g_{\mu\nu} = \eta_{\mu\nu}$ throughout a finite region, but it is always possible to find coordinates around an arbitrary point x^μ_P such that the deviations are of second order: $g_{\mu\nu}\left(\{x^\rho\}\right) = \eta_{\mu\nu} + \mathcal{O}\left[\left(x^\rho - x^\rho_P\right)^2\right]$. These second order corrections characterise the curvature of the spacetime. Also useful is the metric determinant $g \equiv \det\left(g_{\mu\nu}\right) < 0$ which gives the invariant volume element of spacetime: $\mathrm{d}^4x\sqrt{-g}$.

Indices can be raised and lowered using $g_{\mu\nu}$ and the inverse metric $g^{\mu\nu}$, defined by

$$g^{\mu\nu}g_{\nu\lambda} = \delta^\mu_\lambda \equiv \begin{cases} 1 & \mu = \lambda \\ 0 & \mu \neq \lambda \end{cases}$$

For example

$$T^\mu{}_\nu = g^{\mu\lambda}T_{\lambda\nu} = g_{\nu\rho}T^{\mu\rho}.$$

The inner product of two vectors is defined by $V \cdot W \equiv g_{\mu\nu}V^\mu W^\nu$. If $V^2 \equiv V \cdot V > 0, < 0, = 0$ it is referred to as spacelike, timelike or null respectively. The motion of a particle is described by a "world-line" in spacetime $x^\mu(\tau)$. If the world-line parameter obeys $\mathrm{d}\tau = \sqrt{-g_{\mu\nu}\mathrm{d}x^\mu\mathrm{d}x^\nu}$ it is the *proper time* measured by a clock moving along with the particle. The vector $\mathrm{d}x^\mu/\mathrm{d}\tau$ is the *four-velocity* of the particle.

When dealing with spin-$\frac{1}{2}$ particles such as neutrons it is useful to introduce a set of orthonormal basis vector fields or frame fields which are not necessarily related to the coordinate vector fields. These basis vectors are called a *tetrad* or *vierbein* (vier-bein = German "four legs"). The tetrad fields can be written e^μ_a where μ is the component index and a labels which field one is talking about. Orthonormality means

$$g_{\mu\nu}e^\mu_a e^\nu_b = \eta_{ab}. \tag{2.1.2}$$

A simple nontrivial example of frame fields in two dimensions are the unit vectors $\hat{\vec{r}}$, $\hat{\vec{\theta}}$ of ordinary polar coordinates. Greek indices on the tetrad are raised and lowered with the metric as usual, while latin indices are raised and lowered with η_{ab} and η^{ab}. This can be used to show that $g_{\mu\nu} = \eta_{ab}e^a_\mu e^b_\nu$, so it is sometimes said that the tetrad is the square root of the metric. A vector can be expanded in the tetrad basis as well as a coordinate basis: $V = V^a\left(e^\mu_a\partial_\mu\right) = V^\mu\partial_\mu$ which gives the connection between components in different frames: $V^\mu = V^a e^\mu_a$ and $V^a = e^a_\mu V^\mu$.

The tetrad is far from unique: one can perform independent Lorentz transformations on the latin indices at every point in spacetime $e^\mu_a \to \Lambda_a{}^b\left(\{x^\nu\}\right)e^\mu_b$ and produce another valid tetrad. This is *local* Lorentz invariance. Local Lorentz invariance can be thought of as a gauge symmetry in complete analogy with the gauge transformations of the electromagnetic potentials $\vec{A} \to \vec{A} + \nabla f$, $\phi \to \phi - \partial f/\partial t$. These are transformations that leave physical quantities such as the electric and magnetic fields $\vec{E}$, $\vec{B}$, or metric $g_{\mu\nu}$ invariant. In fact, this analogy between gravity and electromagnetism can be exploited completely to formulate gravity as a gauge theory [34]. This formulation is used in attempts to quantise gravity such as [68, 69] but this falls far beyond the scope of this thesis.

A point of notation: greek indices correspond to spacetime coordinates and run over 0, 1, 2, 3

or $t,\ x,\ y,\ z$. Latin indices from the beginning of the alphabet a, b, c, etc. correspond to frame fields and run over $\hat{t},\ \hat{x},\ \hat{y},\ \hat{z}$, the $\hat{}$ distinguishing the two types of index. Finally, in some formulas it is useful to separate the timelike index from the spatial ones. In these formulas a latin index from the middle of the alphabet i, j, k, etc. runs over the spatial indices $\hat{x},\ \hat{y},\ \hat{z}$.

Since one is free to perform transformations independently at different points the difference $V^{\mu}(x+\mathrm{d}x) - V^{\mu}(x)$ is not a tensor. In order to define tensorial derivatives of vector fields one needs a rule, or *connection*, to absorb the extra position dependence of the transformation law. The most general form compatible with linearity and the product rule is

$$\nabla_{\mu} V^{\nu} = \partial_{\mu} V^{\nu} + \Gamma^{\nu}_{\mu\lambda} V^{\lambda}, \tag{2.1.3}$$

$$\nabla_{\mu} V^{a} = \partial_{\mu} V^{a} + \omega^{a}_{\mu b} V^{b}. \tag{2.1.4}$$

Technically ∇_{μ} is the connection, but $\Gamma^{\nu}_{\mu\lambda}$ is often called the connection. $\omega^{a}_{\mu b}$ is called the *spin connection*. If $\Gamma^{\nu}_{\mu\lambda} = \Gamma^{\nu}_{\lambda\mu}$ the connection is called *torsion free*. All the connections in this thesis are torsion free. Notice that a connection is not a tensor, but the difference of two connections is a tensor. There is a canonical choice of connection, called the *Christoffel* connection, which is *metric compatible*, meaning:

$$\nabla_{\mu} g_{\nu\lambda} \equiv \partial_{\mu} g_{\nu\lambda} - \Gamma^{\alpha}_{\mu\nu} g_{\alpha\lambda} - \Gamma^{\alpha}_{\mu\lambda} g_{\nu\alpha} = 0.$$

This condition can be solved explicitly to give:

$$\Gamma^{\alpha}_{\mu\nu} = \frac{1}{2} g^{\alpha\beta} \left(\partial_{\mu} g_{\nu\beta} + \partial_{\nu} g_{\mu\beta} - \partial_{\beta} g_{\mu\nu} \right). \tag{2.1.5}$$

Metric compatibility also determines the spin connection in terms of the Christoffel connection and tetrad:

$$\omega^{a}_{\mu b} = e^{a}_{\lambda} \Gamma^{\lambda}_{\mu\nu} e^{\nu}_{b} - \left(\partial_{\mu} e^{a}_{\nu} \right) e^{\nu}_{b}. \tag{2.1.6}$$

Curvature represents the failure of derivatives to commute. Heuristically: if one parallel transports a vector via two different paths to the same end point the resulting vectors will not in general be parallel to each other at the destination. The Riemann tensor captures this effect[2]:

$$R^{\mu}{}_{\nu\alpha\beta} = \partial_{\alpha} \Gamma^{\mu}_{\nu\beta} - \partial_{\beta} \Gamma^{\mu}_{\nu\alpha} + \Gamma^{\mu}_{\sigma\alpha} \Gamma^{\sigma}_{\nu\beta} - \Gamma^{\mu}_{\sigma\beta} \Gamma^{\sigma}_{\nu\alpha}. \tag{2.1.7}$$

The Ricci tensor and scalar are given by:

$$R_{\mu\nu} \equiv R^{\alpha}_{\mu\alpha\nu},\ R \equiv g^{\mu\nu} R_{\mu\nu}. \tag{2.1.8}$$

The Einstein tensor is

$$G^{\mu\nu} \equiv R^{\mu\nu} - \frac{1}{2} g^{\mu\nu} R. \tag{2.1.9}$$

Importantly, the Einstein tensor is conserved

$$\nabla_{\mu} G^{\mu\nu} = 0,$$

as an automatic consequence of a differential identity obeyed by the Riemann tensor called the Bianchi identity:

$$\nabla_{\lambda} R^{\mu}{}_{\nu\alpha\beta} + \nabla_{\beta} R^{\mu}{}_{\nu\lambda\alpha} + \nabla_{\alpha} R^{\mu}{}_{\nu\beta\lambda} = 0.$$

[2] Note that there are a variety of sign conventions in the literature. The sign here matches [14]. The same remark applies to the Ricci tensor and scalar.

The importance of this identity is that it is entirely geometric in character [14] (i.e., it does not depend in any way on the nature of the matter and radiation appearing in the theory) and allows one to construct theories that automatically conserve energy and momentum.

For later convenience the variation of the Ricci scalar δR with respect to variations of the metric $\delta g^{\mu\nu}$ is quoted here:

$$\delta R = R_{\mu\nu}\delta g^{\mu\nu} + \delta R_{\mu\nu} g^{\mu\nu} = \left(R_{\mu\nu} + g_{\mu\nu}\Box - \nabla_\mu \nabla_\nu\right)\delta g^{\mu\nu} \tag{2.1.10}$$

where $\Box \equiv g^{\mu\nu}\nabla_\mu\nabla_\nu$ is the covariant d'Alambertian (the spacetime generalization of the Laplacian). The variation of the metric determinant is also useful:

$$\delta\sqrt{-g} = -\frac{1}{2}\sqrt{-g}g_{\mu\nu}\delta g^{\mu\nu}. \tag{2.1.11}$$

Conformal transformations are a useful tool in modified gravity, although their physical interpretation has been subject to debate [70]. A conformal transformation is performed by introducing a new metric $\tilde{g}_{\mu\nu}$ which is a rescaled version of the old one:

$$g_{\mu\nu} = \Omega^2 \tilde{g}_{\mu\nu}, \tag{2.1.12}$$

where Ω^2 is a function of spacetime position (note that the convention here is the inverse of that in [70]). For the transformation to be non-degenerate $\Omega^2 > 0$. It is important to note that this is not a coordinate transformation. It is a change of metrics and lengths measured in the new metric are different from those measured in the old metric. A rescaling does not alter the spacelike, timelike or null character of vectors and hence does not change the causal structure of spacetime. Further, angles between vectors, defined by $\cos\theta = (V\cdot W)/|V||W|$, are unchanged.

It is a straightforward, if tedious, exercise to derive the transformation properties of the connection and curvature tensors under conformal transformations. A few useful identities are quoted here without proof (all these identities are for four dimensions, see [70] for further details):

$$g^{\mu\nu} = \Omega^{-2}\tilde{g}^{\mu\nu}, \tag{2.1.13}$$

$$g = \Omega^8 \tilde{g}, \tag{2.1.14}$$

$$\Gamma^\alpha_{\beta\gamma} = \tilde{\Gamma}^\alpha_{\beta\gamma} + \Omega^{-1}\left(\delta^\alpha_\beta \tilde{\nabla}_\gamma\Omega + \delta^\alpha_\gamma\tilde{\nabla}_\beta\Omega - \tilde{g}_{\alpha\beta}\tilde{\nabla}^\alpha\Omega\right), \tag{2.1.15}$$

$$\begin{aligned} R_{\alpha\beta} = {} & \tilde{R}_{\alpha\beta} - 2\tilde{\nabla}_\alpha\tilde{\nabla}_\beta(\ln\Omega) - \tilde{g}_{\alpha\beta}\tilde{g}^{\rho\sigma}\tilde{\nabla}_\sigma\tilde{\nabla}_\rho(\ln\Omega) \\ & + 2\tilde{\nabla}_\alpha(\ln\Omega)\tilde{\nabla}_\beta(\ln\Omega) - 2\tilde{g}_{\alpha\beta}\tilde{g}^{\rho\sigma}\tilde{\nabla}_\rho(\ln\Omega)\tilde{\nabla}_\sigma(\ln\Omega) \end{aligned} \tag{2.1.16}$$

$$R = \Omega^{-2}\left[\tilde{R} - \frac{6\tilde{\Box}\Omega}{\Omega}\right], \tag{2.1.17}$$

$$T_{\alpha\beta} = \Omega^{-2}\tilde{T}_{\alpha\beta}, \tag{2.1.18}$$

$$T_\alpha{}^\beta = \Omega^{-4}\tilde{T}_\alpha{}^\beta, \tag{2.1.19}$$

$$T^{\alpha\beta} = \Omega^{-6}\tilde{T}^{\alpha\beta}, \tag{2.1.20}$$

$$T = \Omega^{-4}\tilde{T}, \tag{2.1.21}$$

where $\tilde{\nabla}$ is the covariant derivative using the Christoffel connection of $\tilde{g}_{\mu\nu}$, $\tilde{\Box} = \tilde{g}^{\mu\nu}\tilde{\nabla}_\mu\tilde{\nabla}_\nu$, $T_{\alpha\beta}$ is the energy-momentum tensor of matter (c.f. equation (2.1.24)) and $T \equiv g^{\alpha\beta}T_{\alpha\beta}$.

2.1.2 General Relativity

General Relativity is without doubt the most successful theory of gravity yet developed. General Relativity is the only theory of gravity that depends only on the metric (*metricity*), is derivable from an action principle and is compatible with the *equivalence principles* [71]:

Weak Equivalence Principle (WEP) If an uncharged test body is placed at an initial event in spacetime and given an initial velocity there, then its subsequent trajectory will be independent of its internal structure and composition.

Einstein Equivalence Principle (EEP) WEP is valid, the outcome of any local non-gravitational test experiment is independent of the velocity of the freely-falling apparatus (Local Lorentz Invariance) and the outcome of any local non-gravitational test experiment is independent of where and when in the universe it is performed (Local Position Invariance).

Strong Equivalence Principle (SEP) EEP holds and is extended to include self-gravitating bodies, not just test bodies, and local gravitational experiments as well as local non-gravitational experiments.

The experimental status of each of these general principles and the detailed predictions of GR are reviewed at length in [20]. Despite these successes it is necessary to investigate alternative theories of gravity in order to shed light on the problems of quantum gravity and the origin of dark energy. It is necessary to relax at least one of the assumptions (metricity, action principle, WEP, EEP, SEP) to go beyond GR. $f(R)$ is a conservative approach to modified gravity in that it relaxes only the strongest and least experimentally constrained assumption: the SEP. $f(R)$ is discussed in Section 2.1.3 after a short review of GR.

The field equations of GR with matter can be derived from the action

$$S = S_{\rm EH} + S_{\rm M} = \int \mathrm{d}^4x\sqrt{-g}\,\frac{1}{2\kappa^2}\left(R - 2\Lambda\right) + \int \mathrm{d}^4x\sqrt{-g}\,\mathcal{L}_{\rm M}, \tag{2.1.22}$$

where $S_{\rm EH}$ is the Einstein-Hilbert action, $S_{\rm M}$ is the matter action, $\kappa \equiv M_{\rm pl}^{-1} \equiv \sqrt{8\pi G} = \left(2.435\times10^{18}\ \text{GeV}\right)^{-1}$ is the inverse Planck mass, Λ is the cosmological constant and $\mathcal{L}_{\rm M}$ is the matter Lagrangian. The matter Lagrangian is taken to depend on a number of matter fields $\Psi^{(i)}$ and their covariant derivatives $\nabla\Psi^{(i)}$ and to be no more than second order in derivatives. Beyond this the matter content of the theory will not be specified until later. Many results can be established without specifying the details of the matter Lagrangian.

There are two approaches (called formalisms) to deriving the field equations from S: the metric and Palatini formalisms. In the metric formalism $S_{\rm EH}$ is regarded to be a functional of the metric only and variations are performed with respect to $\delta g^{\mu\nu}$. In the Palatini formalism (actually developed by Einstein [72]) the action is written $S_{\rm EH} \propto \int \mathrm{d}^4x\sqrt{-g}g^{\mu\nu}R_{\mu\nu}$ where the Ricci tensor is considered a function of the connection $\Gamma^{\alpha}_{\beta\gamma}$, which is now independent of the metric. Taking variations with respect to $\delta g^{\mu\nu}$ and $\delta\Gamma^{\alpha}_{\beta\gamma}$ independently then gives a system of equations equivalent to the usual Einstein field equations. This equivalence is shown in any advanced textbook on relativity, but it fails for $f(R)$ gravity. Thus, while in GR the metric and Palatini formalisms are mathematically and physically identical, in $f(R)$ gravity they are physically distinct and must be considered independently.

Following the metric formalism, the variation of the action with respect to the metric gives the Einstein field equation[3],

$$R_{\mu\nu} - \frac{1}{2} g_{\mu\nu} R + \Lambda g_{\mu\nu} = \kappa^2 T_{\mu\nu}, \tag{2.1.23}$$

where the energy-momentum tensor of matter is defined by

$$T_{\mu\nu} = -\frac{2}{\sqrt{-g}} \frac{\delta S_{\mathrm{M}}}{\delta g^{\mu\nu}}. \tag{2.1.24}$$

The time-time component T_{tt} is the ordinary energy density and the isotropic part of the spatial tensor T_{ij}, where $i, j = x, y, z$, is the ordinary fluid pressure. Off diagonal components of $T_{\mu\nu}$ represent stresses, energy fluxes and momentum densities.

A useful idealisation of real matter and radiation is a *perfect fluid*. A perfect fluid is a gas or fluid that has a four-velocity $u^{\mu}(x)$ which can vary through spacetime, and has an energy density $\rho(x)$ and isotropic pressure $p(x)$ in the rest frame of a fluid element at x [14]. The energy-momentum tensor of a perfect fluid is given by

$$T_{\mu\nu} = (\rho + p) u_{\mu} u_{\nu} + p g_{\mu\nu}. \tag{2.1.25}$$

If the universe is approximated as a perfect fluid and the (spatial) homogeneity assumption is used to set $\rho(x^{\mu}) = \rho(t)$ and $p(x^{\mu}) = p(t)$, it can be shown that the Einstein equation (2.1.23) is equivalent to the Friedmann equation (1.1.1) stated in chapter 1.

The covariant divergence of the left hand side of Einstein's equation vanishes by the Bianchi identity and metric compatibility. This implies

$$\nabla_{\mu} T^{\mu\nu} = 0,$$

which is the conservation of the energy and momentum of matter. This relationship can also be derived as a result of the coordinate invariance of S_{M}. For the energy-momentum tensor of a spatially homogeneous perfect fluid this equation is equivalent to the continuity equation (1.1.2).

2.1.3 $f(R)$ Gravity

$f(R)$ gravity is a conservative modification of GR in that all of the basic ingredients are retained. The only change is that the Einstein-Hilbert action is generalised to

$$S_g = \int \mathrm{d}^4 x \sqrt{-g}\, \frac{1}{2\kappa^2} f(R), \tag{2.1.26}$$

where S_g stands for "gravity." The total action is $S = S_g + S_{\mathrm{M}}$ as before. This simple change has far reaching consequences.

To be clear, there is no suggestion that (2.1.26) is a fundamental theory of gravity for two reasons. First, it suffers many of the same problems with quantization that GR does. Second, there is no known principle which determines the functional form of $f(R)$. The outlook of this thesis is that (2.1.26) is a suitable starting point for studying the low energy (compared to the Planck scale) phenomenology of whatever fundamental theory there might be. Indeed, any more fundamental theory that is correct must contain within it an $f(R)$ limit because GR is a special case of $f(R)$. The hope of $f(R)$ theorists is that the study of (2.1.26) motivates fruitful experimental

[3] Up to a subtlety involving the so called Gibbons-Hawking-York boundary term [73, 74]. This term does not affect any of the results here. It is only relevant to the quantization of gravity and spacetime manifolds which have a boundary.

investigations. Since $f(R)$ is a low energy macroscopic approximation to whatever fundamental quantum gravitational theory there may be, it is not expected that the functional form of $f(R)$ should necessarily be simple. Though theorists tend to be prejudiced towards simple functional forms (polynomial, power law, exponential, etc.), there is no fundamental reason to ignore more complicated forms and, indeed, the known viable models are "complex" in this sense.

This thesis focuses on the metric formalism for $f(R)$ gravity. $f(R)$ gravity in the Palatini formalism is physically distinct from metric $f(R)$. In fact, Palatini $f(R)$ gravity faces grave difficulties: it lacks a well posed Cauchy problem, ordinary matter configurations lead to curvature singularities at surfaces, there are large non-perturbative corrections to the standard model and in most models the Hydrogen atom is explosively unstable [74, 75]. It is not considered any further for these reasons. Finally, there is a metric-affine formalism which is distinct from the metric and Palatini formalisms and is not yet ruled out. It is less well developed than the other two and will not be investigated in this thesis (although it would be a worthwhile topic for future research) [76].

The field equation for metric $f(R)$ gravity can be derived by varying the action with respect to $\delta g^{\mu\nu}$:

$$\begin{aligned}
\delta S &= \frac{1}{2\kappa^2}\int \mathrm{d}^4x\ \delta\left(\sqrt{-g}f(R)\right) + \delta S_{\mathrm{M}} \\
&= \frac{1}{2\kappa^2}\int \mathrm{d}^4x\ \left(\delta\sqrt{-g}f(R) + \sqrt{-g}f_R\delta R\right) - \int \mathrm{d}^4x\sqrt{-g}\ \frac{1}{2}T_{\mu\nu}\delta g^{\mu\nu} \\
&= \frac{1}{2\kappa^2}\int \mathrm{d}^4x\sqrt{-g}\ \left[-\frac{1}{2}g_{\mu\nu}f(R) + f_R\left(R_{\mu\nu} + g_{\mu\nu}\Box - \nabla_\mu\nabla_\nu\right)\right]\delta g^{\mu\nu} \\
&\quad - \int \mathrm{d}^4x\sqrt{-g}\ \frac{1}{2}T_{\mu\nu}\delta g^{\mu\nu},
\end{aligned}$$

using the product rule and (2.1.24) in the second line and (2.1.10) and (2.1.11) in the third line. The shorthand $f_R \equiv \frac{\mathrm{d}f}{\mathrm{d}R}$ was introduced in the second line. Integrating by parts to move the derivatives off the $\delta g^{\mu\nu}$ and dropping the boundary terms leads to the equation of motion

$$\left(R_{\mu\nu} + g_{\mu\nu}\Box - \nabla_\mu\nabla_\nu\right)f_R - \frac{1}{2}g_{\mu\nu}f(R) = \kappa^2 T_{\mu\nu}. \tag{2.1.27}$$

There are several important things to notice about this equation. First, the presence of $\Box$ and $\nabla_\mu\nabla_\nu$ acting on f_R means that the field equations are of fourth order. The theory is sometimes called "fourth order gravity" for this reason. This stands in contrast to GR, whose equations are second order. The higher order nature of the theory brings with it stability concerns, which have been thoroughly investigated in the cosmological context. There are some general restrictions on the functional form of $f(R)$ required for the stability of the theory [3, 4, 77, 78]. These are discussed later. Second, for an arbitrary linear form $f(R) = aR - b$, $f_R = a$ is a constant and the equations become second order:

$$R_{\mu\nu} - \frac{1}{2}g_{\mu\nu}R + \frac{b}{2a}g_{\mu\nu} = \frac{\kappa^2}{a}T_{\mu\nu},$$

which is just GR with an effective gravitational constant $\kappa^2_{\mathrm{eff}} = \kappa^2/a$ and cosmological constant $b/2a$. Thus deviations from GR are obtained only for non-linear $f(R)$. Finally, taking the trace of (2.1.27) gives the so called trace equation:

$$\left(R + 3\Box\right)f_R - 2f(R) = \kappa^2 T. \tag{2.1.28}$$

After a slight rearrangement this gives a wave equation for f_R:

$$\Box f_R = \frac{2f - Rf_R}{3} + \frac{\kappa^2}{3}T.$$

This implies that f_R is a dynamical degree of freedom of the theory. In order to fully specify the initial data requires not just the metric and its time derivative, but also f_R and $\dot{f}_R$. This is in contrast to the trace equation for GR

$$-R + 4\Lambda = \kappa^2 T \tag{2.1.29}$$

which is an algebraic relationship. There is no extra degree of freedom in GR. Of course this is due to the difference in order of the governing field equations.

Simplifying the field equations: the Jordan and Einstein frames

The fact that f_R appears as a dynamical scalar field suggests that the theory could be mapped to a scalar-tensor theory where the field equations governing the metric and the scalar field are of second order. This can be achieved by introducing an auxiliary field χ into the Lagrangian:

$$S_g = \frac{1}{2\kappa^2}\int \mathrm{d}^4x\sqrt{-g}\ \left[f(\chi) + f_\chi(\chi)(R-\chi)\right]. \tag{2.1.30}$$

Performing the variation with respect to χ:

$$\delta S_g = \frac{1}{2\kappa^2}\int \mathrm{d}^4x\sqrt{-g}\ \left[f_\chi(\chi)\,\delta\chi + f_{\chi\chi}(\chi)(R-\chi)\,\delta\chi + f_\chi(\chi)(-\delta\chi)\right],$$

and using the arbitrariness of $\delta\chi$ gives the equation of motion $f_{\chi\chi}(\chi)(R-\chi) = 0$, which implies $\chi = R$ as long as $f_{\chi\chi} \neq 0$. Since this is an algebraic, not differential, relationship it is valid to substitute it back into (2.1.30) which recovers (2.1.26). Thus (2.1.30) is exactly equivalent to the original theory if $f_{\chi\chi} \neq 0$. The case $f_{\chi\chi} = 0$ just reduces to GR. Including a matter action and varying with respect to $g^{\mu\nu}$ gives

$$R_{\mu\nu} - \frac{1}{2}g_{\mu\nu}R - \frac{1}{2}g_{\mu\nu}\frac{f(\chi) - f_\chi(\chi)\chi}{2f_\chi(\chi)} = \left(\frac{\kappa^2}{f_\chi}\right)T_{\mu\nu}.$$

Written in this form $f(R)$ can be viewed as GR with an effective gravitational constant $G_{\text{eff}} = G/f_\chi$ and cosmological constant $\Lambda_{\text{eff}} = \frac{f(\chi)-f_\chi(\chi)\chi}{2f_\chi(\chi)}$ which vary in space and time. The variability of Λ_{eff} is the reason $f(R)$ is studied as a dynamical dark energy candidate. There are strong observational constraints on the variability of G_{eff} and hence on f_χ. Further, it is clear that $f_{\chi\chi}$ must be positive at the current epoch. If $f_{\chi\chi} < 0$ then as matter density increases, the curvature R increases, $f_\chi(\chi = R)$ decreases and G_{eff} increases. This leads to a runaway collapse instability for any inhomogeneous distribution of matter.

It is worth noting that this form of metric $f(R)$ theory is equivalent to a special case of the well studied Brans-Dicke scalar-tensor theory [70, 79]

$$S_{BD} = \frac{1}{16\pi}\int \mathrm{d}^4x\sqrt{-g}\left[\phi_{BD}R - \frac{\omega}{\phi_{BD}}g^{\mu\nu}\nabla_\mu\phi_{BD}\nabla_\nu\phi_{BD} - V(\phi_{BD})\right],$$

where the scalar field ϕ_{BD} is identified as f_χ and the Brans-Dicke parameter is $\omega = 0$. There is a scalar potential $V(f_\chi) = \chi f_\chi - f$ where χ and $f(\chi)$ are found by solving f_χ for χ. The original Brans-Dicke theory lacked a potential V for the scalar field and solar system constraints determine [20, 79] $\omega > 40,000$. $f(R)$ is saved by the potential, which allows the chameleon mechanism to

screen the scalar field on solar system scales [4, 27, 29, 70, 74, 79–84]. The choice of $\omega = 0$ leads to many features atypical of the general Brans-Dicke theory so $f(R)$ theories are worth studying in their own right.

The field equations can be further simplified by a conformal transformation to the so called Einstein frame. The theory as written in equation (2.1.26) is in the Jordan frame. Different conformal frames simply correspond to choosing different metric variables to write down the theory. Changing frames can be considered a field redefinition. Introducing the new metric $\tilde{g}_{\mu\nu}$ by (2.1.12) in (2.1.30) the $f(R)$ action becomes

$$S_g = \frac{1}{2\kappa^2}\int \mathrm{d}^4x\sqrt{-\tilde{g}}\;\Omega^4\left[f_\chi(\chi)\,\Omega^{-2}\left(\tilde{R} - \frac{6\tilde{\Box}\Omega}{\Omega}\right) + f(\chi) - f_\chi(\chi)\,\chi\right],$$

which can be simplified by choosing $\Omega^2 f_\chi = 1$ or $\Omega = f_\chi^{-1/2}$. Thus,

$$S_g = \int \mathrm{d}^4x\sqrt{-\tilde{g}}\;\left[\frac{1}{2\kappa^2}\tilde{R} - \frac{3\tilde{\Box}\Omega}{\kappa^2\Omega} + \frac{\Omega^4\left(f(\chi) - f_\chi(\chi)\,\chi\right)}{2\kappa^2}\right].$$

The second term can be simplified using the identity

$$\tilde{\Box}\Omega = \frac{1}{\sqrt{-\tilde{g}}}\partial_\mu\left(\tilde{g}^{\mu\nu}\sqrt{-\tilde{g}}\partial_\nu\Omega\right),$$

and integrating by parts. The second term becomes

$$\int \mathrm{d}^4x\sqrt{-\tilde{g}}\;\left[-\frac{3}{\kappa^2}\tilde{g}^{\mu\nu}\partial_\mu(\ln\Omega)\,\partial_\nu(\ln\Omega)\right],$$

which can be written as a canonically normalised kinetic term for a scalar field

$$\int \mathrm{d}^4x\sqrt{-\tilde{g}}\;\left(-\frac{1}{2}\tilde{g}^{\mu\nu}\partial_\mu\phi\partial_\nu\phi\right),$$

if one identifies

$$\phi \equiv \sqrt{\frac{6}{\kappa^2}}\ln\Omega = -\frac{1}{2}\sqrt{\frac{6}{\kappa^2}}\ln f_\chi. \tag{2.1.31}$$

It is just as good to write f_R in this equation instead of f_χ since $\chi = R$ by the equations of motion. Both forms of the equation can be found in the literature.

Finally, it is seen that $f(R)$ theory is equivalent to a scalar-tensor theory

$$S_g = \int \mathrm{d}^4x\sqrt{-\tilde{g}}\;\left(\frac{1}{2\kappa^2}\tilde{R} - \frac{1}{2}\tilde{g}^{\mu\nu}\partial_\mu\phi\partial_\nu\phi - V(\phi)\right), \tag{2.1.32}$$

where the scalar potential is

$$V(\phi) = \frac{f_\chi\chi - f}{2\kappa^2 f_\chi^2}. \tag{2.1.33}$$

In this equation χ must be determined in terms of ϕ by solving (2.1.31). Typically it is impossible to invert the relationship (2.1.31) to give χ explicitly. Fortunately, for viable models the deviation of $f(R)$ from GR is very small at laboratory scales so series expansion techniques can be used. When the series is truncated to low enough order $\chi(\phi)$ and $V(\phi)$ can be found. Examples of this technique are given in the section 2.2. Unfortunately the error incurred by truncating the series is hard to gauge.

Under the conformal transformation the matter action changes to

$$S_m = \int \mathrm{d}^4x\sqrt{-\tilde{g}}\Omega^4\mathcal{L}_m\left(\Omega^2\tilde{g}_{\mu\nu}, \psi^{(i)}\right),$$

and the field equations are

$$\tilde{R}_{\mu\nu} - \frac{1}{2}\tilde{g}_{\mu\nu}\tilde{R} = \kappa^2\left(T^{(\phi)}_{\mu\nu} + \tilde{T}_{\mu\nu}\right), \tag{2.1.34}$$

$$\Box\phi = \frac{\mathrm{d}V}{\mathrm{d}\phi} - \frac{\kappa}{\sqrt{6}}\tilde{T}, \tag{2.1.35}$$

where the scalar field energy-momentum tensor is

$$T^{(\phi)}_{\mu\nu} = \partial_\mu\phi\partial_\nu\phi - \tilde{g}_{\mu\nu}\left(\frac{1}{2}\tilde{g}^{\alpha\beta}\partial_\alpha\phi\partial_\beta\phi + V(\phi)\right). \tag{2.1.36}$$

It is important to stress the proper physical interpretation of the variables in the Einstein frame. This issue is often muddled in the literature and a great deal of confusion persists [70, 85, 86]. It is clear that the theories defined by (2.1.30) and (2.1.32) are equivalent, at least at a classical level. Despite this the theories appear very different: in the Jordan frame the gravitational "constant" varies throughout spacetime; in the Einstein frame the gravitational constant is in fact constant, but there is a new matter field ϕ which couples to all other matter fields through the trace of the energy-momentum tensor. This apparent tension is resolved by noticing that the Einstein frame metric $\tilde{g}_{\mu\nu}$ alone is not sufficient to determine physical distances. Both the metric $\tilde{g}_{\mu\nu}$ and the scalar ϕ are required in the specific combination $\Omega^2\tilde{g}_{\mu\nu}$ to determine physical distances. One could say that $\tilde{g}_{\mu\nu}$ measures distances in a system of units which vary throughout spacetime in proportion to Ω. If all one had were the Einstein frame action (2.1.32) this feature would be far from obvious.

A further difficulty with the conformal transformation is that, while the Jordan and Einstein frame theories are classically equivalent, standard quantization procedures yield different quantum theories [85]. One says that conformal transformations do not commute with quantization. One consequence of this is an anomalous coupling of the scalar field to gauge fields [87], which have vanishing $\tilde{T}$. Such couplings could be detected at atomic afterglow experiments [41, 42, 50, 53, 60–63] and helioscope experiments [39, 63, 88]. This thesis only uses the conformal transformation as a classical technique to simplify the field equations. Quantization of the scalar field ϕ is not considered.

The Chameleon Mechanism

In the form of equations (2.1.34) and (2.1.35) $f(R)$ is equivalent to GR with an additional scalar field in the matter sector. The only unusual feature is that the scalar field is coupled to matter through the trace of the energy-momentum tensor $\tilde{T}$. This coupling can be written as an effective potential

$$V_{\text{eff}} = V - \frac{\kappa}{\sqrt{6}}\tilde{T}\phi \approx V + \frac{\kappa}{\sqrt{6}}\tilde{\rho}\phi,$$

where the second equality obtains in the non-relativistic limit if matter is a perfect fluid. This is the special form of interaction mentioned in section 1.2.

The fact that the effective scalar potential depends on the environment through the second term is crucial. The typical shape of the effective potential is shown in Figure 2.1.1. As the density of the environment increases the mass of fluctuations about the minimum of V_{eff} increases, leading

to a decrease in the range of the "fifth force" transmitted by ϕ (in the original chameleon model ϕ really does mediate a fifth force, but in $f(R)$ it mediates the part of the gravitational force responsible for the deviations from GR). This is the *chameleon mechanism* which, for some models at least, allows the modifications to GR to escape notice at solar system scales. The factor of $1/\sqrt{6}$ in V_{eff} is the β mentioned in Section 1.2. In the original chameleon theory the second term in the effective potential is $-\beta\kappa\tilde{T}\phi$ where β is a free parameter [56, 80]. In $f(R)$ the form of the scalar field coupling to matter is completely determined. This is simply a consequence of the fact that in $f(R)$ the scalar field is a part of the gravitational field $g_{\mu\nu}$.

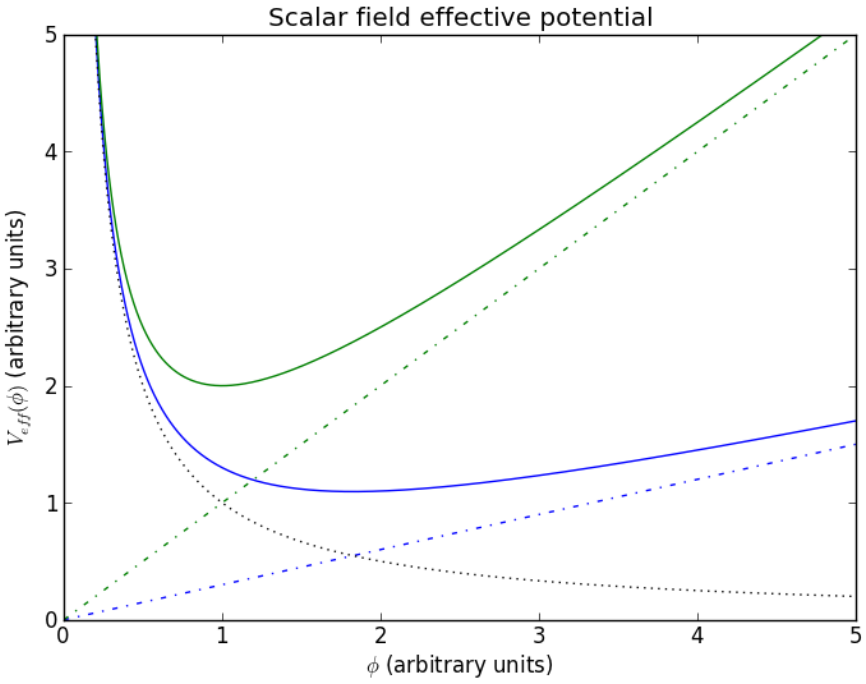

Figure 2.1.1: Effective potential of a chameleon scalar field showing dependence on the environmental density ρ. The dotted curve is the scalar potential $V(\phi)$ (the singular behaviour at $\phi = 0$ is a feature of the original chameleon model but not of $f(R)$ models). The dash dotted curves are the $\rho\phi$ contribution to the effective potential. The coloured curves are the full effective potentials at high (green) and low (blue) ambient densities. The position of the minimum and the curvature there clearly depend on the environment. In particular, the mass of fluctuations about the minimum increases with the density of the environment.

The chameleon mechanism operates through *thin shell* screening. Consider a spherical body such as the Earth, or even a test mass in a gravitational experiment, with uniform density ρ_b and radius[4] R, embedded in a medium of uniform density ρ_m. In order to determine the force exerted by this body on other bodies via the scalar field, the field profile $\phi(r)$ must be found. This involves solving (2.1.35), which is a non-linear Poisson equation. This equation can be solved numerically or, for piecewise constant densities, by an approximate analytical matching procedure [27–30, 37, 54], but the aim here is physical intuition. Near the minimum, $\phi = \phi_{\text{min}}$, the effective potential can be expanded

$$V_{\text{eff}}(\phi = \phi_{\text{min}} + \delta\phi) \approx \text{const.} + \frac{1}{2}m_\phi^2\delta\phi^2 + \mathcal{O}\left(\delta\phi^3\right).$$

[4] R is only the radius in this paragraph. Elsewhere it is the Ricci scalar.

Note that m_ϕ and $\phi_{\min}$ both depend on the density. The Compton wavelength $\lambda_\phi = 1/m_\phi$ determines the distance scale over which the field can vary. This can be seen by solving the linearised version of equation (2.1.35),

$$\nabla^2 \delta\phi = m_\phi^2 \delta\phi,$$

which has the solution

$$\delta\phi = A\frac{\mathrm{e}^{-r/\lambda_\phi}}{r} + B\frac{\mathrm{e}^{+r/\lambda_\phi}}{r}.$$

The physical boundary conditions and matching at the surface $r = R$ determine the constants for both the interior ($r < R$) and exterior ($r > R$) solution. Nevertheless it is clear, even without carrying out the matching procedure, that λ_ϕ is the relevant length scale. If the body is large, i.e. $R \gg \lambda_\phi$, gradients of ϕ at the surface cannot propagate far into the interior of the body. The field profile in the interior of the body is thus a constant $\phi = \phi_{\min}$ except for within a thin shell of thickness $\sim \lambda_\phi$ at the surface. Since only a thin shell of thickness $\Delta R \sim \lambda_\phi$ contributes to the exterior field of the body, the effective scalar "charge" of the body is greatly reduced. Define the scalar charge q_S by analogy to electromagnetism so that the external field of the body is

$$\phi = \frac{q_S}{4\pi r}\mathrm{e}^{-r/\lambda_\phi}.$$

(The exponential factor is absent from the Coulomb potential because the range of electromagnetism is infinite, $\lambda_\phi \to \infty$.) The effective charge of an extended body is

$$q_S \approx \left(\frac{4\pi R^2 \Delta R}{\frac{4}{3}\pi R^3}\right)\frac{\kappa m}{\sqrt{6}} = \left(\frac{3\Delta R}{R}\right)\frac{\kappa m}{\sqrt{6}},$$

which is greatly reduced from the value it would have, $\kappa m/\sqrt{6}$, in the absence of thin shell screening. Further details, including a discussion of the validity of treating atomic matter as a fluid with a smooth density (which is not obviously valid in a non-linear theory), can be found in [84].

2.2 Viable $f(R)$ models

2.2.1 The Linder model: "Exponential gravity"

Now several viable $f(R)$ models are considered. "Viable" means that the models satisfies a number of constraints [31]:

1. Positivity of the effective gravitational coupling
2. Stability of cosmological perturbations
3. Asymptotes to ΛCDM/GR in the high curvature regime
4. Existence of a stable late time de Sitter point (exponential expansion)
5. Compatibility with strong equivalence principle constraints and
6. Compatibility with solar system constraints

The exponential gravity of Linder is the first model to be considered here that satisfies all six constraints [3]. An important advantage of exponential gravity over other viable models is that it only has one free parameter. Exponential gravity is defined by[5]:

[5] Note that the β here is different from the chameleon coupling $\beta = 1/\sqrt{6}$ from Section 1.2.

$$f(R) = R - \beta R_s \left(1 - \mathrm{e}^{-R/R_s}\right). \tag{2.2.1}$$

For cosmologically viable versions of the model the combination βR_s is related to Ω_m so there is only one free parameter. Following [31], take $\beta R_s = 18H_0^2\Omega_m \approx 2 \times 10^{-35}\ \mathrm{s}^{-2}$ and

$$f(R) = R - 18H_0^2\Omega_m \left(1 - \mathrm{e}^{-\beta R/18H_0^2\Omega_m}\right).$$

The model satisfies all viability constraints for $1 < \beta < \exp\left(R/18H_0^2\Omega_m\right)$. The scalar field for exponential gravity is (c.f. equation (2.1.31))

$$\phi = -\frac{1}{2}\sqrt{\frac{6}{\kappa^2}} \ln\left(1 - \beta \mathrm{e}^{-\beta R/18H_0^2\Omega_m}\right).$$

Near the surface of the Earth the approximation $\kappa\phi \ll 1$ is valid. To see this note that, since $f(R)$ must be close to GR near the Earth, it is valid to estimate the curvature using the trace of the Einstein equation (with $\Lambda = 0$, c.f. equation (2.1.29)) $R \approx \kappa^2\rho$. Using this in the equation for ϕ:

$$\kappa\phi = -\frac{1}{2}\sqrt{6} \ln\left(1 - \beta \mathrm{e}^{-\beta\kappa^2\rho/18H_0^2\Omega_m}\right).$$

The exponential is $\sim \exp\left(-10^{29}\right)$ so the second term in the logarithm is exceedingly small. Thus

$$\kappa\phi \approx \frac{1}{2}\sqrt{6}\beta \mathrm{e}^{-\beta\kappa^2\rho/18H_0^2\Omega_m} \ll 1.$$

Even at an ambient density 10^{10} times smaller than the Earth's (comparable to laboratory vacuum) the limit $\kappa\phi \ll 1$ is valid.

The potential (2.1.33) for exponential gravity is

$$V(\phi) = \frac{f_\chi \chi - f}{2\kappa^2 f_\chi^2} = \frac{\beta R_s}{2\kappa^2} \frac{1 - \mathrm{e}^{-\chi/R_s}\left(1 + \frac{\chi}{R_s}\right)}{\left(1 - \beta \mathrm{e}^{-\chi/R_s}\right)^2}.$$

χ can be eliminated in favour of ϕ using

$$\frac{\chi}{R_s} = -\ln\left(\sqrt{\frac{2}{3}}\frac{\kappa\phi}{\beta}\right).$$

Hence

$$V(\phi) = \frac{18H_0^2\Omega_m}{2\kappa^2}\left[1 + \left(2 - \frac{1}{\beta}\right)\sqrt{\frac{2}{3}}\kappa\phi + \sqrt{\frac{2}{3}}\frac{\kappa\phi}{\beta}\ln\left(\sqrt{\frac{2}{3}}\frac{\kappa\phi}{\beta}\right)\right]. \tag{2.2.2}$$

This is pictured in Figure 2.2.1. It is shown in Chapter 3 that this model does not predict an observable shift in the energy levels of the neutron bouncer experiment, so it is necessary to turn to more complicated models.

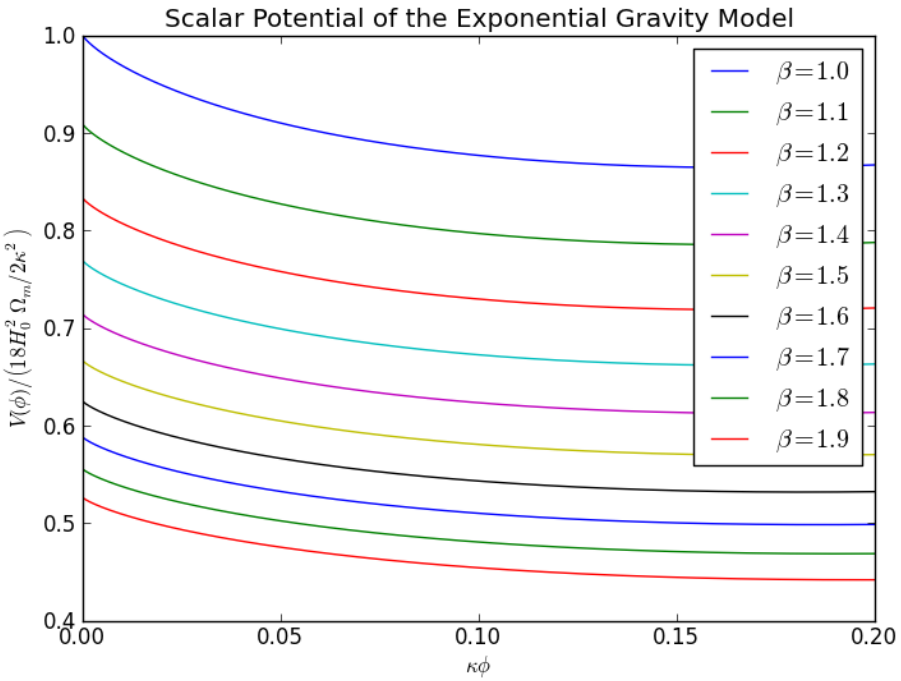

Figure 2.2.1: Scalar potential of Linder's exponential gravity (equation 2.2.2).

2.2.2 The model of Hu and Sawicki

The model of Hu and Sawicki is defined by[6] [4]:

$$f(R) = R - m^2 \frac{c_1 \left(R/m^2\right)^n}{c_2 \left(R/m^2\right)^n + 1}, \tag{2.2.3}$$

with $n > 0$. This theory has four free parameters. Hu and Sawicki make canonical choices for two of the parameters in order to reproduce the expansion history of ΛCDM to the accuracy of current observations. The mass scale m, which sets the scale where deviations from general relativity become $\mathcal{O}(1)$, is taken as [4]

$$m^2 = \frac{\kappa^2 \bar{\rho}_0}{3} = (8315 \text{ Mpc})^{-2} \left(\frac{\Omega_M h^2}{0.13}\right),$$

where $\bar{\rho}_0$ is an average density of the universe today. Taking the current fit values for Ω_M and h (c.f. Chapter 1) this gives[7]

$$m \approx 7.9 \times 10^{-34} \text{ eV}. \tag{2.2.4}$$

The combination m^2/κ^2 frequently appears, so it is convenient to quote its value (restoring $\hbar$ to give the dimensions of a mass density):

$$\frac{m^2}{\kappa^2} = \frac{m^2}{8\pi G \hbar^2} \approx 8.6 \times 10^{-31} \text{ g/cm}^3.$$

[6] There is an important difference in notation between [4] and here. Hu and Sawicki [4] define $f(R)$ by $f^{(HS)}(R) \equiv f^{(\text{here})}(R) - R$. The notation used here is in agreement with the majority of the $f(R)$ literature.

[7] Note that Hu and Sawicki take somewhat different values from those quoted in the first chapter. In particular they set $\Omega_M^{(HS)} = 0.24$ and $\Omega_\Lambda^{(HS)} = 0.76$.

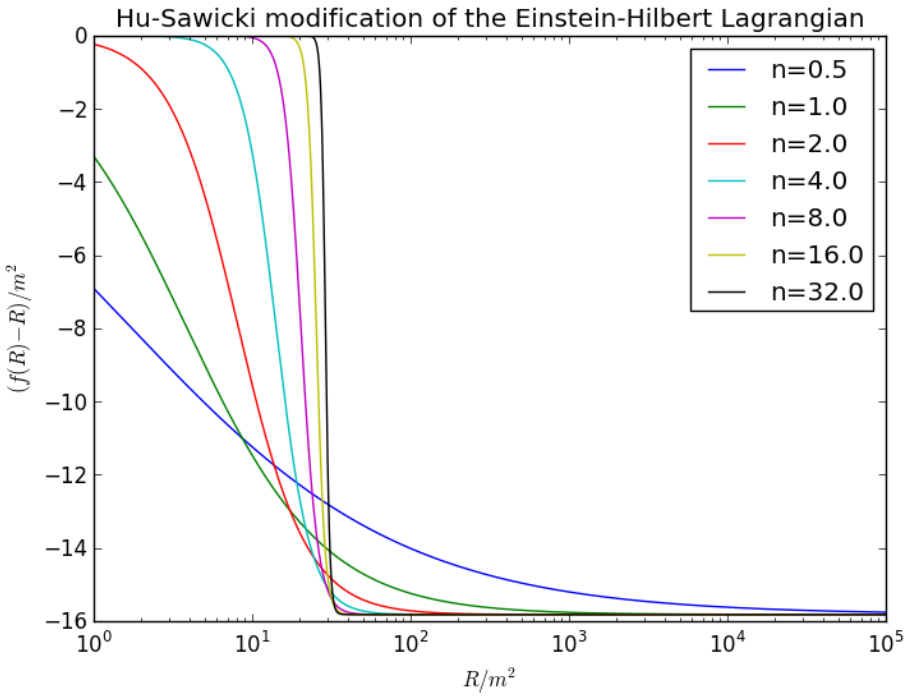

Figure 2.2.2: The modification of the Einstein-Hilbert Lagrangian, the second term of (2.2.3), is shown for the choices (2.2.5) and $|f_{\chi 0}| = 0.05$.

Hu and Sawicki also set

$$\frac{c_1}{c_2} = 6\frac{\Omega_\Lambda}{\Omega_M}. \tag{2.2.5}$$

The remaining free parameters are n and c_1/c_2^2. Because the scalar field ϕ is directly related to f_χ, it is convenient to relate the parameter c_1/c_2^2 to the (cosmological) value of $\bar{f}_\chi$ at the present[8] [4]:

$$\bar{f}_{\chi 0} \equiv \frac{\mathrm{d}f}{\mathrm{d}\chi}(t=0) - 1 \approx -n\frac{c_1}{c_2^2}\left(\frac{12}{\Omega_M} - 9\right)^{-n-1},$$

which allows one to trade the c_1/c_2^2 dependence for $\bar{f}_{\chi 0}$. In particular, using (2.2.5),

$$c_2 \approx -\frac{6n}{\bar{f}_{\chi 0}}\frac{\Omega_\Lambda}{\Omega_M}\left(\frac{12}{\Omega_M} - 9\right)^{-n-1} \approx -15.830\frac{n}{\bar{f}_{\chi 0}} \times 7.552^{-n-1}. \tag{2.2.6}$$

Hu and Sawicki study the $n = 1$ and $n = 4$ models and found solar system tests are satisfied for surprisingly large $|\bar{f}_{\chi 0}|$ (see Figure 2.2.4).

The second term of (2.2.3), i.e. the correction to the Einstein-Hilbert Lagrangian, is shown in Figure 2.2.2 for the cosmologically viable parameters just discussed. In the large R limit (the actual case in the laboratory) all of the models asymptote to GR with a cosmological constant. The n parameter controls the steepness of the transition to an effective cosmological constant, with larger n producing a steeper transition. Because of this and the fact that all laboratory experiments are carried out in the large R regime, small n models predict the largest deviation from GR at laboratory scales. Thus the $n \to 0$ limit is of some interest.

At high curvatures one can use the expansion

[8] The bar is to remind that $\bar{f}_\chi$ is not $\mathrm{d}f^{(\mathrm{here})}/\mathrm{d}\chi$, but is $\mathrm{d}f^{(HS)}/\mathrm{d}\chi$. The confusion is an unfortunate consequence of the notation used in [4].

$$f(R) \approx R - m^2\frac{c_1}{c_2} + m^2\frac{c_1}{c_2^2}\left(\frac{m^2}{R}\right)^n - m^2\frac{c_1}{c_2^3}\left(\frac{m^2}{R}\right)^{2n} + \mathcal{O}\left[\left(\frac{m^2}{R}\right)^{3n}\right], \tag{2.2.7}$$

which can also be viewed as a small m expansion. Using the estimate $R \approx \kappa^2\rho$ from the previous section with the "laboratory vacuum" $\rho = 10^{-10}$ g/cm^3 gives

$$\frac{m^2}{R} \approx \frac{m^2}{\kappa^2\rho} \approx 8.6 \times 10^{-21}, \tag{2.2.8}$$

so truncating the expansion is valid provided

$$\frac{1}{c_2}\left(\frac{m^2}{R}\right)^n \approx \frac{10^{-20n}}{c_2} \ll 1.$$

This is hardly a stringent requirement on c_2, as can be seen from Figure 2.2.3. The solar system constraint on $\left|\bar{f}_{\chi 0}\right|$ is more interesting. Requiring that the model reproduce the known gravitational field of the sun Hu and Sawicki [4] found that

$$\left|\bar{f}_{\chi 0}\right| < 74\left(1.23 \times 10^6\right)^{n-1}\left[\left(\frac{12}{\Omega_M} - 9\right)\frac{\Omega_M h^2}{0.13}\right]^{-(n+1)}. \tag{2.2.9}$$

This translates into a bound on c_2:

$$c_2 > 0.213919 \times n7.552^{-n-1}41.4419^{n+1}\left(1.23 \times 10^6\right)^{1-n}$$

which is also shown in Figure 2.2.3. The $n \to 0$ limit of this bound gives $\left|\bar{f}_{\chi 0}\right| < 1.5 \times 10^{-6}$.

Truncating the expansion to first order in $\left(m^2/R\right)^n$ and using (2.1.31) gives

$$\begin{aligned} f(\chi) &= \chi - m^2\frac{c_1}{c_2} + m^2\frac{c_1}{c_2^2}\left(\frac{m^2}{\chi}\right)^n, \\ f_\chi &= 1 - n\frac{c_1}{c_2^2}\left(\frac{m^2}{\chi}\right)^{n+1}, \\ \kappa\phi &= -\sqrt{\frac{3}{2}}\ln\left[1 - n\frac{c_1}{c_2^2}\left(\frac{m^2}{\chi}\right)^{n+1}\right]. \end{aligned}$$

It is necessary to truncate at this order in order to solve for χ explicitly in terms of ϕ. Doing so gives

$$\chi = m^2\left[\frac{c_2^2}{c_1}\frac{1 - \exp\left(-\sqrt{\frac{2}{3}}\kappa\phi\right)}{n}\right]^{-\frac{1}{n+1}}.$$

Using the estimate $R \approx \kappa^2\rho$ again gives

$$\kappa\phi \approx \sqrt{\frac{3}{2}}n\frac{c_1}{c_2^2}\left(\frac{m^2}{\kappa^2\rho}\right)^{n+1} \approx -\bar{f}_{\chi 0}\sqrt{\frac{3}{2}}\left[\left(\frac{12}{\Omega_M} - 9\right)\frac{m^2}{\kappa^2\rho}\right]^{n+1}, \tag{2.2.10}$$

which, similarly to exponential gravity, is small in the local environment. However, unlike exponential gravity ϕ is not exponentially small. Also, the free parameter c_1/c_2^2, or equivalently $\bar{f}_{\chi 0}$, could possibly be chosen large enough that the scalar field would become observable at the laboratory scale. Also note that the maximum value of ϕ for a given density ρ is obtained in the $n \to 0$ limit. It is shown in section 2.4 that the potential energy of a neutron due to its interaction with the

scalar field is proportional to ϕ. The $n \to 0$ limit then provides the best detection prospects for the Hu-Sawicki model at GRANIT.

The form of the scalar potential (2.1.33) for general n is quite complicated. However, for specific values of n it can be evaluated straightforwardly with a computer algebra package such as Mathematica. Sample code for this is provided in Appendix C. Using (2.2.5) and (2.2.6) to eliminate c_1 and c_2 in terms of the cosmological parameters and $\bar{f}_{\chi 0}$, then using the numerical values of Ω_Λ and Ω_M from the first chapter, gives the scalar potentials for several values of n, where $u \equiv \kappa\phi$:

$$V(\phi) = \frac{m^2}{\kappa^2} \times \begin{cases} 7.91485 - 48.6041\left(\bar{f}_{\chi 0}^2 u\right)^{1/3} + 265.308\left(\bar{f}_{\chi 0}^4 u^2\right)^{1/3} + \left(12.9249 - 1357.69\bar{f}_{\chi 0}^2\right) u & n = \frac{1}{2}, \\ 7.91485 - 31.3262\sqrt{-\bar{f}_{\chi 0}}\sqrt{u} + \left(12.9249 - 92.9895\bar{f}_{\chi 0}\right) u + O\left(u^{3/2}\right) & n = 1, \\ 7.91485 - 22.714\left(-\bar{f}_{\chi 0}\right)^{1/3} u^{2/3} + 12.9249u + O\left(u^{4/3}\right) & n = 2, \\ 7.91485 - 19.852\left(-\bar{f}_{\chi 0}\right)^{1/4} u^{3/4} + 12.9249u + O\left(u^{5/4}\right) & n = 3, \\ 7.91485 - 18.4236\left(-\bar{f}_{\chi 0}\right)^{1/5} u^{4/5} + 12.9249u + O\left(u^{6/5}\right) & n = 4. \end{cases} \tag{2.2.11}$$

Numerical values are used for the coefficients because they are complicated expressions in the model parameters. Analytical expressions can be obtained if needed, however, by using the provided Mathematica code. Examples of $V(\phi)$ are shown in Figures 2.2.5 and 2.2.6. Also note that $V(\phi)$ is $\sim m^2/\kappa^2 \sim 10^{-30}$ g/cm^3 within several orders of magnitude depending on the parameters.

The potential can be expanded at small n, but numerical experiments show that this expansion does not converge fast enough to be useful for practical calculations. Developing techniques to examine the Hu-Sawicki theory in the small n limit may be a topic worthy of further study since this limit is expected to give the largest deviation from GR at laboratory scales.

The stability conditions discussed above are based on a linearised analysis. A study of the fully non-linear Hu-Sawicki model shows that the model develops "weak" singularities at the curvatures relevant to the interior of neutrons stars and the early universe prior to big bang nucleosynthesis (BBN) [89]. These singularities ruin the ability to uniquely predict the future evolution of a given initial state. Appleby *et al.* [89] have shown that these singularity problems must be cured by adding a term proportional to R^2 to $f(R)$:

$$f_{\text{corrected}}(R) = f(R) + \frac{R^2}{6M^2},$$

where M is a parameter with dimensions of mass. M must be sufficiently large to avoid problems with BBN. Surprisingly, Appleby *et al.* [89] found that the R^2 term can produce the early universe inflation required to avoid the flatness, horizon, and monopole problems as discussed in Chapter 1. Thus the corrected model unifies early and late time acceleration of the universe (except that, of course, the scales m and M differ by many orders of magnitude and both must be set by hand).

The corrected Hu-Sawicki model of Appleby *et al.* requires further modification to survive the end of inflation. When inflation ends a process called reheating takes place where fluctuations of the scalar field (either ϕ or any other field which might drive inflation) decay into particle-antiparticle pairs. This conversion must take place rapidly enough, otherwise there will be an over-abundance of scalar particles during BBN [89, 90]. This is ensured by taking M large enough. Also, during reheating the scalar curvature R oscillates violently, becoming large and negative during every oscillation. For the theory to be well defined the function $f(R)$ must be extended smoothly to $R < 0$, which requires that n be an even integer: for non-integer n there is a branch point at $R = 0$

and for odd integer n there is a pole at $R = -m^2 c_2^{-1/n}$. Thus the smallest viable n for the corrected Hu-Sawicki model is $n = 2$.

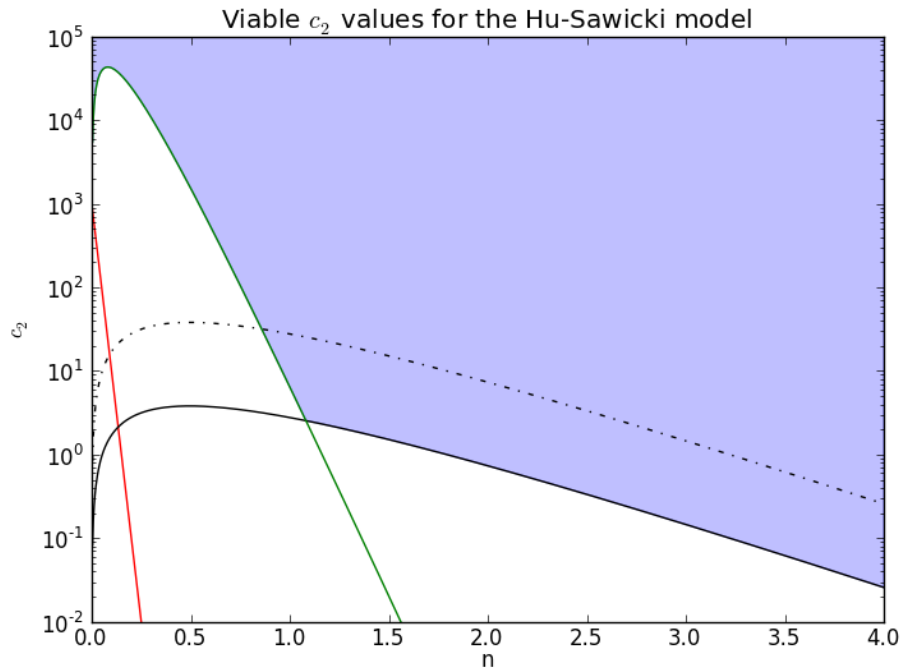

Figure 2.2.3: Parameter space for the cosmologically viable Hu-Sawicki model. The red line is the condition $c_2 \gg 10^{-20n}$, taken as $c_2 > 10^3 \times 10^{-20n}$, for the validity of the small m^2/R expansion on which the present analysis depends. The green line is the constraint on $|\bar{f}_{\chi 0}|$ from solar system tests (equation (2.2.9) and figure 2.2.4). The black line is the constraint $|\bar{f}_{\chi 0}| < 1$. The blue region satisfies both constraints. The black dash dotted line is $|\bar{f}_{\chi 0}| = 0.1$. The viable models form a subset of the blue region, the detailed shape of which has not been computed.

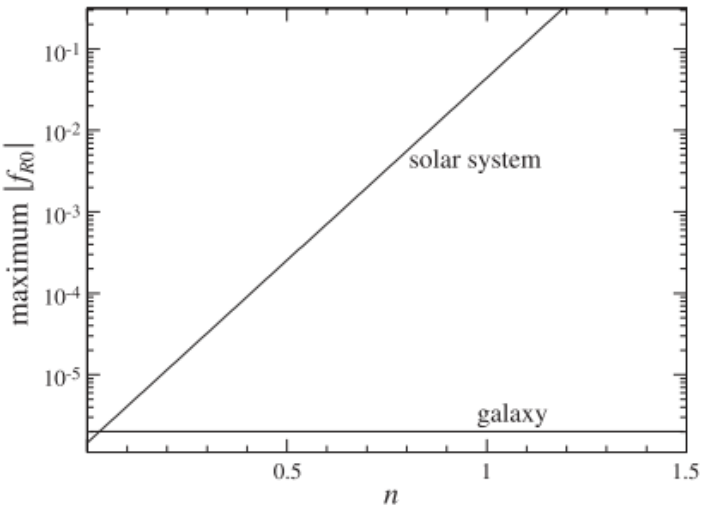

Figure 2.2.4: Limits on $|\bar{f}_{\chi 0}|$ from Solar System constraints [4]. Models above the line labelled "galaxy" predict modified galactic structure formation which could, in principle, be tested by studies of structure formation and galaxy surveys. Reproduction of Figure 9 of [4].

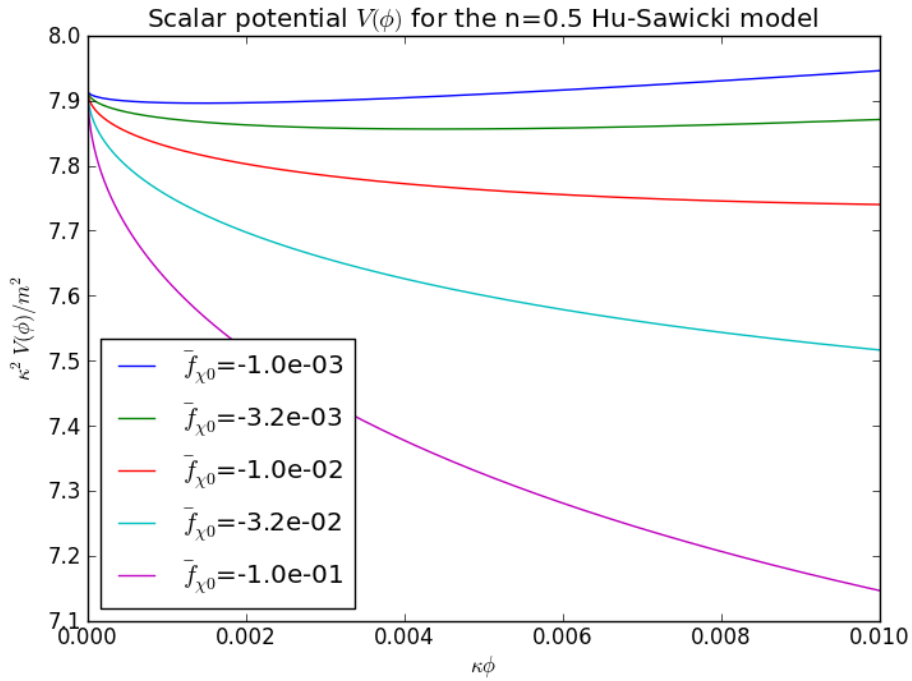

Figure 2.2.6: Scalar potential $V(\phi)$ for the $n = \frac{1}{2}$ Hu-Sawicki model for varying values of $\bar{f}_{\chi 0}$.

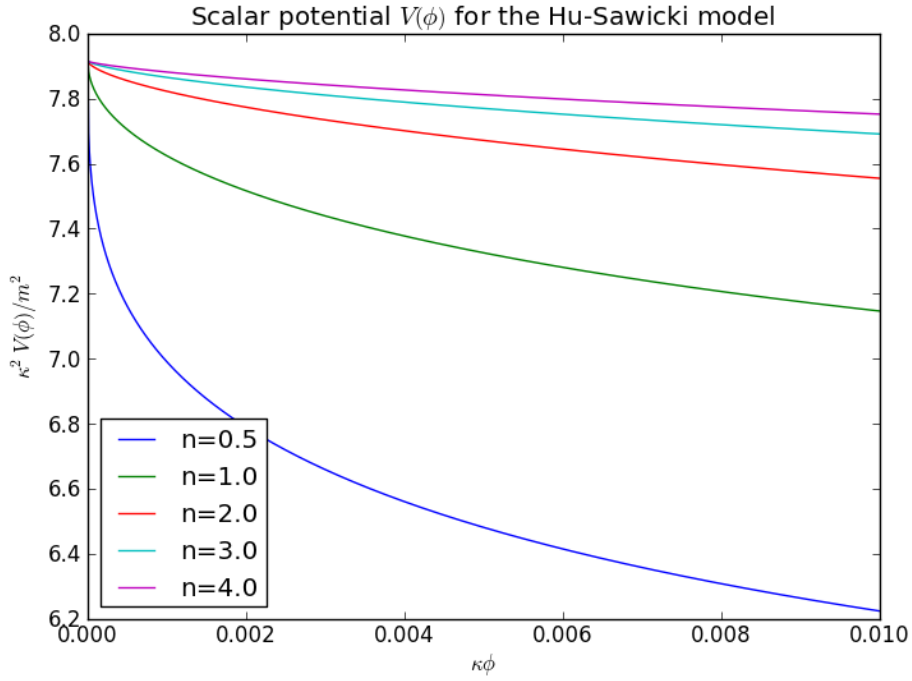

Figure 2.2.5: Scalar potential (2.2.11) for the cosmologically viable Hu and Sawicki model (2.2.3) for $\bar{f}_{\chi 0} = -0.1$.

2.2.3 The model of Xu and Chen: "New Exponential Gravity"

Another viable model is the "new exponential gravity" model of Xu and Chen [5]:

$$f(R) = (R - \lambda c)\, \mathrm{e}^{\lambda (c/R)^{\tilde{n}}}, \tag{2.2.12}$$

where $\lambda \geq 1$, $\tilde{n} > 3$ and $c > 0$ ($\tilde{n}$ is used to distinguish the parameter from the n of the Hu-Sawicki model). These parameter constraints are dictated by stability requirements. In addition the limits $\lambda \gg 1$ and $\tilde{n} \gg 3$ reduce to GR with a cosmological constant. The range of parameters of most interest is $3 < \tilde{n} \leq 4$, $\lambda \sim 1$, which gives the greatest deviation from GR [5]. At large curvatures $R \gg c$ the exponential can be expanded giving

$$f(R) = R - \lambda c + \lambda c^{\tilde{n}} R^{-\tilde{n}+1} - \lambda^2 c^{\tilde{n}+1} R^{-\tilde{n}} + \mathcal{O}\left[(\lambda c)^{2\tilde{n}} \left(\frac{1}{R} \right)^{2\tilde{n}-1} \right].$$

If the fourth term is negligible compared to the third

$$\frac{\lambda^2 c^{\tilde{n}+1} R^{-\tilde{n}}}{\lambda c^{\tilde{n}} R^{-\tilde{n}+1}} = \frac{\lambda c}{R} \ll 1, \tag{2.2.13}$$

then the model can be identified as a Hu-Sawicki model with the parameters related by

$$\begin{aligned} m^2 \frac{c_1}{c_2} &= \lambda c, \\ m^{2n+2} \frac{c_1}{c_2^2} &= \lambda c^{\tilde{n}}, \\ n &= \tilde{n} - 1. \end{aligned}$$

At this level of approximation then, the Xu-Chen models correspond to Hu-Sawicki models with $n > 2$, which are unobservable at GRANIT (to be shown in Chapter 3). Thus the only way the Xu-Chen models could be detectable at neutron bouncer experiments is if the inequality (2.2.13) is not satisfied. However, in the high curvature limit for a cosmologically viable model $\lambda c \to 2\Lambda$ since the theory approaches GR with a cosmological constant, i.e. ΛCDM [5]. Thus, using $R \approx \kappa^2 \rho$ as before,

$$\frac{\lambda c}{R} \approx \frac{2\Lambda}{\kappa^2 \rho} \approx 10^{-19},$$

at a density $\rho = 10^{-10}$ g/cm^3. The deviations from the Hu-Sawicki model are comparably small, thus the model of Xu and Chen is unobservable at neutron bouncer experiments.

Finally, (2.2.12) has an essential singularity at $R = 0$, so it seems likely that this model has problems with reheating in the early universe similar to the Hu-Sawicki model, even with the R^2 correction term of Appleby *et al.* added to the Lagrangian. However, to my knowledge, no detailed examination of this has been carried out.

2.2.4 The models of Appleby *et al.* and Starobinsky

There are two other viable models known to the me. Appleby *et al.* propose [89]:

$$f(R) = (1 - g)\, R + g\epsilon \ln \left[\frac{\cosh\left(\frac{R}{\epsilon} - b \right)}{\cosh b} \right] + \frac{R^2}{6M^2}, \tag{2.2.14}$$

where g, ϵ, b, and M are parameters discussed in their paper. This model is motivated by the desire to unify early and late time inflation and to cure the non-linear stability problems that

plague the Hu-Sawicki model at large curvatures. At intermediate curvatures, such as those in the laboratory environment, (2.2.14) appears qualitatively similar to the Hu-Sawicki model. This model is not studied any further here but it merits further investigation.

Starobinsky proposed a model motivated by a desire to eliminate the cosmological constant [90]:

$$f(R) = R + \lambda R_0 \left[\left(1 + \frac{R^2}{R_0^2} \right)^{-n} - 1 \right].$$

This obeys $f(0) = 0$ so there is no cosmological constant in the model. This qualitatively similar to the Hu-Sawicki model and is not discussed further here.

2.3 The Field of a Mirror

In this section the field equations (2.1.34) and (2.1.35) are solved to obtain the field above a neutron mirror. The weak field non-relativistic limit is valid in this regime. Ignoring the back-reaction of the energy density of the scalar field $T_{00}^{(\phi)}$ on the gravitational field of the Earth[9], the solution of (2.1.34) is the well known Newtonian limit of GR [14, 15]:

$$\mathrm{d}\tilde{s}^2 \equiv \tilde{g}_{\mu\nu}\mathrm{d}x^\mu \mathrm{d}x^\nu = -(1+2\Phi)\,\mathrm{d}t^2 + (1-2\Phi)\left(\mathrm{d}x^2 + \mathrm{d}y^2 + \mathrm{d}z^2\right), \tag{2.3.1}$$

where Φ is the Newtonian gravitational potential. This potential is sourced by a mass density $\tilde{\rho} = \Omega^4\rho$, where ρ is the (physical) Jordan frame matter density. Due to the thin shell screening, ϕ takes on its bulk value ϕ_b throughout the interior of the Earth except for a thin layer at the surface. The effective mass sourcing the Newtonian potential is thus $M_{\text{eff}} = \Omega_b^4 M_\oplus = \exp\left[4\frac{\kappa}{\sqrt{6}}\phi_b\right] M_\oplus$. The approximation $\kappa\phi_b \ll 1$ is valid, so that the potential is $\Phi = \Phi_\oplus + \mathcal{O}(\kappa\phi_b\Phi_\oplus)$ where $\Phi_\oplus = -GM_\oplus/(z + R_\oplus)$ is the classical Newtonian potential. The correction of order $\kappa\phi_b\Phi_\oplus$ is a negligible product of small quantities so from now on the $\oplus$ is dropped from $\Phi_\oplus$. At the surface of the Earth[10] $\Phi \approx 7 \times 10^{-10}$.

The static, non relativistic limit of (2.1.35) is, using $\tilde{T} \approx -\tilde{\rho} = -\Omega^4\rho$,

$$\nabla^2\phi = \frac{\mathrm{d}}{\mathrm{d}\phi}\left[V(\phi) + \frac{1}{4}\exp\left(4\frac{\kappa}{\sqrt{6}}\phi\right)\rho\right].$$

Since the experimental region is of the order of centimetres in size and the neutron wavefunctions extend over several tens of microns [66] the mirror is idealised to a uniform mass density, with a flat horizontal interface in contact with laboratory vacuum [2]. The matter density is

$$\rho = \begin{cases} \rho_m & z < 0, \\ \rho_v & z > 0, \end{cases}$$

where ρ_m is the mirror density and ρ_v is the vacuum density. Brax and Pignol took $\rho_m = 2.6\ \mathrm{g/cm^3}$ in their study of the original chameleon model at GRANIT [2].

Little is available in the literature about the vacuum density currently used at GRANIT. An estimate based on a partial pressure of 10^{-7} torr of Fomblin, an oil used in high vacuum systems [91], gives $\rho_v \approx 10^{-10}\ \mathrm{g/cm^3}$. Baessler *et al.* [92] mention a problem with vacuum degradation of the neutron detector, a polymer based solid state nuclear track detector, which requires a portion

[9] This assumption is checked shortly.

[10] In units where $c = 1$ the gravitational potential, an energy per unit mass, is dimensionless. To restore units multiply Φ by c^2.

of dissolved oxygen to participate in the chemical reactions during track formation. In a high vacuum the oxygen gradually out-gasses, reducing the sensitivity of the detector. Baessler *et al.* [92] suggest performing the experiment in an oxygen atmosphere at a pressure of ~ 100 millibar. At this pressure the vacuum density could be as large as 1.3×10^{-4} g/cm^3. Since the equilibrium field value decreases with increasing density (c.f. Figure 2.1.1) the estimate $\rho_v \sim 10^{-10}$ g/cm^3 provides an optimistic over-estimate of the field, usually by orders of magnitude. Therefore, if a model is found to be undetectable at $\rho_v \sim 10^{-10}$ g/cm^3 it will certainly be undetectable at a more realistic operating point. It is important to note that this is a technological limitation which could conceivably be eliminated, not a fundamental one.

The field equation (2.1.35) reduces to

$$\frac{\mathrm{d}^2\phi}{\mathrm{d}z^2} = \frac{\mathrm{d}V}{\mathrm{d}\phi} + \frac{\kappa}{\sqrt{6}}\rho, \tag{2.3.2}$$

with boundary conditions appropriate to a planar slab: $\mathrm{d}\phi/\mathrm{d}z \to 0$ as $z \to \pm\infty$. Continuity of ϕ and $\mathrm{d}\phi/\mathrm{d}z$ are required at $z = 0$. These are satisfied if the field reaches an extremum of the effective potential

$$V_{\text{eff}} \equiv V + \frac{1}{4}\exp\left(4\frac{\kappa}{\sqrt{6}}\phi\right)\rho$$

as $z \to \pm\infty$. Let the extrema of the effective potential be denoted $\phi_\pm$, where the sign indicates the sign of z. To leading order in $\kappa^2\phi\rho$ the extrema are given by,

$$\frac{\mathrm{d}V_\pm}{\mathrm{d}\phi} \equiv \frac{\mathrm{d}V}{\mathrm{d}\phi}\left(\phi = \phi_\pm\right) = -\frac{\kappa}{\sqrt{6}}\rho_{v,m}. \tag{2.3.3}$$

This can be used to eliminate ρ from equation (2.3.2):

$$\frac{\mathrm{d}^2\phi}{\mathrm{d}z^2} = \frac{\mathrm{d}V}{\mathrm{d}\phi} - \frac{\mathrm{d}V_\pm}{\mathrm{d}\phi} + \mathcal{O}\left(\kappa^2\phi\rho\right),$$

where the $\pm$ sign corresponds to $z \gtrless 0$ respectively. The effective potential is

$$V_{\text{eff}} = V - \phi\frac{\mathrm{d}V_\pm}{\mathrm{d}\phi}.$$

There is a simple mechanical analogy for equation (2.3.2). If one thinks of z as time and ϕ as a spatial coordinate then equation (2.3.2) is Newton's law for a particle moving in one dimension under the influence of a time dependent potential $-V_{\text{eff}}\left(\phi, \rho\left(z\right)\right)$. A thin shell solution has the following interpretation: the particle starts near the top of a potential hill at ϕ_- and begins rolling down. Then at $z = 0$ the particle receives a sudden kick from the discontinuous change in $\rho\left(z\right)$, and the potential hill moves to ϕ_+. The particle then rolls up the new hill with just enough energy to come to rest at the top, $\phi = \phi_+$. This analogy shows that away from $z = 0$ the "energy" is conserved:

$$\epsilon = \frac{1}{2}\left(\frac{\mathrm{d}\phi}{\mathrm{d}z}\right)^2 - V_{\text{eff}}.$$

Applying the boundary conditions to this equation gives

$$\frac{1}{2}\left(\frac{\mathrm{d}\phi}{\mathrm{d}z}\right)^2 - V_{\text{eff}} = \begin{cases} -V_{\text{eff}}\left(\phi_+, \rho_v\right) & z > 0, \\ -V_{\text{eff}}\left(\phi_-, \rho_m\right) & z < 0. \end{cases} \tag{2.3.4}$$

Algorithm 1 Algorithm for finding the scalar field profile above a mirror.

Given $V(\phi)$, ρ_m, ρ_v:

1. Compute $\phi_\pm$ by solving (2.3.3).
2. Find ϕ_0 using (2.3.5).
3. Find $z(\phi)$ by integrating (2.3.7).
4. Invert $z(\phi)$ and interpolate onto the desired z grid to obtain $\phi(z)$.

Continuity of ϕ and $\mathrm{d}\phi/\mathrm{d}z$ at $z = 0$ gives

$$V_{\text{eff}}(\phi_0, \rho_m) - V_{\text{eff}}(\phi_-, \rho_m) = V_{\text{eff}}(\phi_0, \rho_v) - V_{\text{eff}}(\phi_+, \rho_v),$$

allowing ϕ_0 to be found:

$$\phi_0 = \frac{V(\phi_-) - V(\phi_+) + \phi_+ \frac{\mathrm{d}V_+}{\mathrm{d}\phi} - \phi_- \frac{\mathrm{d}V_-}{\mathrm{d}\phi}}{\frac{\mathrm{d}V_+}{\mathrm{d}\phi} - \frac{\mathrm{d}V_-}{\mathrm{d}\phi}}. \tag{2.3.5}$$

Once ϕ_0 is in hand, (2.3.4) can be integrated to give an implicit expression for $\phi(z)$:

$$z = \int_{\phi_0}^{\phi(z)} \frac{\mathrm{d}\phi}{\sqrt{2\left[V_{\text{eff}}(\phi, \rho_v) - V_{\text{eff}}(\phi_+, \rho_v)\right]}} \tag{2.3.6}$$

$$= \int_{\phi_0}^{\phi(z)} \frac{\mathrm{d}\phi}{\sqrt{2\left[V(\phi) - V(\phi_+) + \frac{\kappa}{\sqrt{6}}\rho_v(\phi - \phi_+)\right]}}, \tag{2.3.7}$$

for $z > 0$ and an analogous (though not of interest) equation for $z < 0$. A procedure for finding the field profile above the mirror is Algorithm 1.

Finally, the assumption that the back-reaction of the scalar field can be neglected must be checked. This requires $T_{00}^{(\phi)} \ll \rho$. Using equation (2.1.36) for a static, nearly homogeneous $\phi = \phi_b$ gives

$$T_{00}^{(\phi)} = (1 + 2\Phi) V(\phi_b) \approx V(\phi_b).$$

Unfortunately this quantity is model dependent. Using exponential gravity (2.2.2) as the basis for an estimate,

$$V(\phi_b) \approx \frac{18 H_0^2 \Omega_m}{2\kappa^2} \sim \frac{H_0^2}{\kappa^2} \sim 10^{-30}\ \mathrm{g/cm^3},$$

which is totally negligible compared to the density of the Earth. Similarly for the Hu-Sawicki model $V(\phi) \sim m^2/\kappa^2 \sim 10^{-30}\ \mathrm{g/cm^3}$. Hence the back-reaction can be safely neglected.

2.4 Bouncing Neutrons

To find the gravitational energies of neutrons confined above a mirror it is necessary to solve the Schrödinger equation in the curved spacetime above the mirror, which requires knowledge of the metric. Working in the Jordan frame ensures that the energy eigenvalues correspond to the physical energies of the system, thus the Jordan frame metric is required. Combining equations (2.1.12),

(2.1.31) and (2.3.1) gives

$$g_{\mu\nu}\mathrm{d}x^\mu\mathrm{d}x^\nu = -\exp\left(2\frac{\kappa}{\sqrt{6}}\phi\right)(1+2\Phi)\,\mathrm{d}t^2 + \exp\left(2\frac{\kappa}{\sqrt{6}}\phi\right)(1-2\Phi)\left(\mathrm{d}x^2+\mathrm{d}y^2+\mathrm{d}z^2\right).$$

Neglecting terms of order $(\kappa\phi)^2$ and $\kappa\phi\Phi$,

$$g_{\mu\nu}\mathrm{d}x^\mu\mathrm{d}x^\nu = -(1+2\mathcal{A})\,\mathrm{d}t^2 + (1-2\mathcal{B})\left(\mathrm{d}x^2+\mathrm{d}y^2+\mathrm{d}z^2\right), \tag{2.4.1}$$

where the effective gravitational potentials are

$$\begin{aligned}\mathcal{A} &= \Phi + \frac{\kappa}{\sqrt{6}}\phi, \\ \mathcal{B} &= \Phi - \frac{\kappa}{\sqrt{6}}\phi.\end{aligned} \tag{2.4.2}$$

Since there are two gravitational potentials this expression differs from the standard Newtonian limit of GR. One could simply postulate that the gravitational potential energy is $m_N\mathcal{A}$ where m_N is the neutron mass (this is what [2] did), but it is worth re-deriving the Schrödinger equation from a fully relativistic theory to verify that this is correct. The natural place to begin is the Dirac equation for a neutral particle in curved spacetime. This theory is standard but not well known outside of a specialist community. Further information can be found in [93–95]. The Dirac equation in curved spacetime is[11]:

$$\left(\gamma^a e_a^\mu \nabla_\mu + m_N\right)\Psi = 0. \tag{2.4.3}$$

Here γ^a are the 4x4 Dirac gamma matrices which obey the algebra [34]

$$\left\{\gamma^a,\gamma^b\right\} \equiv \gamma^a\gamma^b + \gamma^b\gamma^a = 2\eta^{ab}, \tag{2.4.4}$$

and Hermiticity conditions $\left(\gamma^{\hat{t}}\right)^\dagger = -\gamma^{\hat{t}}$, $\left(\gamma^k\right)^\dagger = \gamma^k$. Only the algebraic properties of the γ^a matrices matter. Many explicit representations of the gamma matrices exist, and all are unitarily equivalent to each other. That said, it is often useful to choose a specific representation (this is done in Appendix B). Covariant quantities can be constructed out of the spinor field Ψ using the adjoint $\bar{\Psi} \equiv \Psi^\dagger i\gamma^{\hat{t}}$. For instance, $J^a \equiv \bar{\Psi}i\gamma^a\Psi$ is a conserved current. The time component $J^{\hat{t}}$ is the neutron density and the normalisation condition is

$$\int \mathrm{d}^3x\sqrt{-g^{(3)}}J^{\hat{t}} = \int \mathrm{d}^3x\sqrt{-g^{(3)}}\Psi^\dagger\Psi = 1,$$

where $g^{(3)}_{\mu\nu}$ is the restriction of the metric to a $t=$ constant surface.

The other quantities in (2.4.3) are the tetrad fields e_a^μ (c.f. (2.1.2)) and the spinor covariant derivative ∇_μ,

$$\nabla_\mu = \partial_\mu + \frac{1}{8}\omega_{\mu bc}\left[\gamma^b,\gamma^c\right],$$

where $\omega_{\mu bc}$ is the spin connection (c.f. (2.1.6)). The spin connection term keeps track of the interaction of the gravitational field with the spin of the neutron. The computation of the spin connection and covariant derivative is not enlightening. The only point worth noting is that in the weak field limit only terms of order $\mathcal{A}$, $\mathcal{B}$ and their derivatives are kept. Refer to Appendix A for

[11] Note: there are several conventions which differ by factors of i in various places.

details. The result for the spinor covariant derivative is equation (A.0.6).

The Dirac equation is valid for neutrons at any speed. However, the neutrons in the bouncer experiment are slow, with typical speeds of the order of metres per second. The reduction of the Dirac equation to the non-relativistic limit is more tedious algebra (Appendix B), but the result is simply the Schrödinger equation (B.0.6)

$$-\frac{1}{2m_N}\nabla^2\psi + \mathcal{A}m_N\psi = \mathcal{E}\psi, \tag{2.4.5}$$

with gravitational potential energy $m\mathcal{A}$. This verifies the form of Schrödinger equation used in [2]. The nature of the higher order terms are relativistic kinetic energy corrections, couplings between spin and the gravitational field, and gradients of the gravitational field. In the absence of spin dependent couplings the Hamiltonian

$$\mathcal{H} \equiv -\frac{1}{2m_N}\nabla^2 + \mathcal{A}m_N$$

commutes with the spin angular momentum operators $S_k = \frac{1}{2}\sigma_k$, where σ_k are the Pauli matrices. As a result the wavefunction can be factorised $\psi = \psi(\vec{r})\,\chi_\pm$ where $\chi_\pm$ are two linearly independent constant two component spinors. The two spin states for each energy level are degenerate and (2.4.5) can be considered as an equation for the scalar wavefunction $\psi(\vec{r})$ in the absence of spin. The spin part of the wavefunction is dropped hereafter as irrelevant. If a perturbing magnetic field is introduced to induce transitions between the gravitational energy levels, as will be done at GRANIT, it would be necessary to consider spin dependent Hamiltonians. This thesis focuses on the stationary states of the unperturbed Hamiltonian for simplicity.

The boundary conditions on ψ are those appropriate to a bound system. The mirror is approximated as a hard wall for simplicity. In reality the mirror is a potential barrier with a height of 90 neV. As a result the neutron wavefunction penetrates several angstroms or nanometres into the mirror surface [1, 66]. This effect was also neglected in the chameleon theory study [2]. Quantifying the error caused by neglecting the mirror penetration is left to future work, but the error is expected to be small because 90 neV $\gg \mathcal{E}$ for the states of interest. The problem statement is thus completed by the conditions

$$\psi(0) = 0,$$
$$\psi \to 0 \text{ as } z \to \infty.$$

Finally, it is important to note that by the uncertainty principle the measurement of the energy levels is fundamentally limited by the time available to perform the measurement:

$$\Delta E \sim \frac{\hbar}{\tau} = \hbar\left(\frac{1}{\tau_{\text{loss}}} + \frac{1}{\tau_\beta}\right),$$

where $\tau_\beta = 881.5 \pm 1.5$ s is the neutron lifetime due to beta decay [7, 96] and τ_{loss}^{-1} represents all other loss mechanisms. The current GRANIT experiment operates in "flow through" mode [67] where the neutrons pass through the experiment in 75 ms. Other loss mechanisms are scattering from imperfections in the mirror or wall surfaces, losses due to vibrations of the apparatus (either thermal or seismic), and absorption into the nuclei of impurity atoms on the exposed surfaces of the experiment. At present these loss mechanisms dominate over β decay, hence GRANIT claims a sensitivity of 0.01 peV [1, 66]. By converting to a "neutron trap mode," where the neutrons are

trapped for several seconds in a well (consisting of a 30×30 cm^2 mirror and 500 μm high walls), the sensitivity is expected to increase by one or two orders of magnitude in the next several years. The Coriolis effect causes a broadening of the gravitational levels due to the horizontal velocity of the neutrons. This broadening is not currently important but could become so if the sources of neutron loss are reduced. The ultimate sensitivity defined by the neutron lifetime is 10^{-7} peV.

Chapter 3

Solution of the problem

This chapter deals with the solution of the neutron bouncer eigenvalue problem. Chapter 2 developed the formalism and discussed the theory of $f(R)$ gravity applied to the neutron bouncer. The resulting mathematical problem is defined by equations (2.3.2) (equivalently (2.3.7)), (2.4.2) and (2.4.5). In this chapter the classical neutron bouncer (with $\phi = 0$) is reviewed, and the field profile and Schrödinger equations for $f(R)$ are dealt with. For reference, the problem statement is reiterated here.

A horizontal mirror with mass density ρ_m is placed at $z < 0$ under a vacuum of density ρ_v at $z > 0$. Neutrons bounce in the Earth's gravitational field above the mirror, with the effects of modified gravity being accounted for through the inclusion of a scalar field ϕ in addition to the ordinary Newtonian potential Φ.

The scalar field ϕ is determined by

$$\frac{\mathrm{d}^2\phi}{\mathrm{d}z^2} = \frac{\mathrm{d}V}{\mathrm{d}\phi} + \frac{\kappa}{\sqrt{6}}\rho, \tag{3.0.1}$$

where

$$\rho = \begin{cases} \rho_m & z < 0, \\ \rho_v & z > 0. \end{cases}$$

For $f(R)$ gravity the scalar potential $V(\phi)$ is related to the functional form of $f(R)$ by equation (2.1.33). The only thing that differs between different $f(R)$ models is the scalar potential $V(\phi)$. The scalar field equation (3.0.1) is solved subject to the boundary conditions

$$\phi \to \phi_\pm \text{ as } z \to \pm\infty,$$

where the $\phi_\pm$ are constants determined by requiring that the right hand side of (3.0.1) goes to zero:

$$\frac{\mathrm{d}V}{\mathrm{d}\phi}(\phi = \phi_\pm) = -\frac{\kappa}{\sqrt{6}} \begin{cases} \rho_m & \phi = \phi_- \\ \rho_v & \phi = \phi_+ \end{cases}. \tag{3.0.2}$$

Equation (3.0.1) can be solved implicitly by quadrature and the solution is given by (2.3.7):

$$z(\phi) = \int_{\phi_0}^{\phi(z)} \frac{\mathrm{d}\phi}{\sqrt{2\left[V(\phi) - V(\phi_+) + \frac{\kappa}{\sqrt{6}}\rho_v(\phi - \phi_+)\right]}}, \tag{3.0.3}$$

where ϕ_0 is obtained by equation (2.3.5), rewritten somewhat as

$$\kappa\phi_0 = \frac{\sqrt{6}\left[V\left(\phi_-\right) - V\left(\phi_+\right)\right] + \kappa\phi_-\rho_m - \kappa\phi_+\rho_v}{\rho_m - \rho_v}. \tag{3.0.4}$$

The Schrödinger equation for the neutron in the gravitational field above the mirror is

$$\mathcal{E}\psi = -\frac{1}{2m_N}\nabla^2\psi + \left(\Phi + \frac{\kappa}{\sqrt{6}}\phi\right) m_N\psi,$$

where the Newtonian potential is

$$\Phi = -\frac{GM_\oplus}{z + R_\oplus} \approx -\frac{GM_\oplus}{R_\oplus} + \frac{GM_\oplus}{R_\oplus^2}z,$$

where $M_\oplus$, $R_\oplus$ are the mass and radius of the Earth, respectively. The motion in the x and y directions is free and is ignored for simplicity. Writing $g \equiv GM_\oplus/R_\oplus^2$, the Schrödinger equation is

$$\mathcal{E}'\psi = -\frac{1}{2m_N}\frac{\mathrm{d}^2\psi}{\mathrm{d}z^2} + \left(gz + \frac{\kappa}{\sqrt{6}}\phi\right) m_N\psi, \tag{3.0.5}$$

where

$$\mathcal{E}' = \mathcal{E} + \frac{GM_\oplus m_N}{R_\oplus}.$$

A uniform shift of the energy levels is unobservable and can be dropped. This is equivalent to measuring the gravitational potential relative to $z = 0$ rather than infinity, a convenient arrangement for the neutron bouncer problem. The prime on $\mathcal{E}'$ is dropped hereafter. The higher order corrections to the Newtonian potential are suppressed by $z/R_\oplus$ relative to the leading term. For the low lying gravitational states of neutrons this suppression is $\sim 10\ \mu\mathrm{m}/6400\ \mathrm{km} \sim 10^{-12}$.

In the absence of a magnetic field and neglecting relativistic corrections to (3.0.5), the spin part of the wavefunction separates and the two spin degrees of freedom of the neutron are energy degenerate. Thus, for the purposes of this thesis, it is sufficient to treat (3.0.5) as a scalar equation. Perfect reflection at the mirror surface and normalisability impose the boundary conditions

$$\psi\left(0\right) = 0,$$
$$\psi \to 0 \text{ as } z \to \infty.$$

In reality the neutron wavefunction penetrates into the mirror a distance of the order of nanometres, but this has a negligible impact on the energy levels.

Thus in broad outline the full computation has three steps:

1. Compute $V\left(\phi\right)$ for a given $f\left(R\right)$ model.
2. Compute $\phi\left(z\right)$ above the neutron mirror.
3. Find the eigenvalues of the Schrödinger equation.

The first step was already carried out for the exponential gravity and Hu-Sawicki models in Section 2.2.

For numerical purposes it is useful to introduce dimensionless quantities relative to the characteristic energy, length and density scales

$$\begin{aligned}\epsilon &= 1 \text{ peV} = 10^{-12} \text{ eV},\\ \ell &= 1\ \mu\text{m} = 10^{-6} \text{ m},\\ \rho_0 &= 10^{-10} \text{ g/cm}^3 = 4.31013 \times 10^{56} \text{ peV}^4,\end{aligned}$$

where the last equality follows in units where $\hbar = c = 1$. Let the dimensionless energy, coordinate and density be $E = \mathcal{E}/\epsilon$, $\zeta = z/\ell$ and $\bar{\rho} = \rho/\rho_0$ respectively (note that ρ_0 is chosen to be of the order of ρ_v) and define the dimensionless scalar field $\varphi = \kappa\phi/a$ where a is an adjustable constant. Using these variables and restoring factors of $\hbar$ and c (assigning $V(\phi) = \rho_0 \bar{V}(\phi)$ dimensions of mass density) equations (3.0.1) and (3.0.5) become

$$\frac{\mathrm{d}^2\varphi}{\mathrm{d}\zeta^2} = \frac{\hbar c^3 \kappa^2 \ell^2 \rho_0}{a^2}\frac{\mathrm{d}\bar{V}}{\mathrm{d}\varphi} + \frac{\hbar c^3 \kappa^2 \ell^2 \rho_0}{a\sqrt{6}}\bar{\rho}, \tag{3.0.6}$$

$$\frac{2m_N \ell^2 \epsilon}{\hbar^2} E\psi = -\frac{\mathrm{d}^2\psi}{\mathrm{d}\zeta^2} + \left(\frac{2m_N^2 g \ell^3}{\hbar^2}\zeta + \frac{2m_N^2 \ell^2 c^2}{\sqrt{6}\hbar^2} a\varphi\right)\psi. \tag{3.0.7}$$

All of the coefficients in the Schrödinger equation can be made $\mathcal{O}(1)$ if a is chosen appropriately as $a \sim \hbar^2/m_N^2 \ell^2 c^2 \approx 4.41 \times 10^{-20}$. Take $a = 10^{-20}$ exactly. Ideally the gravitational acceleration at the site of the experiment would be used, but here the standard value of 9.8 m/s^2 is used. Then, with the numerical values of the coefficients, the system becomes

$$\frac{\mathrm{d}^2\varphi}{\mathrm{d}\zeta^2} = A\frac{\mathrm{d}\bar{V}}{\mathrm{d}\varphi} + B\bar{\rho}, \tag{3.0.8}$$

$$\frac{\mathrm{d}^2\psi}{\mathrm{d}\zeta^2} = (C\zeta + D\varphi - KE)\,\psi, \tag{3.0.9}$$

where

$$\begin{aligned}A &\equiv \frac{\hbar c^3 \kappa^2 \ell^2 \rho_0}{a^2} = 1.8658 \times 10^{-5},\\ B &\equiv \frac{\hbar c^3 \kappa^2 \ell^2 \rho_0}{a\sqrt{6}} = 7.61709 \times 10^{-26},\\ C &\equiv \frac{2m_N^2 g \ell^3}{\hbar^2} = 0.00494419,\\ D &\equiv \frac{2m_N^2 \ell^2 c^2}{\sqrt{6}\hbar^2} a = 0.185122,\\ K &\equiv \frac{2m_N \ell^2 \epsilon}{\hbar^2} = 0.0482596.\end{aligned}$$

The φ equation appears badly scaled, but recall that in exponential gravity and the Hu-Sawicki model $V \sim 10^{-30}$ g/cm^3 and for laboratory vacuum $\rho \sim 10^{-10}$ g/cm^3 so both terms on the right hand side are of the order 10^{-25} within a few orders of magnitude.

The quadrature formula can be adapted to the new variables:

$$\zeta(\varphi) = L\int_{\varphi_0}^{\varphi} \frac{\mathrm{d}\varphi}{\sqrt{\bar{V} - \bar{V}_+ + \frac{a}{\sqrt{6}}\bar{\rho}_v(\varphi - \varphi_+)}}, \tag{3.0.10}$$

Table 3.1: Roots of the Airy function, energy, average height and height squared for the first ten energy levels of the Newtonian ($\phi = 0$) neutron bouncer.

n	a_n	$\mathcal{E}_n$ (peV)	$\langle z \rangle$ (μm)	$\langle z^2 \rangle$ (μm^2)
1	-2.33811	1.406	9.15	100
2	-4.08795	2.458	16.00	307
3	-5.52056	3.320	21.60	560
4	-6.78671	4.081	26.56	846
5	-7.94413	4.777	31.09	1159
6	-9.02265	5.426	35.31	1495
7	-10.0402	6.038	39.29	1852
8	-11.0085	6.620	43.08	2226
9	-11.9360	7.178	46.71	2617
10	-12.8288	7.715	50.20	3023

where the constant is

$$L = \frac{ac}{\kappa \ell \sqrt{2\rho_0}} = 163.701.$$

3.1 The Newtonian Problem

In the Newtonian case $\phi = 0$ the Schrödinger equation can be solved exactly [65]. The normalizable wavefunctions are Airy functions

$$u_n(z) = \frac{1}{\mathrm{Ai}'(a_n)} \left(\frac{\hbar^2}{2m_N^2 g}\right)^{-\frac{1}{6}} \mathrm{Ai}\left[\left(\frac{\hbar^2}{2m_N^2 g}\right)^{-\frac{1}{3}} \left(z - \frac{\mathcal{E}_n}{m_N g}\right)\right],$$

where $\mathrm{Ai}'(z) \equiv \frac{\mathrm{d}}{\mathrm{d}z}\mathrm{Ai}(z)$ and the energies are

$$\mathcal{E}_n = -m_N g \left(\frac{\hbar^2}{2m_N^2 g}\right)^{\frac{1}{3}} a_n = -\left(\frac{1}{2}\hbar^2 m_N g^2\right)^{\frac{1}{3}} a_n,$$

where a_n are the zeros of the Airy function. The first ten eigenvalues and the corresponding average heights $\langle z \rangle \equiv \langle u_n | z | u_n \rangle$ of the neutron are given in Table 3.1. Later the mean squared heights $\langle z^2 \rangle \equiv \langle u_n | z^2 | u_n \rangle$ will be useful, so these are given as well.

In terms of the dimensionless variables the wavefunctions and energies are

$$\sqrt{\ell} u_n(z) = \frac{C^{\frac{1}{6}}}{\mathrm{Ai}'(a_n)} \mathrm{Ai}\left[C^{\frac{1}{3}}\left(\zeta - \frac{K}{C}E_n\right)\right],$$
$$E_n = -\frac{C^{\frac{2}{3}}}{K} a_n.$$

3.2 The $f(R)$ Problem

In this section the scalar field profiles are examined, specializing to the exponential gravity and Hu-Sawicki models. The model of Xu and Chen was already shown to be indistinguishable from a Hu-Sawicki model at laboratory scales (c.f. Section 2.2.3). Since the actual field profile is bounded above by ϕ_+, a crude limit on the size of the predicted energy level shift can be computed with relatively little effort. This is used to show that only a small range of model-space is worth considering any further.

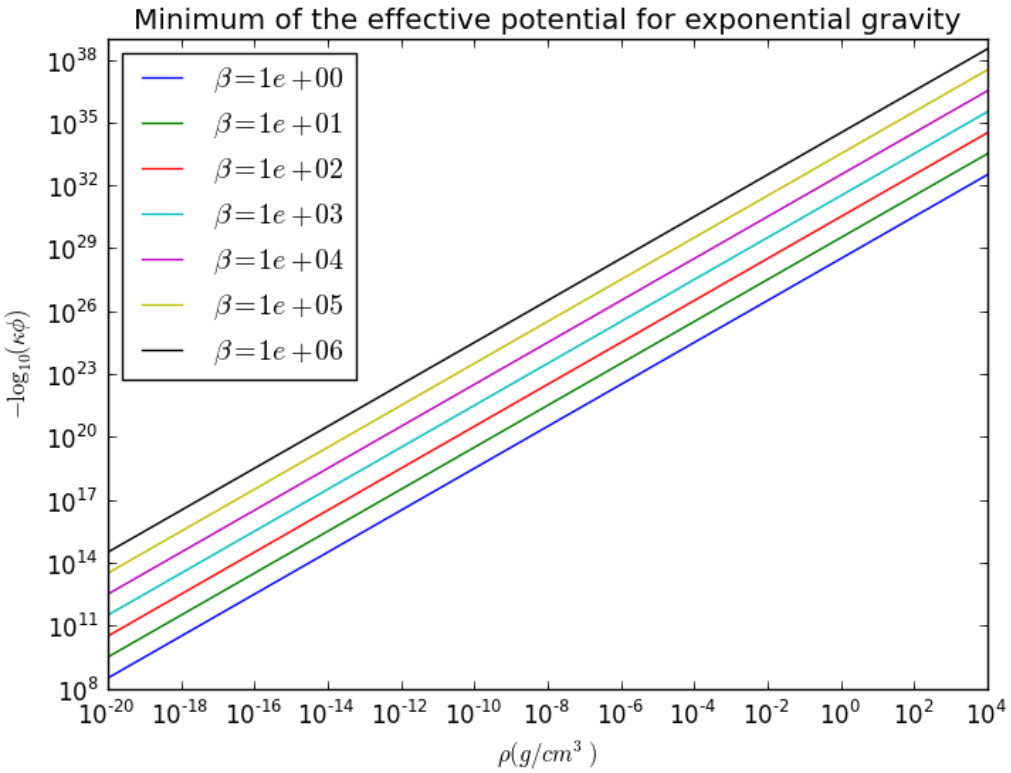

Figure 3.2.1: (Base 10 logarithm of) the minimum of $V_{\text{eff}}(\phi)$ for exponential gravity for several values of β. Since the model is constrained by $\beta > 1$ the field ϕ is bound to have an extremely small value at all but cosmological densities.

3.2.1 Exponential gravity

For exponential gravity the boundary conditions (3.0.2) on ϕ read

$$\kappa\phi_{\pm} = \sqrt{\frac{3}{2}}\beta \exp\left[-\beta\left(2 + \frac{\rho_{v,m}}{\rho_c}\right)\right], \tag{3.2.1}$$

where

$$\rho_c = \frac{18H_0^2\Omega_m}{\hbar c^5\kappa^2} = 1.344 \times 10^{-29}\ \text{g/cm}^3,$$

using $\Omega_m = 0.23$. It is worth noting that this density is comparable to the critical density of the universe (equation (1.1.3)):

$$\frac{\rho_{\text{crit}}}{\rho_c} = \frac{1}{6\Omega_m} \approx 0.725.$$

Even for the most rarefied laboratory vacuum available $\rho_v/\rho_c \gg 2$. The equilibrium field is shown as a function of density in Figure 3.2.1. Note that $\kappa\phi$ is exponentially small as promised in section 2.2.1.

It is worth estimating the contribution of the scalar field perturbation to the neutron energy before embarking on the full computation of the field profile. Since the field is small the interaction $\frac{\kappa}{\sqrt{6}}\phi m_N\psi$ can be treated as a perturbation. The well known result from time independent first order perturbation theory is [65]

$$\Delta\mathcal{E}_n^{(1)} = \left\langle u_n \left| \frac{\kappa}{\sqrt{6}}\phi m_N \right| u_n \right\rangle, \tag{3.2.2}$$

for the first order perturbation $\Delta\mathcal{E}_n^{(1)}$ to the n-th state. Since ϕ is bounded by ϕ_0 and ϕ_+ in the region $z > 0$ an upper bound can be estimated on the energy level shift

$$\Delta\mathcal{E}_n^{(1)} \lesssim \left\langle u_n \left| \frac{\kappa}{\sqrt{6}}\phi_+ m_N \right| u_n \right\rangle = \frac{\kappa}{\sqrt{6}}\phi_+ m_N \approx \frac{1}{2}\beta \exp\left\{-\beta\frac{\rho_v}{\rho_c}\right\} m_N,$$

where (3.2.1) was used in the last step. This gives, in the most optimistic case where $\beta \sim 1$,

$$\Delta\mathcal{E}_n^{(1)} \lesssim \exp\left(-10^{19}\right) m_N,$$

which is utterly undetectable. In fact, due to the uncertainty principle the minimum time necessary to measure an energy to this precision is

$$\tau \sim \frac{\hbar}{\Delta\mathcal{E}_n^{(1)}} \sim \exp\left(+10^{19}\right),$$

and it hardly matters what units are used. The time required is vastly greater than the age of the universe. Hence, exponential gravity will never be detectable in a neutron bouncer experiment. No further effort is spent on it here. Note that to reach a first order perturbation estimate of 1 peV would require a field of at least $\kappa\phi \sim 3 \times 10^{-21}$.

3.2.2 Hu and Sawicki

Recall the scalar potential for the Hu-Sawicki model (2.2.11):

$$V(\phi) = \frac{m^2}{\kappa^2} \times \begin{cases} 7.91485 - 48.6041\left(\bar{f}_{\chi 0}^2 u\right)^{1/3} + 265.308\left(\bar{f}_{\chi 0}^4 u^2\right)^{1/3} + \left(12.9249 - 1357.69\bar{f}_{\chi 0}^2\right) u & n = \frac{1}{2}, \\ 7.91485 - 31.3262\sqrt{-\bar{f}_{\chi 0}}\sqrt{u} + \left(12.9249 - 92.9895\bar{f}_{\chi 0}\right) u + O\left(u^{3/2}\right) & n = 1, \\ 7.91485 - 22.714\left(-\bar{f}_{\chi 0}\right)^{1/3} u^{2/3} + 12.9249u + O\left(u^{4/3}\right) & n = 2, \\ 7.91485 - 19.852\left(-\bar{f}_{\chi 0}\right)^{1/4} u^{3/4} + 12.9249u + O\left(u^{5/4}\right) & n = 3, \\ 7.91485 - 18.4236\left(-\bar{f}_{\chi 0}\right)^{1/5} u^{4/5} + 12.9249u + O\left(u^{6/5}\right) & n = 4, \end{cases}$$

where $u \equiv \kappa\phi$ and $\bar{f}_{\chi 0} \equiv \frac{\mathrm{d}f}{\mathrm{d}\chi}(t=0) - 1$ parametrises the present day deviation from general relativity at cosmological scales. The canonical choice of m gives $m^2/\kappa^2 \approx 8.6 \times 10^{-31}$ g/cm^3 (c.f. Section 2.2.2). The bounds on $\bar{f}_{\chi 0}$ depend on n, becoming weaker at large n. Recall from the discussion in section 2.2.2 that smaller values of n yield better detection prospects. Focus on the case $n = 1$ for the moment. The minimum of the effective potential can be found by a small extension of the Mathematica script in Appendix C:

$$\begin{aligned} \kappa\phi_{\min} = &\left(-2.58445 \times 10^3 \bar{f}_{\chi 0}\right) / \left[9.10921 \times 10^4 \bar{f}_{\chi 0}^2 - 2.53223 \times 10^4 \bar{f}_{\chi 0}\right. \\ &\left. -1.59967 \times 10^3 \frac{\kappa^2\rho}{m^2}\bar{f}_{\chi 0} + 7.02299\left(\frac{\kappa^2\rho}{m^2}\right)^2 + 1.75981 \times 10^3 + 2.22344 \times 10^2 \frac{\kappa^2\rho}{m^2}\right]. \end{aligned}$$

Since $\left|\bar{f}_{\chi 0}\right|$ is $\mathcal{O}(1)$ and $\kappa^2\rho/m^2 \gtrsim 10^{20}$ (c.f. (2.2.8)),

$$\kappa\phi_{\min} \lesssim -\frac{2.58445 \times 10^3 \bar{f}_{\chi 0}}{7.02299\left(\frac{\kappa^2\rho}{m^2}\right)^2} \lesssim 3 \times 10^{-38}.$$

Table 3.2: First order perturbation theory estimate (3.2.2) applied to the Hu-Sawicki model with $|f_{\chi 0}| \sim 1$ and various integer values of n.

n	$\Delta\mathcal{E}_k^{(1)}$ (peV)
1	10^{-17}
2	10^{-36}
3	10^{-54}
4	10^{-73}
5	10^{-92}
6	10^{-111}

Repeating the first order perturbation theory argument from the previous section,

$$\Delta\mathcal{E}_k^{(1)} \lesssim \left\langle u_k \left| \frac{\kappa}{\sqrt{6}}\phi_+ m_N \right| u_k \right\rangle = \frac{\kappa}{\sqrt{6}}\phi_+ m_N \approx 10^{-17} \text{ peV},$$

which is ten orders of magnitude below the ultimate gravitational sensitivity of 10^{-7} peV. Further, $\Delta\mathcal{E}_k^{(1)}$ is a rapidly decreasing function of n, as can be seen from Table 3.2. Thus the $n \geq 1$ Hu-Sawicki models are undetectable at a neutron bouncer experiment. However, these models are power-law suppressed rather than exponentially suppressed as in the exponential gravity model. This suggests that the $n < 1$ case is promising. This view is supported by Table 3.2. Unfortunately it becomes increasingly difficult to solve (3.0.2) for non-integer n. Also, recall from the discussion in Section 2.2.3, the unobservability of the $n > 2$ Hu-Sawicki models at GRANIT implies that the model of Xu and Chen is unobservable there as well.

Consider now the $n = 1/2$ case. Equation (3.0.2) can be rearranged to

$$-\frac{8\pi G\hbar^2}{\sqrt{6}m^2}\rho = -\frac{48.6041}{3}\left(\bar{f}_{\chi 0}^2 u_{\min}^{-2}\right)^{1/3} + \frac{265.308 \times 2}{3}\left(\bar{f}_{\chi 0}^4 u_{\min}^{-1}\right)^{1/3} + 12.9249 - 1357.69\bar{f}_{\chi 0}^2.$$

Since $u_{\min} \ll 1$ the first term dominates, hence

$$u_{\min} = \kappa\phi_{\min} \approx \frac{-\bar{f}_{\chi 0}}{\left(7.18458 \times 10^{28}\frac{\text{cm}^3}{\text{g}}\rho\right)^{3/2}}. \tag{3.2.3}$$

This is shown in Figure 3.2.2. It can be seen that $n = 1/2$ models which pass solar system tests require a very high vacuum $\rho_v \lesssim 10^{-13}$ g/cm^3 to approach the ultimate gravitational sensitivity level and a density of $\rho_v \lesssim 10^{-16}$ g/cm^3 to approach the current claimed GRANIT sensitivity. The latter density is 10^{12} times less dense than the suggested GRANIT operating point [92]. It must also be recalled that this is a necessary but not sufficient condition for the detectability of the energy level shifts. The high level of vacuum required is not promising for the detection of the $n = 1/2$ model, although undetectability is not shown rigorously until the next section.

It is worth checking (3.2.3) against the estimate (2.2.10) based on the approximation $R \approx \kappa^2\rho$. The ratio of (2.2.10) to (3.2.3) is ≈ 3.8. Thus the naive estimate (2.2.10) over-estimates the equilibrium field by less than an order of magnitude. An advantage of (2.2.10) is that it can be used for all n. The result for $n < 1/2$ is shown in Figure 3.2.3 for a large cosmological field $\bar{f}_{\chi 0}$. It can be seen that the Hu-Sawicki model is undetectable at GRANIT except possibly at the high vacuum, small n regime, and only then if several orders of magnitude improvement in the experimental sensitivity are made.

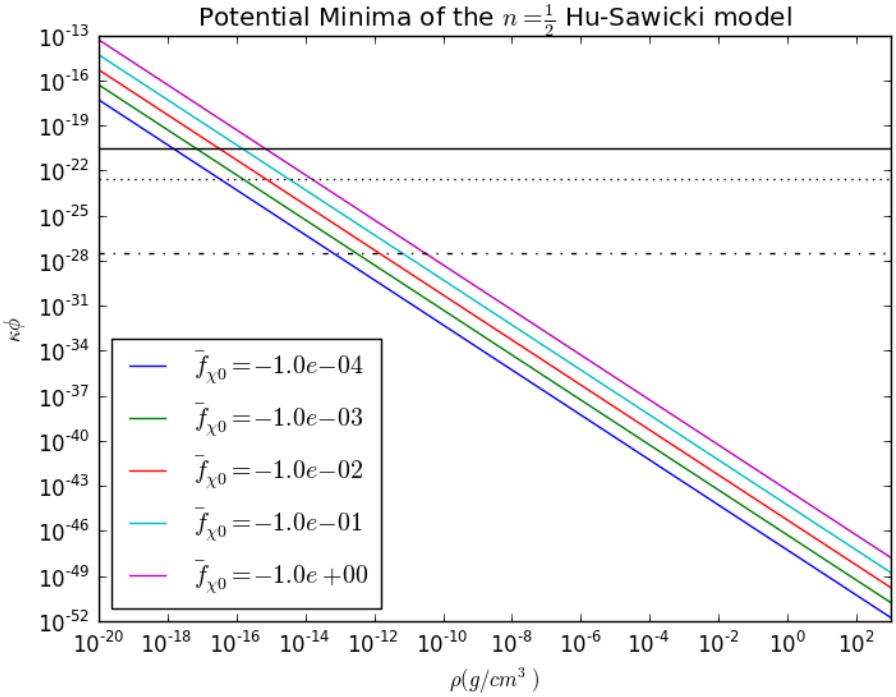

Figure 3.2.2: Minima of the effective potential $V_{\text{eff}}(\phi)$ for the $n = 1/2$ Hu-Sawicki model (2.2.11). The horizontal lines are the crude upper bound (3.2.2) on the energy level shifts for 1 peV (solid line), 0.01 peV (dotted line) - the claimed GRANIT sensitivity, and 10^{-7} peV (dash dotted line) - the ultimate gravitational sensitivity. Section 3.3 shows that the crude limit grossly overestimates the energy level shifts by about ten orders of magnitude because the thin shell effect is not sufficiently strong and the field never reaches ϕ_+ in the region just above the mirror where the neutrons are.

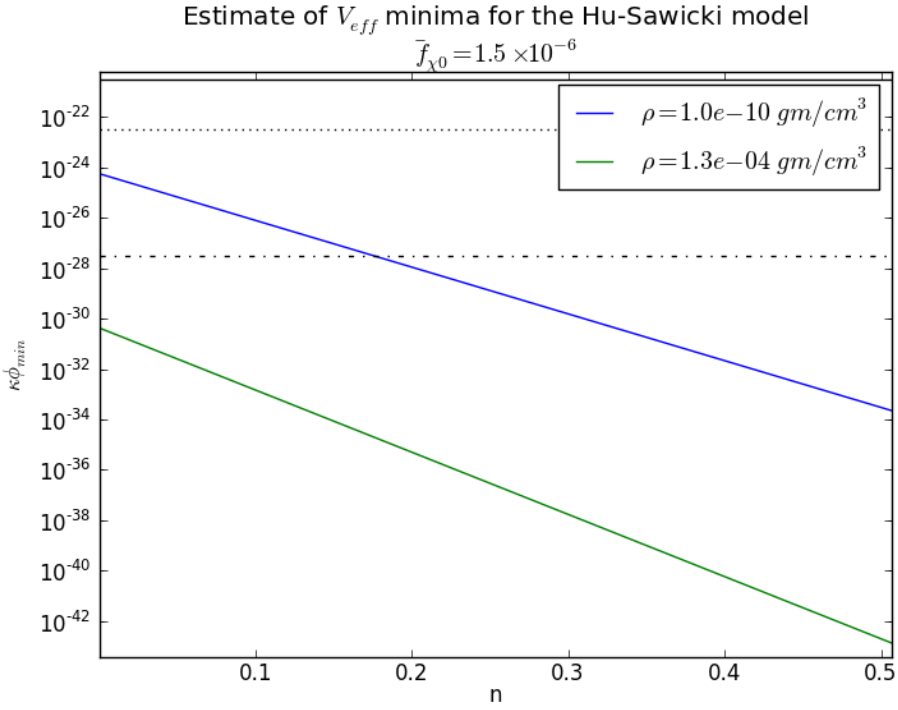

Figure 3.2.3: Estimates of the minimum of the effective potential for the Hu-Sawicki model obtained from (2.2.10) with the cosmological field $\bar{f}_{\chi 0} = 1.5 \times 10^{-6}$ near the limit imposed by solar system tests as $n \to 0$ (c.f. Figure 2.2.4). The horizontal lines are the same as in Figure 3.2.2, and the same remark about the crude estimate applies here. The two densities are those appropriate to a high vacuum (blue) and the realistic operating point of GRANIT (green).

3.3 Comparison to the original chameleon theory

These results stand in remarkable contrast to the results for the original chameleon theory. Brax and Pignol found that energy level shifts in the original chameleon theory (OCT[1]) could be detectable [2]. There are several differences between OCT and $f(R)$ gravity that could potentially explain the discrepancy. These differences were mentioned in Section 1.2:

1. OCT is formulated with fixed units in the Einstein frame. $f(R)$ has fixed units in the Jordan frame.
2. The potential $V(\phi)$ of OCT has a different form than in $f(R)$.
3. The coupling of the scalar to matter is given by a free parameter β in OCT while $\beta = 1/\sqrt{6}$ in $f(R)$. The primary case of interest in [2] is strong coupling $\beta \gg 1$.

These are examined in turn.

The Einstein and Jordan frames differ by a conformal rescaling of the metric and units of measure by powers of $\Omega = \exp(\beta\kappa\phi)$ where $\beta = 1/\sqrt{6}$ in $f(R)$ and is a free parameter in OCT. Since $\kappa\phi \ll 1$ at laboratory scales in both theories, the rescaling is negligibly different from 1 in both cases. Thus the choice of conformal frame has negligible practical impact and does not account for the differing results.

The potential used in [2] is an inverse power law typical of quintessence theories (up to a shift by a constant):

$$V(\phi) = \frac{M^{4+n}}{\phi^n},$$

where M is a parameter, with dimensions of mass, which is commonly taken to be the dark energy scale 2.4×10^{-3} eV and $n \geq 1$. To my knowledge no known $f(R)$ model has a $V(\phi)$ which approximates to this potential. The Hu-Sawicki model certainly does not approximate to an inverse power law potential. In principle, any desired $V(\phi)$ can be obtained from $f(R)$ simply by setting the left hand side of (2.1.33) for the $f(R)$ potential to the desired expression. The resulting condition is a complicated implicit non-linear differential equation for $f(R)$. I know of no means to make progress along these lines. The difference in the form of the potentials leads to different field profiles in the two theories.

Brax and Pignol found, after a number of approximations, that in OCT the field profile above the mirror is a power law [2]:

$$\phi = M\left(\frac{2+n}{\sqrt{2}}Mz\right)^{\frac{2}{2+n}}.$$

Remarkably this profile is independent of ρ_m, ρ_v and the coupling β. Brax and Pignol found that all dependence on these quantities drops out for strongly coupled chameleons with $\beta \gg 1$. Since Mz is $\mathcal{O}(1)$ for $z \sim 100$ μm and $\left[(2+n)/\sqrt{2}\right]^{2/2+n}$ is bounded between 1 and 2 for all $n > 0$,

$$\kappa\phi \sim \kappa M \sim 10^{-30},$$

within an order of magnitude, almost independent of n. The actual field profiles are shown in Figure 3.3.1.

The OCT field profiles are to be compared to those of the Hu-Sawicki model. For definiteness take an optimistic $n = \frac{1}{2}$ case. The field profile is obtained by evaluating (3.0.10) by numerical quadrature. The result is shown in Figure 3.3.2. There are several important features to note. First, the field profile for $f(R)$ is varies over a much greater range of height, i.e. the thin shell

[1] This is not a standard acronym.

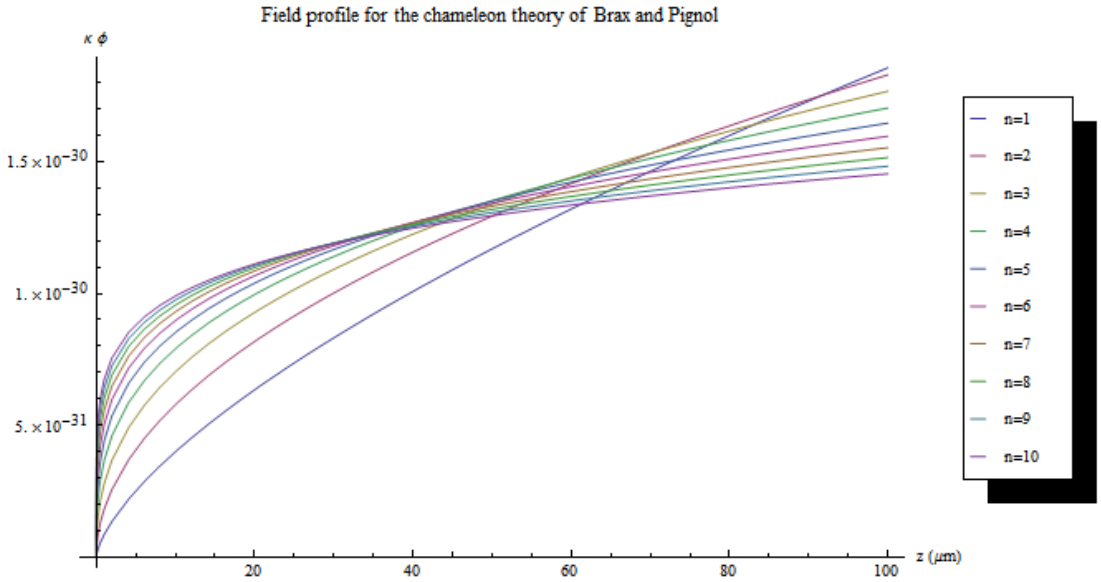

Figure 3.3.1: Field profiles of the original chameleon theory examined by Brax and Pignol [2] for several values of n.

is not as thin as in OCT. The influence of the mirror on the scalar field extends several metres, invalidating the idealization of the experiment as an infinite symmetric system. The mirror itself is ~ 30 cm in horizontal dimension and there are many other components of the experiment within several metres of the mirror, all of which would contribute significantly to the resulting field profile. The net effect would be a reduction of the field in the region above the mirror, further suppressing the induced energy level shifts. Second, the field is several orders of magnitude smaller than the OCT field. Figure 3.3.3 shows the range of z relevant to GRANIT. It can be seen that the Hu-Sawicki field is seven orders of magnitude smaller than the field from OCT. Third, the Hu-Sawicki field profile is nearly linear up to, and actually well past, $z = 100$ μm whereas the OCT field is non-linear in this region. (Figure 3.3.4 shows the relative residuals of equation (3.0.1) to benchmark the accuracy of the numerical solution.)

The fact that the Hu-Sawicki field profile is almost linear for the relevant z is further bad news for experimental detection of the model at GRANIT. Consider the potential energy $U(z)$ of a bouncing neutron from (3.0.5), restoring units:

$$U(z) \equiv \left(gz + \frac{1}{\sqrt{6}} c^2 \kappa\phi \right) m_N.$$

It is apparent from Figure 3.3.3 that a low order Taylor series for ϕ will suffice. Thus

$$U(z) \equiv \left(gz + \frac{1}{\sqrt{6}} c^2 \left(a_0 + a_1 z + a_2 z^2 + \mathcal{O}\left(z^3\right) \right) \right) m_N,$$

where the Taylor series for ϕ is

$$\kappa\phi = a_0 + a_1 z + a_2 z^2 + \mathcal{O}\left(z^3\right).$$

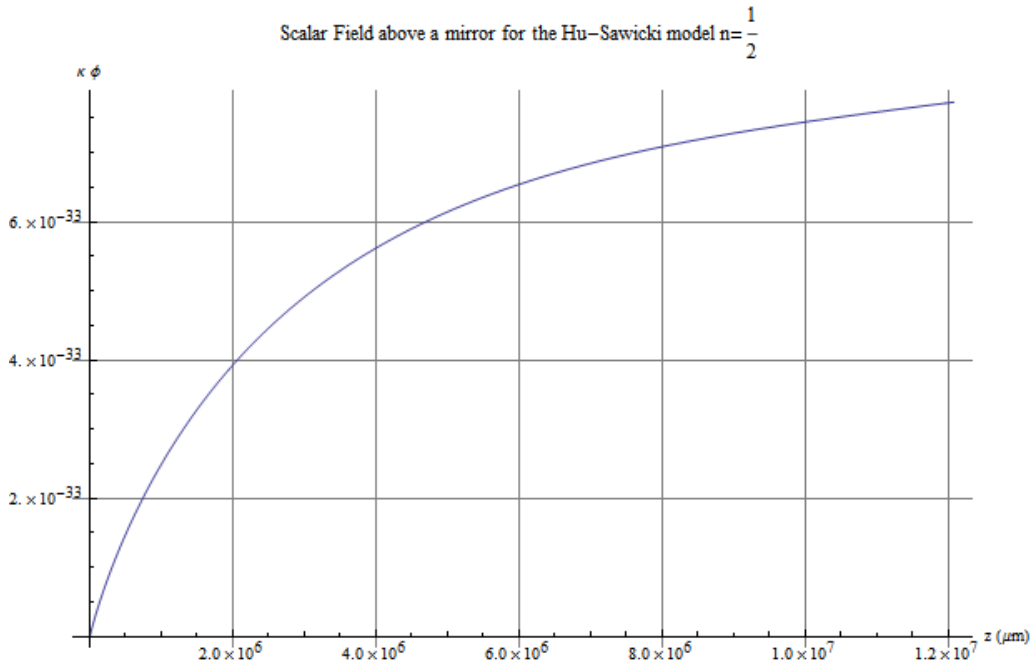

Figure 3.3.2: Scalar field $\kappa\phi$ above a mirror with density $\rho_m = 2.6$ g/cm^3 under a vacuum $\rho_v = 10^{-10}$ g/cm^3 for the $n = 1/2$ Hu-Sawicki model. The m and c_1 parameters are canonical (c.f. (2.2.4) and (2.2.5)) and $c_2 = 10^3$ is near the solar system limit (c.f. Figure 2.2.3).

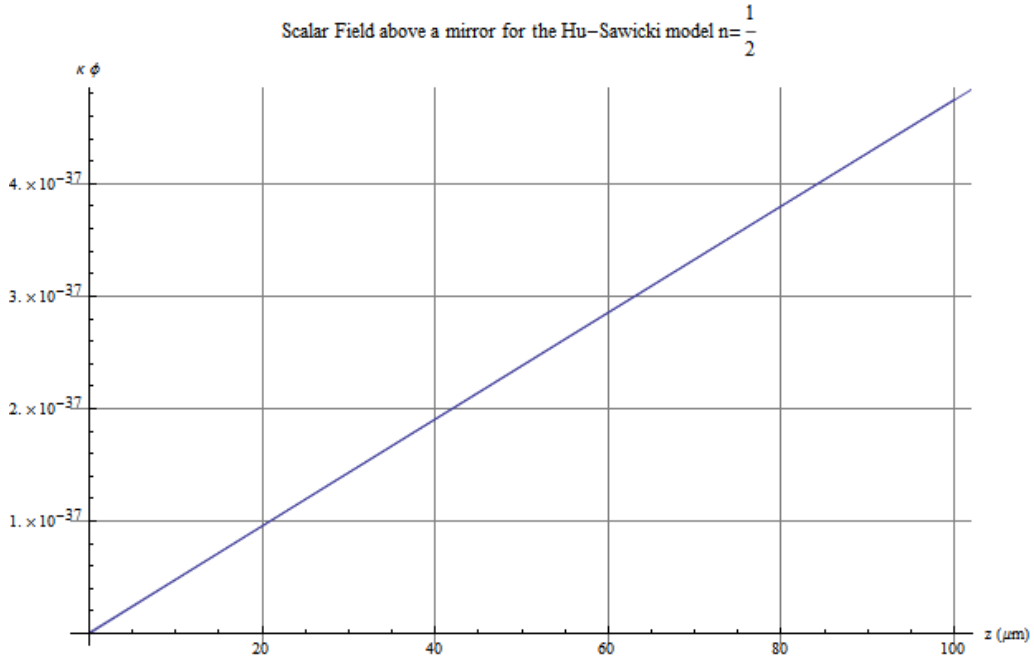

Figure 3.3.3: The same field profile as Figure 3.3.2 zoomed in to the range of z relevant to GRANIT. Notice the close approximation to a linear profile.

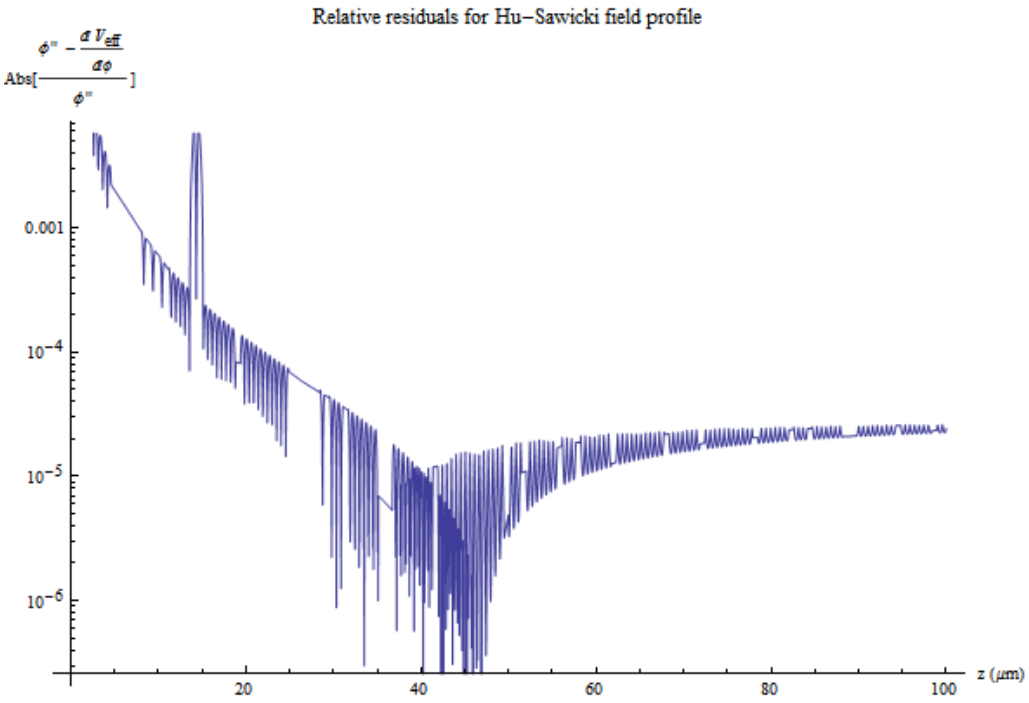

Figure 3.3.4: Relative residual of equation (3.0.1) for the field profile obtained by numerical quadrature as shown in Figure 3.3.3. This shows that numerical errors are controlled to the percent level. The odd feature around $z = 45$ μm is due to the residual changing sign.

The constant term a_0 produces an unobservable overall shift of the energy levels and can be dropped. The linear term can be understood as changing the effective gravitational acceleration:

$$g_{\text{eff}} \equiv g + \frac{1}{\sqrt{6}} a_1 c^2.$$

A fit of the field profile gives $a_1 \approx 5 \times 10^{-39}$ μm^{-1}, so

$$\frac{\delta g}{g} \equiv \frac{g_{\text{eff}} - g}{g} = \frac{1}{\sqrt{6}} \frac{a_1 c^2}{g} \approx 2 \times 10^{-17},$$

which would be easily lost in the error of the measurement of the local value of g.

The leading order observable shift is produced by the quadratic term. In first order perturbation theory:

$$\Delta \mathcal{E}_k^{(1)} = \frac{a_2 m_N c^2}{\sqrt{6}} \left\langle u_k \left| z^2 \right| u_k \right\rangle.$$

A fit to the field profile gives $a_2 \approx -4 \times 10^{-43}$ μm^{-2}. The corresponding energy shifts for the first ten states are tabulated in Table 3.3. All of the predicted shifts are unobservable. Further, the predicted shifts are roughly ten orders of magnitude smaller than the crude limit given in the previous section. This is because the bound was set based on $\phi < \phi_+$, although in reality the scalar field does not reach its ultimate value ϕ_+ until far into the tail of the wavefunction ($z \gg \langle z \rangle$). In the region where $\psi(z)$ is large, one has $\phi \ll \phi_+$. If this remains true for all $n < 1/2$ then no viable Hu-Sawicki model is detectable at GRANIT.

The coupling $\beta = 1/\sqrt{6}$ affects the neutron potential energy both directly, by multiplying the scalar field in $U(z)$, and indirectly by affecting the field profile. The fact that $1/\sqrt{6}$ is much less than the β values considered in OCT [2] reduces the energy level shifts through three mechanisms:

Table 3.3: Energy level shifts for the $n = 1/2$ Hu-Sawicki model with the same "optimistic" parameters as in Figure 3.3.2.

k	$\Delta\mathcal{E}_k^{(1)}$ (peV)
1	-2×10^{-20}
2	-4×10^{-20}
3	-9×10^{-20}
4	-1×10^{-19}
5	-2×10^{-19}
6	-2×10^{-19}
7	-3×10^{-19}
8	-3×10^{-19}
9	-4×10^{-19}
10	-5×10^{-19}

1. The thin shell is not sufficiently thin. ϕ does not approach its ultimate value ϕ_+ sufficiently close to the mirror to affect the neutron motion.

2. The field profile near the mirror is approximately linear, producing energy level shifts indistinguishable from an error in the measurement of the local gravitational acceleration g.

3. The perturbing potential is reduced relative to OCT because it is multiplied by a much smaller β.

These three mechanisms conspire to make the $f(R)$ models examined in this thesis unobservable at neutron bouncer experiments.

Chapter 4

Discussion

$f(R)$ gravity is a modification of General Relativity which shows promise for addressing several of the mysteries of cosmology, principally the nature of dark energy. Whenever a theory is proposed to fix problems at one scale it is important to consider what experimental and observation techniques might be available to test the theory at other scales. After all, physics is a unified whole, and modifying something as fundamental as the law of gravity while also satisfying all known constraints and making new predictions is no trivial matter. Precision tests of gravity at the laboratory scale have the potential to constrain physics at the cosmological scale. This thesis has focused on the prediction of $f(R)$ gravity for the energy levels of neutrons bound in the Earth's gravitational field. The experimental collaboration GRANIT at Institut Laue–Langevin (ILL) in Grenoble is making rapid progress in the measurement of the properties of gravitationally bound neutrons, expected to soon reach a sensitivity of 0.01 peV in the measurement of the neutron energy levels. A previous investigation by Brax and Pignol [2] of the closely related chameleon scalar-tensor theory demonstrated the potential of GRANIT to detect modifications of the Newtonian gravitational potential due to chameleons. This motivates the investigation of whether known viable models of $f(R)$ gravity are detectable at GRANIT. Three known viable models were studied in this thesis: the exponential gravity model of Linder, the model of Hu and Sawicki, and the "new" exponential gravity model of Xu and Chen. None of these models are detectable at GRANIT. Critical evaluation of these results follows.

4.1 Review of the results

Three known viable models of $f(R)$ gravity were investigated. For the exponential gravity model (c.f. sections 2.2.1 and 3.2.1) the energy level shifts were found to be

$$\Delta\mathcal{E}_n^{(1)} \lesssim \exp\left(-10^{19}\right) m_N,$$

which is undetectable at GRANIT. In fact, the minimum time necessary to resolve an energy to this precision due to the uncertainty principle is vastly greater than the age of the universe.

The Hu-Sawicki model (c.f. sections 2.2.2 and 3.2.2) predicts larger energy level shifts which depend on the model parameters n and $\bar{f}_{\chi 0}$ (equivalently small c_2). Models with smaller n and larger $\bar{f}_{\chi 0}$ predict larger energy level shifts. Table 3.3 summarises the shifts of the first ten energy levels computed using first order perturbation theory for an "optimistic" $n = 1/2$ model, i.e., one where $\bar{f}_{\chi 0}$ saturates the solar system bound. The shifts are of the order 10^{-19} peV, twelve orders of magnitude below the ultimate gravitational sensitivity level. Thus $n \geq 1/2$ Hu-Sawicki models are

shown to be undetectable at neutron bouncer experiments. The case of $n \ll 1$ is more promising, but the computations become more difficult. A crude estimate (c.f. Figure 3.2.3) suggests that the Hu-Sawicki model might be observable at small enough n, but the same estimate is over-optimistic for $n = 1/2$ and its validity for $n \ll 1$ can be called into question.

The Xu-Chen model (c.f. section 2.2.3) was shown to be observationally indistinguishable from $n > 2$ Hu-Sawicki models at laboratory scales. Thus the Xu-Chen model is also unobservable at GRANIT.

4.2 The approximations used

A number of approximations were made in Chapters 2 and 3 to simplify the analysis. All of the manipulations in Chapter 2 leading up to the field equations (2.1.34) and (2.1.35):

$$\tilde{R}_{\mu\nu} - \frac{1}{2}\tilde{g}_{\mu\nu}\tilde{R} = \kappa^2\left(T^{(\phi)}_{\mu\nu} + \tilde{T}_{\mu\nu}\right),$$
$$\Box\phi = \frac{\mathrm{d}V}{\mathrm{d}\phi} - \frac{\kappa}{\sqrt{6}}\tilde{T},$$

were exact. However, the scalar potential $V(\phi)$ for a given model is typically difficult to compute and approximations must be made. Recall that (2.1.33):

$$V(\phi) = \frac{f_\chi \chi - f}{2\kappa^2 f_\chi^2},$$

where χ and $f(\chi)$ must be found from ϕ by inverting (2.1.31)

$$\phi = -\frac{1}{2}\sqrt{\frac{6}{\kappa^2}}\ln f_\chi.$$

In the exponential gravity model terms of order $(\kappa\phi)^2$ and higher were dropped, however, since $\kappa\phi$ is super-exponentially small in this model the truncation has negligible impact. The situation is more serious in the Hu-Sawicki model, where one cannot even invert the relationship for ϕ without first truncating $f(R)$ to the lowest non-trivial order. For most values of the parameters this is no problem because the expansion converges rapidly at laboratory scales. However, convergence fails precisely for the most interesting limit ($n \to 0$ and $\bar{f}_{\chi 0}$ as large as possible c.f. solar system constraints). This makes the accuracy of the truncation difficult to assess, and going to higher orders in the expansion dramatically increases the computational burden. Using the crude estimate of the scalar curvature $R \approx \kappa^2\rho$ raises hopes that the small n models might be observable at sufficiently high vacuum (c.f. Figure 3.2.3). However, experience with the detailed computation of the energy level shifts for the $n = 1/2$ case shows that the crude estimate can be overly optimistic by several orders of magnitude. The observability of $n \to 0$ Hu-Sawicki models at neutron bouncer experiments remains an open question, but my opinion is that the answer is likely negative. Similar points apply to the Xu-Chen model, which, using a series expansion technique, was approximately mapped to a Hu-Sawicki model. The accuracy of the mapping depends on the order of magnitude of the largest neglected term, but including this term leads to technical difficulties similar to those faced in the Hu-Sawicki model.

The most important physical approximation used is the simplification of the geometry of the experiment. It was shown in Section 3.3 that the "thin" shell solution of the $n = 1/2$ Hu-Sawicki model in fact extends over several metres. This should be compared to the horizontal scale of

the mirror ~ 30 cm. This shows that the idealisation of the geometry to a semi-infinite mirror at $z < 0$ and a homogeneous vacuum at $z > 0$ fails. To accurately compute the field profile above the mirror one must account for the true geometry of the experiment, not an exciting task. However, the general effect of the disturbing influence of other bodies is to reduce the scalar field ϕ. This can be seen qualitatively in the following way. Consider any distribution of matter which contains an empty region $\mathcal{R}$. The scalar field takes the form which minimises the field energy

$$\int \mathrm{d}^3x \ \left[\frac{1}{2}\left(\nabla\phi\right)^2 + V_{\text{eff}}\left(\phi\right)\right].$$

Now introduce a body $\mathcal{B}$ into the empty region $\mathcal{R}$. Because the field equations are non-linear ϕ will adjust to the new matter distribution in a non-trivial way, but the general tendencies can be seen simply. Because $\mathcal{B}$ is far denser than $\mathcal{R}$ the effective potential inside $\mathcal{B}$ is minimised at a value ϕ_b smaller than the minimum ϕ_r inside $\mathcal{R}$. This will tend to reduce the field inside $\mathcal{B}$ from the value it had before. However, to reduce the field inside $\mathcal{B}$ without also reducing it outside would cost a great deal in gradient energy $\frac{1}{2}\left(\nabla\phi\right)^2$. The energetically favourable arrangement is for the field to be reduced inside $\mathcal{B}$, but not quite to ϕ_b, and for the reduction to propagate smoothly some distance outside the body. In the case of the $n = 1/2$ Hu-Sawicki model, at GRANIT, that distance is of the order of metres. Thus the field will not reach the idealised value above the mirror, as to do so would cost too much gradient energy. The result is that all of the energy level shifts computed in Chapter 3 overestimate the actual value for the true geometry.

Another simplification used is the choice of densities ρ_v and ρ_m. The mirror density $\rho_m = 2.6\ \mathrm{g/cm^3}$ was taken from the Brax and Pignol paper [2] in an attempt to match their results. The literature on ρ_v is sparse. Two crude estimates were made in Section 2.3: the first, $10^{-10}\ \mathrm{g/cm^3}$, is based on high vacuum systems reportedly used for other ultra-cold neutron research [91] and the second based on recommendations for future sensitivity improvements [92]. The current value of ρ_v being used at GRANIT could not be found but, in light of the previous discussion and the results of section 3.2, no practically obtainable vacuum would seem to change the qualitative results.

A number of perturbations of the Schrödinger equation, such as relativistic corrections, non-uniformity of the Earth's gravitational field and the Coriolis effect, produce energy level shifts comparable to or larger than the predicted shifts due to modified gravity. All of these influences were neglected for simplicity but must be included to accurately predict the energy levels of gravitationally bound neutrons. Finally, all of the numerical computations are of course approximate. A detailed error analysis has not been carried out, but examination of the relative residuals of the numerical solution for ϕ (c.f. Figure 3.3.4) suggests that numerical errors do not significantly affect the result. Of the physical constants appearing in the problem the least precisely known are the cosmological parameters Ω_M, Ω_Λ and H_0 which determine the scale of modifications to general relativity.

4.3 Directions for future work

There are several viable models which have not been studied here, including the Hu-Sawicki model corrected for large curvature stability (c.f. the discussion at the end of 2.2.2 or [89]), the Appleby et. al. and Starobinsky models (c.f. section 2.2.4). The corrected Hu-Sawicki model will probably not be observable at GRANIT because: a) the R^2 term in $f\left(R\right)$ is not relevant at laboratory scales, b) stability during reheating requires that n be an even integer ≥ 2 and c) the $n \geq 1/2$ Hu-Sawicki models are unobservable at GRANIT. The Starobinsky model is qualitatively similar to the vanilla Hu-Sawicki model. The Appleby et. al. model (2.2.14) merits further investigation. A technical

point meriting investigation is whether there is a way to carry out the energy level computation entirely in the Jordan frame without introducing the scalar field ϕ. This would eliminate the difficulty in computing $V(\phi)$ and also provide a more direct route to the solution.

More broadly it is worth studying whether there are any viable metric-affine $f(R)$ theories and non-$f(R)$ modified gravity theories which make predictions for GRANIT. The original chameleon theory is an example in the latter category, but the fact that the scalar-matter interaction is fixed by hand, arbitrarily, makes the theory seem poorly motivated. Certainly there are other, well motivated, modified gravity theories that could be relevant at GRANIT.

Dark energy, dark matter, and neutrino oscillations can be read as experimental clues that known physics has a low energy frontier as well as a high energy one. Theoretical clues come in the form of the hierarchy problem (the vast difference in energy scales in physics, which can be taken to include the cosmological constant problem as a special case), the strong CP problem (the unnatural smallness of CP violation in strong interactions), and the existence of models of the kind discussed in this thesis. The development of new clever experiments such as GRANIT is a key to shedding light on the low energy frontier. One can only hope that after several decades of experimental drought in fundamental physics future theoreticians will struggle to keep up with the experimentalists.

A final thought in closing: recently the smallest known chameleon was discovered (Figure 4.3.1). Perhaps this tiny creature is a fitting metaphor for this thesis, faced with the mysteries of gravitation.

Figure 4.3.1: Adult *Brookesia micra*, the smallest known species of chameleon, on the head of a match [9].

Bibliography

[1] Stefan Baessler, Mathieu Beau, Michael Kreuz, Vladimir N. Kurlov, Valery V. Nesvizhevsky, Guillaume Pignol, Konstantin V. Protasov, Francis Vezzu, and Aleksey Yu. Voronin. The GRANIT spectrometer. *Comptes Rendus Physique*, 12(8):707–728, October 2011. ISSN 16310705. doi: 10.1016/j.crhy.2011.04.010. URL http://linkinghub.elsevier.com/retrieve/pii/S1631070511000934.

[2] Philippe Brax and Guillaume Pignol. Strongly Coupled Chameleons and the Neutronic Quantum Bouncer. May 2011. URL http://arxiv.org/abs/1105.3420.

[3] Eric V. Linder. Exponential gravity. *Physical Review D*, 80(12), December 2009. ISSN 1550-7998. doi: 10.1103/PhysRevD.80.123528. URL http://prd.aps.org/abstract/PRD/v80/i12/e123528.

[4] Wayne Hu and Ignacy Sawicki. Models of f(R) cosmic acceleration that evade solar system tests. *Physical Review D*, 76(6), September 2007. ISSN 1550-7998. doi: 10.1103/PhysRevD.76.064004. URL http://prd.aps.org/abstract/PRD/v76/i6/e064004.

[5] Qiang Xu and Bin Chen. A New Exponential Gravity. March 2012. URL http://arxiv.org/abs/1203.6706.

[6] Steven Weinberg. *Cosmology*. Oxford University Press, Oxford, 2008. ISBN 978-0-19-852682-7. URL http://www.oup.com/us/catalog/general/subject/Physics/Astronomy/?view=usa&ci=9780198526827#reviews.

[7] K Nakamura. Review of Particle Physics. *Journal of Physics G: Nuclear and Particle Physics*, 37(7A):075021, July 2010. ISSN 0954-3899. doi: 10.1088/0954-3899/37/7A/075021. URL http://pdg.lbl.gov/http://stacks.iop.org/0954-3899/37/i=7A/a=075021?key=crossref.de0390bfb70101fa23c6dbe588ea1324.

[8] E. Komatsu, K. M. Smith, J. Dunkley, C. L. Bennett, B. Gold, G. Hinshaw, N. Jarosik, D. Larson, M. R. Nolta, L. Page, D. N. Spergel, M. Halpern, R. S. Hill, A. Kogut, M. Limon, S. S. Meyer, N. Odegard, G. S. Tucker, J. L. Weiland, E. Wollack, and E. L. Wright. SEVEN-YEAR WILKINSON MICROWAVE ANISOTROPY PROBE (WMAP) OBSERVATIONS: COSMOLOGICAL INTERPRETATION. *The Astrophysical Journal Supplement Series*, 192(2): 18, February 2011. ISSN 0067-0049. doi: 10.1088/0067-0049/192/2/18. URL http://stacks.iop.org/0067-0049/192/i=2/a=18?key=crossref.7c358756e608597b4941051eb0ae0afa.

[9] Frank Glaw, Jörn Köhler, Ted M Townsend, and Miguel Vences. Rivaling the world's smallest reptiles: discovery of miniaturized and microendemic new species of leaf chameleons (Brookesia) from northern Madagascar. *PloS one*, 7(2):e31314, January 2012. ISSN 1932-6203. doi: 10.1371/journal.pone.0031314. URL http://www.pubmedcentral.nih.gov/articlerender.fcgi?artid=3279364&tool=pmcentrez&rendertype=abstract.

[10] Nobelprize.org. The Nobel Prize in Physics 2011, 2011. URL http://www.nobelprize.org/nobel_prizes/physics/laureates/2011/.

[11] Sean M. Carroll. Dark Energy and the Preposterous Universe. Technical report, July 2001. URL http://arxiv.org/abs/astro-ph/0107571.

[12] Sean M. Carroll. The Cosmological Constant. *Living Rev. Relativity*, 4, 2001. URL http://www.livingreviews.org/lrr-2001-1.

[13] Jerome Martin. Everything You Always Wanted To Know About The Cosmological Constant Problem (But Were Afraid To Ask). May 2012. URL http://arxiv.org/abs/1205.3365.

[14] Charles W. Misner, Kip S. Thorne, and John Archibald Wheeler. *Gravitation*. W. H. Freeman and Company, New York, 1973. ISBN 0-7167-0334-3.

[15] Sean M. Carroll. Lecture Notes on General Relativity, December 1997. URL http://arxiv.org/abs/gr-qc/9712019.

[16] R. Bernabei, P. Belli, F. Cappella, R. Cerulli, C. J. Dai, A. D'Angelo, H. L. He, A. Incicchitti, H. H. Kuang, X. H. Ma, F. Montecchia, F. Nozzoli, D. Prosperi, X. D. Sheng, R. G. Wang, and Z. P. Ye. New results from DAMA/LIBRA. *The European Physical Journal C*, 67(1-2):39–49, March 2010. ISSN 1434-6044. doi: 10.1140/epjc/s10052-010-1303-9. URL http://www.springerlink.com/index/10.1140/epjc/s10052-010-1303-9.

[17] C. Aalseth, P. Barbeau, J. Colaresi, J. Collar, J. Diaz Leon, J. Fast, N. Fields, T. Hossbach, M. Keillor, J. Kephart, A. Knecht, M. Marino, H. Miley, M. Miller, J. Orrell, D. Radford, J. Wilkerson, and K. Yocum. Search for an Annual Modulation in a p-Type Point Contact Germanium Dark Matter Detector. *Physical Review Letters*, 107(14), September 2011. ISSN 0031-9007. doi: 10.1103/PhysRevLett.107.141301. URL http://link.aps.org/doi/10.1103/PhysRevLett.107.141301.

[18] CDMS Collaboration, Z. Ahmed, D. S. Akerib, A. J. Anderson, S. Arrenberg, C. N. Bailey, D. Balakishiyeva, L. Baudis, D. A. Bauer, P. L. Brink, T. Bruch, R. Bunker, B. Cabrera, D. O. Caldwell, J. Cooley, P. Cushman, M. Daal, F. DeJongh, P. C. F. Di Stefano, M. R. Dragowsky, S. Fallows, E. Figueroa-Feliciano, J. Filippini, J. Fox, M. Fritts, S. R. Golwala, J. Hall, S. A. Hertel, T. Hofer, D. Holmgren, L. Hsu, M. E. Huber, O. Kamaev, M. Kiveni, M. Kos, S. W. Leman, S. Liu, R. Mahapatra, V. Mandic, K. A. McCarthy, N. Mirabolfathi, D. C. Moore, H. Nelson, R. W. Ogburn, A. Phipps, K. Prasad, M. Pyle, X. Qiu, W. Rau, A. Reisetter, Y. Ricci, T. Saab, B. Sadoulet, J. Sander, R. W. Schnee, D. Seitz, B. Serfass, D. Speller, K. M. Sundqvist, M. Tarka, R. B. Thakur, A. N. Villano, B. Welliver, S. Yellin, J. Yoo, B. A. Young, and J. Zhang. Search for annual modulation in low-energy CDMS-II data. March 2012. URL http://arxiv.org/abs/1203.1309.

[19] E. Aprile, K. Arisaka, F. Arneodo, A. Askin, L. Baudis, A. Behrens, K. Bokeloh, E. Brown, T. Bruch, G. Bruno, J. Cardoso, W.-T. Chen, B. Choi, D. Cline, E. Duchovni, S. Fattori, A. Ferella, F. Gao, K.-L. Giboni, E. Gross, A. Kish, C. Lam, J. Lamblin, R. Lang, C. Levy, K. Lim, Q. Lin, S. Lindemann, M. Lindner, J. Lopes, K. Lung, T. Marrodán Undagoitia, Y. Mei, A. Melgarejo Fernandez, K. Ni, U. Oberlack, S. Orrigo, E. Pantic, R. Persiani, G. Plante, A. Ribeiro, R. Santorelli, J. dos Santos, G. Sartorelli, M. Schumann, M. Selvi,

P. Shagin, H. Simgen, A. Teymourian, D. Thers, O. Vitells, H. Wang, M. Weber, and C. Weinheimer. Dark Matter Results from 100 Live Days of XENON100 Data. *Physical Review Letters*, 107(13), September 2011. ISSN 0031-9007. doi: 10.1103/PhysRevLett.107.131302. URL http://link.aps.org/doi/10.1103/PhysRevLett.107.131302.

[20] Clifford M. Will. The Confrontation between General Relativity and Experiment. *Living Rev. Relativity*, 9, 2006. URL http://www.livingreviews.org/lrr-2006-3.

[21] Cliff P. Burgess. Quantum Gravity in Everyday Life: General Relativity as an Effective Field Theory. *Living Rev. Relativity*, 7, 2004. URL http://www.livingreviews.org/lrr-2004-5.

[22] Roy Maartens and Kazuya Koyama. Brane-World Gravity. April 2010. URL http://arxiv.org/abs/1004.3962.

[23] Andrei Linde. Particle Physics and Inflationary Cosmology. March 2005. URL http://arxiv.org/abs/hep-th/0503203.

[24] Neil Turok and Paul J. Steinhardt. Beyond Inflation A Cyclic Universe Scenario. *Physica Scripta*, page 76, 2005. ISSN 0031-8949. doi: 10.1238/Physica.Topical.117a00076. URL http://www.physica.org/xml/article.asp?article=t117a00076.xml.

[25] Kazuharu Bamba, Salvatore Capozziello, Shin'ichi Nojiri, and Sergei D. Odintsov. Dark energy cosmology: the equivalent description via different theoretical models and cosmography tests. May 2012. URL http://arxiv.org/abs/1205.3421.

[26] Edmund J. Copeland, M. Sami, and Shinji Tsujikawa. Dynamics of dark energy. March 2006. doi: 10.1142/S021827180600942X. URL http://arxiv.org/abs/hep-th/0603057.

[27] Steven S. Gubser and Justin Khoury. Scalar self-interactions loosen constraints from fifth force searches. *Physical Review D*, 70(10):19, November 2004. ISSN 1550-7998. doi: 10.1103/PhysRevD.70.104001. URL http://arxiv.org/abs/hep-ph/0405231.

[28] Justin Khoury and Amanda Weltman. Chameleon Fields: Awaiting Surprises for Tests of Gravity in Space. *Physical Review Letters*, 93(17):4, October 2004. ISSN 0031-9007. doi: 10.1103/PhysRevLett.93.171104. URL http://arxiv.org/abs/astro-ph/0309300.

[29] Justin Khoury. Theories of Dark Energy with Screening Mechanisms. November 2010. URL http://arxiv.org/abs/1011.5909.

[30] T. P. Waterhouse. An Introduction to Chameleon Gravity. November 2006. URL http://arxiv.org/abs/astro-ph/0611816.

[31] Kazuharu Bamba, Chao-Qiang Geng, and Chung-Chi Lee. Cosmological evolution in exponential gravity. *Journal of Cosmology and Astroparticle Physics*, 2010(08):021–021, August 2010. ISSN 1475-7516. doi: 10.1088/1475-7516/2010/08/021. URL http://stacks.iop.org/1475-7516/2010/i=08/a=021?key=crossref.deb4b3fe55077f2cf43b03cf26aac495.

[32] Santiago Esteban Perez Bergliaffa. An overview of f(R) theories. July 2011. URL http://arxiv.org/abs/1107.5183.

[33] Salvatore Capozziello and Mariafelicia De Laurentis. Extended Theories of Gravity. August 2011. URL http://arxiv.org/abs/1108.6266.

[34] A. Zee. *Quantum Field Theory in a Nutshell: Second Edition (In a Nutshell (Princeton))*. Princeton University Press, 2010. ISBN 0691140340. URL http://www.amazon.com/Quantum-Field-Theory-Nutshell-Princeton/dp/0691140340.

[35] Kurt Hinterbichler and Justin Khoury. Screening Long-Range Forces through Local Symmetry Restoration. *Physical Review Letters*, 104(23):4, June 2010. ISSN 0031-9007. doi: 10.1103/PhysRevLett.104.231301. URL http://arxiv.org/abs/1001.4525http://link.aps.org/doi/10.1103/PhysRevLett.104.231301.

[36] Nathan Chow and Justin Khoury. Galileon Cosmology. Technical report, May 2009. URL http://arxiv.org/abs/0905.1325.

[37] Philippe Brax, Carsten van de Bruck, Anne-Christine Davis, Justin Khoury, and Amanda Weltman. Detecting dark energy in orbit: The cosmological chameleon. *Physical Review D*, 70(12):31, December 2004. ISSN 1550-7998. doi: 10.1103/PhysRevD.70.123518. URL http://arxiv.org/abs/astro-ph/0408415.

[38] Ph. Brax. Chameleon Dark Energy. In *AIP Conference Proceedings*, volume 736, pages 105–110. AIP, October 2004. doi: 10.1063/1.1835177. URL http://arxiv.org/abs/astro-ph/0410103http://link.aip.org/link/?APC/736/105/1&Agg=doi.

[39] Philippe Brax, Carsten van de Bruck, and Anne-Christine Davis. Compatibility of the Chameleon-Field Model with Fifth-Force Experiments, Cosmology, and PVLAS and CAST Results. *Physical Review Letters*, 99(12):4, September 2007. ISSN 0031-9007. doi: 10.1103/PhysRevLett.99.121103. URL http://arxiv.org/abs/hep-ph/0703243.

[40] Philippe Brax, Carsten van de Bruck, Anne-Christine Davis, David Mota, and Douglas Shaw. Detecting chameleons through Casimir force measurements. *Physical Review D*, 76(12):39, December 2007. ISSN 1550-7998. doi: 10.1103/PhysRevD.76.124034. URL http://arxiv.org/abs/0709.2075.

[41] Philippe Brax, Carsten van de Bruck, Anne-Christine Davis, David Mota, and Douglas Shaw. Testing chameleon theories with light propagating through a magnetic field. *Physical Review D*, 76(8):24, October 2007. ISSN 1550-7998. doi: 10.1103/PhysRevD.76.085010. URL http://arxiv.org/abs/0707.2801.

[42] Philippe Brax and Clare Burrage. Chameleon induced atomic afterglow. *Physical Review D*, 82(9):13, November 2010. ISSN 1550-7998. doi: 10.1103/PhysRevD.82.095014. URL http://arxiv.org/abs/1009.1065http://link.aps.org/doi/10.1103/PhysRevD.82.095014.

[43] Philippe Brax, Clare Burrage, Anne-Christine Davis, David Seery, and Amanda Weltman. Higgs production as a probe of chameleon dark energy. *Physical Review D*, 81(10):24, May 2010. ISSN 1550-7998. doi: 10.1103/PhysRevD.81.103524. URL http://arxiv.org/abs/0911.1267http://link.aps.org/doi/10.1103/PhysRevD.81.103524.

[44] Ph. Brax, C. van de Bruck, A. Davis, D. Shaw, and D. Iannuzzi. Tuning the Mass of Chameleon Fields in Casimir Force Experiments. *Physical Review Letters*, 104(24), June 2010. ISSN 0031-9007. doi: 10.1103/PhysRevLett.104.241101. URL http://arxiv.org/abs/1003.1605.

[45] Philippe Brax, Carsten van de Bruck, David Mota, Nelson Nunes, and Hans Winther. Chameleons with field-dependent couplings. *Physical Review D*, 82(8):17, October 2010. ISSN 1550-7998. doi: 10.1103/PhysRevD.82.083503. URL http://arxiv.org/abs/1006.2796.

[46] Philippe Brax. Lorentz Invariance Violation in Modified Gravity. February 2012. URL http://arxiv.org/abs/1202.0740.

[47] Piyabut Burikham and Sirachak Panpanich. Effects of Chameleon Scalar Field on Rotation Curves of the Galaxies. March 2011. URL http://arxiv.org/abs/1103.1198.

[48] C. Burrage. Supernova brightening from chameleon-photon mixing. *Physical Review D*, 77 (4):17, February 2008. ISSN 1550-7998. doi: 10.1103/PhysRevD.77.043009. URL http://arxiv.org/abs/0711.2966.

[49] Clare Burrage, Anne-Christine Davis, and Douglas Shaw. Detecting chameleons: The astronomical polarization produced by chameleonlike scalar fields. *Physical Review D*, 79 (4):34, February 2009. ISSN 1550-7998. doi: 10.1103/PhysRevD.79.044028. URL http://arxiv.org/abs/0809.1763.

[50] A. Chou, W. Wester, A. Baumbaugh, H. Gustafson, Y. Irizarry-Valle, P. Mazur, J. Steffen, R. Tomlin, A. Upadhye, A. Weltman, X. Yang, and J. Yoo. Search for Chameleon Particles Using a Photon-Regeneration Technique. *Physical Review Letters*, 102(3):4, January 2009. ISSN 0031-9007. doi: 10.1103/PhysRevLett.102.030402. URL http://arxiv.org/abs/0806.2438.

[51] V. Dzhunushaliev, V. Folomeev, and D. Singleton. Chameleon stars. June 2011. URL http://arxiv.org/abs/1106.1267.

[52] Radouane Gannouji, Bruno Moraes, David Mota, David Polarski, Shinji Tsujikawa, and Hans Winther. Chameleon dark energy models with characteristic signatures. *Physical Review D*, 82(12):16, December 2010. ISSN 1550-7998. doi: 10.1103/PhysRevD.82.124006. URL http://arxiv.org/abs/1010.3769.

[53] Holger Gies, David Mota, and Douglas Shaw. Hidden in the light: Magnetically induced afterglow from trapped chameleon fields. *Physical Review D*, 77(2):17, January 2008. ISSN 1550-7998. doi: 10.1103/PhysRevD.77.025016. URL http://arxiv.org/abs/0710.1556.

[54] Katherine Jones-Smith and Francesc Ferrer. Detecting Chameleon Dark Energy via an Electrostatic Analogy. *Physical Review Letters*, 108(22), May 2012. ISSN 0031-9007. doi: 10.1103/PhysRevLett.108.221101. URL http://arxiv.org/abs/1105.6085http://link.aps.org/doi/10.1103/PhysRevLett.108.221101.

[55] Piyali Bagchi Khatua and Ujjal Debnath. Role of chameleon field in accelerating Universe. *Astrophysics and Space Science*, 326(1):53–60, December 2009. ISSN 0004-640X. doi: 10.1007/s10509-009-0207-3. URL http://arxiv.org/abs/1012.1443http://www.springerlink.com/index/10.1007/s10509-009-0207-3.

[56] Justin Khoury and Amanda Weltman. Chameleon Cosmology. *Physical Review D*, 69(4):25, September 2003. ISSN 1550-7998. doi: 10.1103/PhysRevD.69.044026. URL http://arxiv.org/abs/astro-ph/0309411.

[57] David F. Mota and Camilla A. O. Schelpe. Requirement of a Primordial Magnetic Field in Chameleon Models. August 2011. URL http://arxiv.org/abs/1108.0892.

[58] Johannes Noller. Derivative Chameleons. March 2012. URL http://arxiv.org/abs/1203.6639.

[59] Alessandra Silvestri. Scalar Radiation from Chameleon-Shielded Regions. *Physical Review Letters*, 106(25):4, June 2011. ISSN 0031-9007. doi: 10.1103/PhysRevLett.106.251101. URL http://arxiv.org/abs/1103.4013.

[60] Jason H. Steffen and for the GammeV Collaboration. Constraints on chameleons and axion-like particles from the GammeV experiment. October 2008. URL http://arxiv.org/abs/0810.5070.

[61] J. Steffen, A. Upadhye, A. Baumbaugh, A. Chou, P. Mazur, R. Tomlin, A. Weltman, and W. Wester. Laboratory Constraints on Chameleon Dark Energy and Power-Law Fields. *Physical Review Letters*, 105(26):5, December 2010. ISSN 0031-9007. doi: 10.1103/PhysRevLett.105.261803. URL http://arxiv.org/abs/1010.0988.

[62] Jason H. Steffen. The CHASE laboratory search for chameleon dark energy. November 2010. URL http://arxiv.org/abs/1011.3802.

[63] A. Upadhye, J. H. Steffen, and A. Weltman. Constraining chameleon field theories using the GammeV afterglow experiments. *Physical Review D*, 81(1):17, January 2010. ISSN 1550-7998. doi: 10.1103/PhysRevD.81.015013. URL http://arxiv.org/abs/0911.3906.

[64] Gong-Bo Zhao, Baojiu Li, and Kazuya Koyama. Testing Gravity Using the Environmental Dependence of Dark Matter Halos. *Physical Review Letters*, 107(7):5, August 2011. ISSN 0031-9007. doi: 10.1103/PhysRevLett.107.071303. URL http://arxiv.org/abs/1105.0922http://link.aps.org/doi/10.1103/PhysRevLett.107.071303.

[65] L.D. Landau and E.M. Lifshitz. *Quantum Mechanics (Non-relativistic Theory)*. Butterworth-Heinemann, Oxford, third edition, 1977. ISBN 0-08-029140-6.

[66] Stephan Baessler, Alexei Gagarski, Ludmilla Grigorieva, Michael Kreuz, Fabrice Naraghi, Valery Nesvizhevsky, Guillaume Pignol, Konstantin Protassov, Dominique Rebreyend, Francis Vezzu, and Alexei Voronin. The GRANIT project: Status and Perspectives. February 2012. URL http://arxiv.org/abs/1202.2784.

[67] M. Kreuz, V.V. Nesvizhevsky, P. Schmidt-Wellenburg, T. Soldner, M. Thomas, H.G. Börner, F. Naraghi, G. Pignol, K.V. Protasov, D. Rebreyend, F. Vezzu, R. Flaminio, C. Michel, N. Morgado, L. Pinard, S. Baeß ler, A.M. Gagarski, L.A. Grigorieva, T.M. Kuzmina, A.E. Meyerovich, L.P. Mezhov-Deglin, G.A. Petrov, A.V. Strelkov, and A.Yu. Voronin. A method to measure the resonance transitions between the gravitationally bound quantum states of neutrons in the GRANIT spectrometer. *Nuclear Instruments and Methods in Physics Research Section A: Accelerators, Spectrometers, Detectors and Associated Equipment*, 611(2-3):326–330, December 2009. ISSN 01689002. doi: 10.1016/j.nima.2009.07.059. URL http://arxiv.org/abs/0902.0156http://linkinghub.elsevier.com/retrieve/pii/S0168900209015551.

[68] Zvi Bern. Perturbative Quantum Gravity and its Relation to Gauge Theory. *Living Rev. Relativity*, 5, 2002. URL http://www.livingreviews.org/lrr-2002-5.

[69] Carlo Rovelli. Loop Quantum Gravity. *Living Rev. Relativity*, 11, 2008. URL http://www.livingreviews.org/lrr-2008-5.

[70] Valerio Faraoni and Salvatore Capozziello. *Beyond Einstein Gravity*. Springer Netherlands, Dordrecht, 2011. ISBN 978-94-007-0164-9. doi: 10.1007/978-94-007-0165-6. URL http://www.springerlink.com/index/10.1007/978-94-007-0165-6.

[71] Thomas P. Sotiriou. *Modified Actions for Gravity: Theory and Phenomenology*. PhD thesis, International School for Advanced Studies, Trieste, October 2007. URL http://arxiv.org/abs/0710.4438.

[72] M. Ferraris, M. Francaviglia, and C. Reina. Variational formulation of general relativity from 1915 to 1925 Palatini's method discovered by Einstein in 1925. *General Relativity and Gravitation*, 14(3):243–254, March 1982. ISSN 0001-7701. doi: 10.1007/BF00756060. URL http://www.springerlink.com/content/w162047g07804167/.

[73] G. W. Gibbons and S. W. Hawking. Action integrals and partition functions in quantum gravity. *Physical Review D*, 15(10):2752–2756, May 1977. ISSN 0556-2821. doi: 10.1103/PhysRevD.15.2752. URL http://prd.aps.org/abstract/PRD/v15/i10/p2752_1.

[74] Thomas P. Sotiriou. f(R) theories of gravity. *Reviews of Modern Physics*, 82(1):451–497, March 2010. ISSN 0034-6861. doi: 10.1103/RevModPhys.82.451. URL http://link.aps.org/doi/10.1103/RevModPhys.82.451.

[75] Gonzalo J. Olmo. Hydrogen atom in Palatini theories of gravity. *Physical Review D*, 77(8), April 2008. ISSN 1550-7998. doi: 10.1103/PhysRevD.77.084021. URL http://prd.aps.org/abstract/PRD/v77/i8/e084021.

[76] Thomas P. Sotiriou and Stefano Liberati. Metric-affine f(R) theories of gravity. *Annals of Physics*, 322(4):935–966, April 2007. ISSN 00034916. doi: 10.1016/j.aop.2006.06.002. URL http://dx.doi.org/10.1016/j.aop.2006.06.002.

[77] Luca Amendola, David Polarski, and Shinji Tsujikawa. Are f(R) Dark Energy Models Cosmologically Viable? *Physical Review Letters*, 98(13), March 2007. ISSN 0031-9007. doi: 10.1103/PhysRevLett.98.131302. URL http://prl.aps.org/abstract/PRL/v98/i13/e131302http://link.aps.org/doi/10.1103/PhysRevLett.98.131302.

[78] Stephen A. Appleby and Richard A. Battye. Do consistent models mimic general relativity plus Λ? *Physics Letters B*, 654(1-2):7–12, October 2007. ISSN 03702693. doi: 10.1016/j.physletb.2007.08.037. URL http://dx.doi.org/10.1016/j.physletb.2007.08.037http://linkinghub.elsevier.com/retrieve/pii/S0370269307010052.

[79] Antonio De Felice and Shinji Tsujikawa. f(R) Theories. *Living Rev. Relativity*, 13, 2010. URL http://www.livingreviews.org/lrr-2010-3.

[80] Philippe Brax, Carsten van de Bruck, Anne-Christine Davis, and Douglas Shaw. f(R) gravity and chameleon theories. *Physical Review D*, 78(10):18, November 2008. ISSN 1550-7998. doi: 10.1103/PhysRevD.78.104021. URL http://arxiv.org/abs/0806.3415.

[81] Valerio Faraoni. R^{n} gravity and the chameleon. *Physical Review D*, 83(12):5, June 2011. ISSN 1550-7998. doi: 10.1103/PhysRevD.83.124044. URL http://arxiv.org/abs/1106.0328.

[82] Thomas Faulkner, Max Tegmark, Emory F. Bunn, and Yi Mao. Constraining f(R) gravity as a scalar-tensor theory. *Physical Review D*, 76(6):15, September 2007. ISSN 1550-7998. doi: 10.1103/PhysRevD.76.063505. URL http://arxiv.org/abs/astro-ph/0612569http://link.aps.org/doi/10.1103/PhysRevD.76.063505.

[83] Je-An Gu and Wei-Ting Lin. Solar-System Constraints on f(R) Chameleon Gravity. August 2011. URL http://arxiv.org/abs/1108.1782.

[84] David Mota and Douglas Shaw. Evading equivalence principle violations, cosmological, and other experimental constraints in scalar field theories with a strong coupling to matter. *Physical Review D*, 75(6):72, March 2007. ISSN 1550-7998. doi: 10.1103/PhysRevD.75.063501. URL http://arxiv.org/abs/hep-ph/0608078http://link.aps.org/doi/10.1103/PhysRevD.75.063501.

[85] Valerio Faraoni and Shahn Nadeau. (Pseudo)issue of the conformal frame revisited. *Physical Review D*, 75(2), January 2007. ISSN 1550-7998. doi: 10.1103/PhysRevD.75.023501. URL http://link.aps.org/doi/10.1103/PhysRevD.75.023501.

[86] THOMAS P. SOTIRIOU, STEFANO LIBERATI, and VALERIO FARAONI. THEORY OF GRAVITATION THEORIES: A NO-PROGRESS REPORT. *International Journal of Modern Physics D*, 17(03 & 04):399, 2008. ISSN 0218-2718. doi: 10.1142/S0218271808012097. URL http://www.worldscinet.com/ijmpd/17/1703n04/S0218271808012097.html.

[87] Philippe Brax, Clare Burrage, Anne-Christine Davis, David Seery, and Amanda Weltman. Anomalous coupling of scalars to gauge fields. *Physics Letters B*, 699(1-2):5–9, May 2011. ISSN 03702693. doi: 10.1016/j.physletb.2011.03.047. URL http://arxiv.org/abs/1010.4536http://linkinghub.elsevier.com/retrieve/pii/S0370269311003200.

[88] I. G. Irastorza, F. T. Avignone, S. Caspi, J. M. Carmona, T. Dafni, M. Davenport, A. Dudarev, G. Fanourakis, E. Ferrer-Ribas, J. Galan, J. A. Garcia, T. Geralis, I. Giomataris, H. Gomez, D. H. H. Hoffmann, F. J. Iguaz, K. Jakovcic, M. Krcmar, B. Lakic, G. Luzon, M. Pivovaroff, T. Papaevangelou, G. Raffelt, J. Redondo, A. Rodriguez, S. Russenschuck, J. Ruz, I. Shilon, H. Ten Kate, A. Tomas, S. Troitsky, K. van Bibber, J. A. Villar, J. Vogel, L. Walckiers, and K. Zioutas. Towards a new generation axion helioscope. March 2011. URL http://arxiv.org/abs/1103.5334.

[89] Stephen A Appleby, Richard A Battye, and Alexei A Starobinsky. Curing singularities in cosmological evolution of F (R) gravity. *Journal of Cosmology and Astroparticle Physics*, 2010(06), June 2010. ISSN 1475-7516. doi: 10.1088/1475-7516/2010/06/005. URL http://stacks.iop.org/1475-7516/2010/i=06/a=005?key=crossref.c9666ff75242b59a26a8953fc3796990http://arxiv.org/abs/0909.1737.

[90] Alexei A. Starobinsky. Disappearing cosmological constant in f(R) gravity. *JETP Letters*, 86(3):157–163, October 2007. ISSN 0021-3640. doi: 10.1134/S0021364007150027. URL http://arxiv.org/abs/0706.2041http://www.springerlink.com/index/10.1134/S0021364007150027.

[91] J M Pendlebury. Fundamental Physics with Ultracold Neutrons. *Annual Review of Nuclear and Particle Science*, 43(1):687–727, December 1993. ISSN 0163-8998. doi: 10.1146/annurev.ns.43.120193.003351. URL http://www.annualreviews.org/doi/abs/10.1146/annurev.ns.43.120193.003351.

[92] S. Baessler, A.M. Gagarski, E.V. Lychagin, A. Mietke, A.Yu. Muzychka, V.V. Nesvizhevsky, G. Pignol, A.V. Strelkov, B.P. Toperverg, and K. Zhernenkov. New methodical developments for GRANIT. *Comptes Rendus Physique*, 12(8):729–754, October 2011. ISSN 16310705. doi: 10.1016/j.crhy.2011.04.014. URL http://dx.doi.org/10.1016/j.crhy.2011.04.014.

[93] Dieter Brill and John Wheeler. Interaction of Neutrinos and Gravitational Fields. *Reviews of Modern Physics*, 29(3):465–479, July 1957. ISSN 0034-6861. doi: 10.1103/RevModPhys.29.465. URL http://rmp.aps.org/abstract/RMP/v29/i3/p465_1.

[94] N. D. Birrell and P. C. W. Davies. *Quantum Fields in Curved Space*. Cambridge University Press, Cambridge, 1982. ISBN 0521278589.

[95] Nicolas Boulanger, Philippe Spindel, and Fabien Buisseret. Bound states of Dirac particles in gravitational fields. *Physical Review D*, 74(12), December 2006. ISSN 1550-7998. doi: 10.1103/PhysRevD.74.125014. URL http://link.aps.org/doi/10.1103/PhysRevD.74.125014.

[96] Stephan Paul. The puzzle of neutron lifetime. *Nuclear Instruments and Methods in Physics Research Section A: Accelerators, Spectrometers, Detectors and Associated Equipment*, 611 (2-3):157–166, December 2009. ISSN 01689002. doi: 10.1016/j.nima.2009.07.095. URL http://linkinghub.elsevier.com/retrieve/pii/S0168900209015174.

Appendix A

Spin Connection Coefficients and Covariant Derivative

The connection coefficients for the metric (2.4.1) can be evaluated by a standard procedure [14]. The action for a massive test particle in special and general relativity is

$$S = -m \int \mathrm{d}\tau = -m \int \mathrm{d}\lambda \; L,$$

where τ is the proper time, which is given by $\mathrm{d}\tau^2 = g_{\mu\nu}\mathrm{d}x^\mu \mathrm{d}x^\nu$ and the Lagrangian is

$$L = -m\sqrt{g_{\mu\nu}\dot{x}^\mu \dot{x}^\nu},$$

where $x^\mu = x^\mu(\lambda)$ and $\dot{x}^\mu \equiv \mathrm{d}x^\mu/\mathrm{d}\lambda$ and λ is any (smooth, monotonic) parameter on the world-line of the particle. The connection coefficients $\Gamma^\mu_{\rho\sigma}$ can be read off by comparing the Euler-Lagrange equations

$$\frac{\mathrm{d}}{\mathrm{d}\lambda}\left(\frac{\partial L}{\partial \dot{x}^\mu}\right) - \frac{\partial L}{\partial x^\mu} = 0,$$

to the equations for a geodesic in curved spacetime:

$$\ddot{x}^\mu + \Gamma^\mu_{\rho\sigma}\dot{x}^\rho \dot{x}^\sigma = 0,$$

and the spin connection can be found by equation (2.1.6). Work can be saved, however, by the standard result that the same equations of motion follow from the simpler Lagrangian:

$$L = \frac{1}{2} g_{\mu\nu}\dot{x}^\mu \dot{x}^\nu.$$

For the field of a mirror

$$L = -\frac{1}{2}(1+2\mathcal{A})\,\dot{t}^2 + (1-2\mathcal{B})\,\frac{1}{2}\left(\dot{x}^2 + \dot{y}^2 + \dot{z}^2\right).$$

The Euler-Lagrange equations are

$$
\begin{aligned}
0 &= \ddot{t} + \frac{2\mathcal{A}_z}{(1+2\mathcal{A})}\dot{z}\dot{t}, \\
0 &= \ddot{x} - \frac{2\mathcal{B}_z}{(1-2\mathcal{B})}\dot{z}\dot{x}, \\
0 &= \ddot{y} - \frac{2\mathcal{B}_z}{(1-2\mathcal{B})}\dot{z}\dot{y}, \\
0 &= \ddot{z} + \frac{\mathcal{A}_z}{(1-2\mathcal{B})}\dot{t}^2 + \frac{\mathcal{B}_z}{(1-2\mathcal{B})}\left(\dot{x}^2 + \dot{y}^2 - \dot{z}^2\right),
\end{aligned}
$$

where the subscript z means derivative with respect to z. Keeping terms of first order in $\mathcal{A}_z$, $\mathcal{B}_z$:

$$
\begin{aligned}
&\Gamma^t_{zt} = \Gamma^t_{tz} = \Gamma^z_{tt} = \mathcal{A}_z, \\
&\Gamma^x_{zx} = \Gamma^x_{xz} = \Gamma^y_{zy} = \Gamma^y_{yz} = -\Gamma^z_{xx} = -\Gamma^z_{yy} = \Gamma^z_{zz} = -\mathcal{B}_z.
\end{aligned}
\tag{A.0.1}
$$

All the other connection coefficients vanish. These can be conveniently arranged as a set of matrices, with the upper index labeling the row and the lower index labeling the column:

$$
\begin{aligned}
(\Gamma^\mu_{t\nu}) &= \begin{pmatrix} 0 & 0 & 0 & \mathcal{A}_z \\ 0 & 0 & 0 & 0 \\ 0 & 0 & 0 & 0 \\ \mathcal{A}_z & 0 & 0 & 0 \end{pmatrix}, \\
(\Gamma^\mu_{x\nu}) &= \begin{pmatrix} 0 & 0 & 0 & 0 \\ 0 & 0 & 0 & -\mathcal{B}_z \\ 0 & 0 & 0 & 0 \\ 0 & \mathcal{B}_z & 0 & 0 \end{pmatrix}, \\
(\Gamma^\mu_{y\nu}) &= \begin{pmatrix} 0 & 0 & 0 & 0 \\ 0 & 0 & 0 & 0 \\ 0 & 0 & 0 & -\mathcal{B}_z \\ 0 & 0 & \mathcal{B}_z & 0 \end{pmatrix}, \\
(\Gamma^\mu_{z\nu}) &= \begin{pmatrix} \mathcal{A}_z & 0 & 0 & 0 \\ 0 & -\mathcal{B}_z & 0 & 0 \\ 0 & 0 & -\mathcal{B}_z & 0 \\ 0 & 0 & 0 & -\mathcal{B}_z \end{pmatrix}.
\end{aligned}
$$

The tetrad e^a_λ and inverse tetrad e^λ_a are needed to compute the spin connection. e^a_λ can be read off from the metric by equation (2.1.2). Written in matrix form with the upper index labeling the row and the lower index the column, and to first order in $\mathcal{A}$, $\mathcal{B}$:

$$
(e^a_\lambda) = \begin{pmatrix} 1+\mathcal{A} & 0 & 0 & 0 \\ 0 & 1-\mathcal{B} & 0 & 0 \\ 0 & 0 & 1-\mathcal{B} & 0 \\ 0 & 0 & 0 & 1-\mathcal{B} \end{pmatrix},
$$

and

$$\left(e_a^\lambda\right) = \begin{pmatrix} 1-\mathcal{A} & 0 & 0 & 0 \\ 0 & 1+\mathcal{B} & 0 & 0 \\ 0 & 0 & 1+\mathcal{B} & 0 \\ 0 & 0 & 0 & 1+\mathcal{B} \end{pmatrix}.$$

Now equation (2.1.6) for the spin connection is arranged in the form of matrix multiplication:

$$\omega_{\mu b}^a = e_\lambda^a \Gamma_{\mu\nu}^\lambda e_b^\nu - \left(\partial_\mu e_\nu^a\right) e_b^\nu.$$

Thus, to first order in small quantities

$$\left(\omega_{tb}^a\right) = \begin{pmatrix} 0 & 0 & 0 & \mathcal{A}_z \\ 0 & 0 & 0 & 0 \\ 0 & 0 & 0 & 0 \\ \mathcal{A}_z & 0 & 0 & 0 \end{pmatrix}, \tag{A.0.2}$$

$$\left(\omega_{xb}^a\right) = \begin{pmatrix} 0 & 0 & 0 & 0 \\ 0 & 0 & 0 & -\mathcal{B}_z \\ 0 & 0 & 0 & 0 \\ 0 & \mathcal{B}_z & 0 & 0 \end{pmatrix}, \tag{A.0.3}$$

$$\left(\omega_{yb}^a\right) = \begin{pmatrix} 0 & 0 & 0 & 0 \\ 0 & 0 & 0 & 0 \\ 0 & 0 & 0 & -\mathcal{B}_z \\ 0 & 0 & \mathcal{B}_z & 0 \end{pmatrix}, \tag{A.0.4}$$

$$\left(\omega_{zb}^a\right) = 0. \tag{A.0.5}$$

Lowering the a index with $\eta_{ac}\omega_{\mu b}^c$ changes the sign of the top right entry of ω_{tb}^a and leaves all of the others unchanged.

The spinor covariant derivative can now be simplified,

$$\begin{aligned} \gamma^a e_a^\mu \nabla_\mu &= \gamma^a e_a^\mu \left(\partial_\mu + \frac{1}{8}\omega_{\mu bc}\left[\gamma^b, \gamma^c\right]\right) \\ &= \gamma^a e_a^\mu \partial_\mu + \frac{1}{2} e_a^\mu \sum_{b<c} \omega_{\mu bc} \gamma^a \gamma^b \gamma^c \\ &= \gamma^a e_a^\mu \partial_\mu + \frac{1}{2} e_{\hat{t}}^t \omega_{t\hat{t}\hat{z}} \gamma^{\hat{t}} \gamma^{\hat{t}} \gamma^{\hat{z}} \\ &+ \frac{1}{2} e_{\hat{x}}^x \omega_{x\hat{x}\hat{z}} \gamma^{\hat{x}} \gamma^{\hat{x}} \gamma^{\hat{z}} + \frac{1}{2} e_{\hat{y}}^y \omega_{y\hat{y}\hat{z}} \gamma^{\hat{y}} \gamma^{\hat{y}} \gamma^{\hat{z}} \\ &= \gamma^a e_a^\mu \partial_\mu + \frac{1}{2}\left(-\mathcal{A}_z\right)(-1)\gamma^{\hat{z}} + \left(-\mathcal{B}_z\right)(+1)\gamma^{\hat{z}}. \end{aligned}$$

Finally,

$$\gamma^a e_a^\mu \nabla_\mu = \left(1-\mathcal{A}\right)\gamma^{\hat{t}}\partial_t + \left(1+\mathcal{B}\right)\left(\gamma^{\hat{x}}\partial_x + \gamma^{\hat{y}}\partial_y\right) + \left[\left(1+\mathcal{B}\right)\partial_z + \frac{1}{2}\mathcal{A}_z - \mathcal{B}_z\right]\gamma^{\hat{z}}. \tag{A.0.6}$$

Appendix B

Non-relativistic Reduction of the Dirac Equation

In order to proceed with the non-relativistic limit of (2.4.3) it is necessary to introduce a specific representation of the gamma matrices. The most useful representation is the Dirac representation

$$\gamma^{\hat{t}} = \begin{pmatrix} -i\mathbb{I}_2 & 0 \\ 0 & i\mathbb{I}_2 \end{pmatrix}, \ \gamma^k = \begin{pmatrix} 0 & -i\sigma_k \\ i\sigma_k & 0 \end{pmatrix}, \tag{B.0.1}$$

where $\mathbb{I}_2$ is the 2x2 identity matrix and the σ_k are the Pauli matrices

$$\sigma_{\hat{x}} = \begin{pmatrix} 0 & 1 \\ 1 & 0 \end{pmatrix}, \ \sigma_{\hat{y}} = \begin{pmatrix} 0 & -i \\ i & 0 \end{pmatrix}, \ \sigma_{\hat{z}} = \begin{pmatrix} 1 & 0 \\ 0 & -1 \end{pmatrix}.$$

From here on $\mathbb{I}_2$ is suppressed for concision.

A constant energy solution has the form

$$\Psi = \mathrm{e}^{-i(m_N+\mathcal{E})t} \begin{pmatrix} \psi \\ \chi \end{pmatrix}, \tag{B.0.2}$$

where ψ and χ are time independent spinors and $\mathcal{E} \ll m_N$ in the non-relativistic limit. The standard theory of the Dirac equation shows that $\chi \ll \psi$. Inserting (B.0.2) and (A.0.6) in the Dirac equation (2.4.3) gives

$$\left\{ (1-\mathcal{A})\,\gamma^{\hat{t}}\left[-i\left(m_N+\mathcal{E}\right)\right] + (1+\mathcal{B})\left(\gamma^{\hat{x}}\partial_x + \gamma^{\hat{y}}\partial_y\right) + \left[(1+\mathcal{B})\,\partial_z + \frac{1}{2}\mathcal{A}_z - \mathcal{B}_z\right]\gamma^{\hat{z}} + m_N \right\} \begin{pmatrix} \psi \\ \chi \end{pmatrix} = 0.$$

Using the Dirac representation,

$$\left[\mathcal{A}m_N - (1-\mathcal{A})\,\mathcal{E}\right]\psi - (K+D)\,\chi = 0, \tag{B.0.3}$$

$$(K+D)\,\psi + \left[(2-\mathcal{A})\,m_N + (1-\mathcal{A})\,\mathcal{E}\right]\chi = 0, \tag{B.0.4}$$

where

$$K \equiv i\sigma_k \partial_k = i\sigma_{\hat{x}} \partial_x + i\sigma_{\hat{y}} \partial_y + i\sigma_{\hat{z}} \partial_z,$$
$$D \equiv \mathcal{B}K + \left(\frac{1}{2}\mathcal{A}_z - \mathcal{B}_z\right) i\sigma_{\hat{z}}.$$

The equation (B.0.4) can be used to eliminate χ from equation (B.0.3). Solving (B.0.4) for χ gives

$$\chi = -\left[(2-\mathcal{A})\, m_N + (1-\mathcal{A})\, \mathcal{E}\right]^{-1} (K+D)\, \psi.$$

Using this, (B.0.3) becomes

$$0 = \left[\mathcal{A}m_N - (1-\mathcal{A})\, \mathcal{E}\right] \psi + (K+D)\left[(2-\mathcal{A})\, m_N + (1-\mathcal{A})\, \mathcal{E}\right]^{-1} (K+D)\, \psi. \tag{B.0.5}$$

Since $\mathcal{E} \ll m_N$ and $\mathcal{A} \ll 1$ and for the neutron quantum bouncer $\mathcal{A} \sim 10^{-10}$ and $\mathcal{E}/m_N \sim 10^{-21} \sim \mathcal{A}^2$,

$$\left[(2-\mathcal{A})\, m_N + (1-\mathcal{A})\, \mathcal{E}\right]^{-1} \approx (2m_N)^{-1} \left(1 - \mathcal{A} + \frac{\mathcal{E}}{m_N}\right)^{-1} \approx \frac{1+\mathcal{A}}{2m_N}.$$

The second term of (B.0.5) simplifies to

$$\frac{1}{2m_N}\left\{(K+D)\left[(1+\mathcal{A})\, K\right] + (K+D)\, D\right\} \psi = \frac{1}{2m_N}\left(K^2 + K\mathcal{A}K + DK + KD\right) \psi.$$

to leading order in small quantities. This can be simplified with the identities

$$K^2 = -\sigma_k \sigma_l \partial_k \partial_l = -\nabla^2,$$
$$K\mathcal{A}K\psi = -\sigma_k \partial_k \left(\mathcal{A}\sigma_l \partial_l \psi\right) = (K\mathcal{A})\, K\psi - \mathcal{A}\nabla^2 \psi,$$

and

$$\begin{aligned}
(DK + KD)\, \psi &= \left[\mathcal{B}K + \left(\frac{1}{2}\mathcal{A}_z - \mathcal{B}_z\right) i\sigma_z\right] K\psi \\
&\quad + K\left[\mathcal{B}K + \left(\frac{1}{2}\mathcal{A}_z - \mathcal{B}_z\right) i\sigma_z\right] \psi \\
&= 2\mathcal{B}K^2\psi + \left(\frac{1}{2}\mathcal{A}_z - \mathcal{B}_z\right) i\left(\sigma_z K + K\sigma_z\right) \psi \\
&\quad + \left[K\left(\mathcal{B}\right) K + K\left(\frac{1}{2}\mathcal{A}_z - \mathcal{B}_z\right) i\sigma_z\right] \psi \\
&= 2\mathcal{B}K^2\psi - \left(\mathcal{A}_z - 2\mathcal{B}_z\right) \partial_z \psi \\
&\quad + \left[K\left(\mathcal{B}\right) K + K\left(\frac{1}{2}\mathcal{A}_z - \mathcal{B}_z\right) i\sigma_z\right] \psi.
\end{aligned}$$

Now $K\mathcal{A}_z \sim K\mathcal{B}_z \sim g/R_\oplus$ where g is the gravitational acceleration. This is much smaller than $K\mathcal{A}\partial_z\psi \sim K\mathcal{B}\partial_z\psi \sim \mathcal{A}_z\partial_z\psi \sim \mathcal{B}_z\partial_z\psi$ which is of the order of g/ℓ where ℓ is the extent of the neutron wavefunction. Thus the $K\mathcal{A}_z, K\mathcal{B}_z$ terms can be dropped:

$$(DK + KD)\, \psi = 2\mathcal{B}K^2\psi - \left(\mathcal{A}_z - 2\mathcal{B}_z\right) \partial_z \psi + K\left(\mathcal{B}\right) K\psi.$$

The first term is of the order $\mathcal{B}/\ell^2$ and remaining two are much smaller at $\mathcal{B}/R_\oplus\ell$. Putting the dominant terms together,

$$\frac{1}{2m_N}\left(K^2 + K\mathcal{A}K + DK + KD\right)\psi = -\frac{1}{2m_N}\left(1 + \mathcal{A} + 2\mathcal{B}\right)\nabla^2\psi.$$

Since $\mathcal{A}, \mathcal{B} \ll 1$ equation (B.0.5) finally becomes

$$0 = \left(\mathcal{A}m_N - \mathcal{E}\right)\psi - \frac{1}{2m_N}\nabla^2\psi. \tag{B.0.6}$$

Appendix C

Mathematica code to find $V(\phi)$ for the Hu-Sawicki model

```
(*
 * Mathematica notebook for computing the scalar potential
 * of the Hu–Sawicki f(R) model.
 *
 * Michael Brown 19 Jun 2012
 * Developed and tested on Mathematica 8.0.4.0 for Students.
 *
 * The original model definition is found in
 * Hu,W.,& Sawicki,I.(2007). Models of f(R) cosmic acceleration
 * that evade solar system tests. Physical Review D, 76 (6).
 * doi:10.1103/PhysRevD.76.064004
*)

Clear[m, c, n]

(* The model of Hu and Sawicki is defined by *)

f[R_] := R - (m^2*(c1*(R/m^2)^n))/(c2*(R/m^2)^n + 1)

(* Unfortunately this cannot explicitly be put in terms of
 * a scalar field except at large R/m^2. The second term will
 * be expanded to lowest order in m^2/R.
*)

expandedf[R_] := R + (
 Normal[
  Series[Simplify[
   f[R] - R /. R -> m^2/u^n^(-1),
   {m > 0, u > 0, n > 0, c1 > 0, c2 > 0}],
  {u, 0, 1}]] //. u -> (R/m^2)^(-n))
```

```
(* The scalar field is defined in terms of the derivative of f[R] as follows: *)

\[Phi][R_] := -((Sqrt[6]*Log[D[expandedf[R], R]])/(2*\[Kappa]))

(* Now R can be found in terms of \[Phi] by inverting the relationship. *)

solvedform = FullSimplify[Solve[\[Phi][R] == \[Phi], R][[1]],
 {m > 0, \[Kappa] > 0, \[Phi] > 0, n > 0, c2 > 0, c1 > 0}];

(* The scalar potential can now be found for specific values of n.
 * The variable substitution u = \[Kappa] \[Phi] is used,
 * as is the canonical value of c1 from Hu and Sawicki.
 * "OL" means Subscript[\[CapitalOmega], \[CapitalLambda]] and
 * "OM" means Subscript[\[CapitalOmega], M].
*)

MatrixForm[FullSimplify[
 Table[
  {k, FullSimplify[
   (D[f[R], R]*R - f[R])/(2*\[Kappa]^2*D[f[R], R]^2) /. solvedform /.
    {\[Phi] -> u/\[Kappa]} /. {n -> k} /. {c1 -> ((6*OL)/OM)*c2},
   {m > 0, n > 0, c1 > 0, c2 > 0, OL > 0,
    OM > 0, u > 0}]}, {k, {1, 4}}]]]

(* Less complicated expressions can be found by expanding about u=0. *)

MatrixForm[FullSimplify[
 Table[{k, FullSimplify[
  Series[
   (D[f[R], R]*R - f[R])/(2*\[Kappa]^2*D[f[R], R]^2) /. solvedform /.
    {\[Phi] -> u/\[Kappa]} /. {n -> k} /. {c1 -> ((6*OL)/OM)*c2},
  {u, 0, 1}], {m > 0, n > 0, c1 > 0, c2 > 0,
   OL > 0, OM > 0, u > 0}]}, {k, {1, 2, 3, 4}}]]]
```